BMT Group

“Where will our knowledge take you?”

Alternate Welding Processes for In-Service Welding

Final Report

Darren Begg

Reference: 5637C.FR
Date: April 24, 2009

5637C.FR

ALTERNATE WELDING PROCESSES FOR IN-SERVICE WELDING

FINAL REPORT

April 24, 2009

Submitted to:

US Department of Transportation
Pipeline and Hazardous Materials Safety Administration (PHMSA)
400-7th Street S.W.
Washington, D.C. 20590-0001

Submitted by:

BMT FLEET TECHNOLOGY LIMITED
311 Legget Drive
Kanata, Ontario
Canada K2K 1Z8

BMT Contact: Darren Begg
Ph.: (613) 592-2830, Ext. 229
Fax: (613) 592-4950
Email: dbegg@fleetech.com

BMT FTL DOCUMENT QUALITY CONTROL DATA SHEET

PROPOSAL/REPORT: Alternate Welding Processes for In-Service Welding”

DATE: April 24, 2009

PREPARED BY:

Darren Begg
Program Manager, Welding and Inspection

REVIEWED :

Nick Pussegoda, Phd, P. Eng.
Program Manager, Materials and Metallurgy

REVIEWED AND APPROVED BY:

Aaron Dinovitzer, P. Eng.
President

EXECUTIVE SUMMARY

Conducting weld repairs and attaching hot tap tees onto pressurized pipes has the advantage of avoiding loss of service and revenue. However, the risks involved with in-service welding need to be managed by ensuring that welding is performed in a reproducible and consistent manner within an optimal heat input window. The optimal heat input window avoids burn-through (upper limit of heat input) and weld faults or hydrogen induced cold cracking (lower limit of heat input).

Welding on live pipelines has been successfully performed for years, using mainly the shielded metal arc welding (SMAW) process. Over the past 25 years, failures have occurred in welds deposited on in-service pipelines, and these failures have been attributed to weldment hydrogen cracking, and inconsistent bead size or penetration profile. Numerous investigations have been completed to address the most significant in-service welding hazards, namely burn-through and hydrogen-induced cracking. Weld procedures designed to avoid burn-through and hydrogen cracking consider primarily the thermal cycle, while pipe chemistry and internal pressure are additional influencing parameters for delayed cracking and burn-through, respectively. The thermal cycle itself depends on the welding heat energy input, heat sink capacity of the pipeline (pipe wall thickness, fluid type and flow rate), and any preheat or post heat applied.

A significant, process dependant, in-service welding concern that can be addressed by modern power sources is the reliable control of heat input and weld size that are often difficult to maintain in all position welding. To increase in-service welding productivity, improve welder safety and assure weld integrity, alternative arc welding processes and other recent technological developments were evaluated with the objective of defining parameters and conditions associated that can preclude hydrogen cracking and burn-through in a reproducible manner.

The five alternative welding processes that were identified and evaluated in comparison to the benchmark (i.e., SMAW with low hydrogen electrodes) were:

- Self-shielded flux cored arc welding (SS-FCAW):
- Gas metal arc welding with Controlled Dip Transfer Technology, (Miller Electric's Regulated Metal Discharge (RMD)):
- Pulsed Gas Metal Arc Welding (PGMAW) using state-of-the-art power sources with closed loop feedback control:
- Gas Shielded Flux Cored Arc Welding (GS-FCAW):
- Pulsed Metal Cored Arc Welding (PMCAW):

Each of the advanced welding processes has the benefit of:

- allowing higher deposition rate without burn-through. This can be achieved by virtue of a soft arc and reduced penetration, or by running a cold arc, i.e., by allowing a lower heat input for a given deposition rate;
- allowing lower heat input without causing hydrogen induced delayed cracking. This can be achieved through the use of processes/consumables with lower weld metal hydrogen potential. The arc efficiency of each process is another factor which can influence cooling rate, and hence the susceptibility of the weld zone microstructures to delayed cracking at a given energy input;
- having a reduced susceptibility to weld flaws;
- providing better and consistent control of the weld metal puddle;
- rugged and portable equipment for field use; and
- requiring reduced operator skill.

Each of these semi-automatic processes can be used with mechanical tracking devices, and thus remove the variability in weld deposition and thus improve the safety and integrity of in-service welding.

To assess if the alternative processes/variations do indeed offer some or all of the expected advantages, the alternative processes were subjected to mutual head to head experimental comparisons, as well as with the current practice, viz., shielded metal arc welding using low hydrogen electrodes. The comparison or performance trials focused on the prevention of hydrogen cracking, burn-through, and weld flaws. The results of the trials can be used to demonstrate the range of welding parameters that could be expected to produce sound welds for each process and develop comments on ease of welding, preparation requirements, and productivity. The evaluations were performed on instrumented pipe of both low and high strength pipe with a range of heat sink conditions, including static air and water backing, thus representing the extremes of expected in-service heat sink conditions that could be encountered during welding on thin wall live pipelines.

Based on the results of the alternative welding processes evaluated

(a) Each have the potential to provide slower cooling rates over a range of heat inputs, compared to the SMAW process.
   - Slower cooling resulted in lower CGHAZ hardness and thus lower susceptibility to hydrogen cracking
   - PMCAW and PGMAW demonstrated lower CGHAZ hardness compared to SMAW at the same calculated heat input level.

(b) Each alternative process exhibited a higher susceptibility to burn-though compared to SMAW, likely due to their higher process arc efficiencies and resulting higher peak inside surface temperature for a given calculated heat input level. The SSFCAW process had demonstrated the highest susceptibility to burn-through, however SMAW with 2.4mm electrodes had demonstrated the lowest.
   - Possible that adjusting pulse waveform parameters could reduce their susceptibility

(c) Alternative processes offer the advantage of mechanization to enhance consistency of the welding procedure in all positions of welding as well as enhanced productivity with continuous wire feed and less interruptions.
   - PMCAW and PMCAW processes demonstrated enhanced tempering of HAZ’s in previously weld deposits at heat inputs 50% lower than the FCAW process, as demonstrated in Task 8.

(d) Alternate welding processes passed the requirements for bend and nick break testing as per API 1104 specifications.

(e) Each process demonstrated longer hydrogen delay times in the simulated hydrogen model when welding on water filled pipe compared to the static air conditions.

ACKNOWLEDGEMENTS

The author would like to thank the following organizations for their participation and support in this project:

- US Department of Transportation
- TransCanada Pipelines
- TDW/Williamson Industries
- RMS Welding Systems
- ESAB
- Hobart Brothers
- Miller Electric
- Bohler Thyssen
- Enbridge Pipelines

TABLE OF CONTENTS

APPENDICES

LIST OF FIGURES

LIST OF TABLES

LIST OF ACRONYMS

BMT FTL	BMT Fleet Technology Limited
CGHAZ	Coarse Grain Heat Affected Zone
ESO	Electrical Stick-out
EWI	Edison Welding Institute
FCAW	Flux Cored Arc Welding
IPM	Inches per Minute
PGMAW	Pulse Gas Metal Arc Welding
PHMSA	Pipeline and Hazardous Materials Safety Administration
PMCAW	Pulse Metal Cored
PRCI	Pipeline Research Council International
RMD	Regulated Metal Deposition
SMAW	Shielded Metal Arc Welding
TCPL	TransCanada Pipeline Limited
TS	Travel Speed
USDOT	US Department of Transportation
WFS	Wire Feed Speed

1 BACKGROUND

Conducting weld repairs and attaching hot tap tees onto pressurized pipes has the advantage of avoiding loss of service and revenue. However, the risks involved with in-service welding need to be managed by ensuring that welding is performed in a reproducible and consistent manner within an optimal heat input window. The optimal heat input window avoids burn-through (upper limit of heat input) and weld faults or hydrogen induced cold cracking (lower limit of heat input).

Numerous investigations have been undertaken in the past to study welding on pressurized pipelines. Some of these are numerical in nature and aim to model heat flow to determine:

(a) the heat input to cause burn-through in pipes of various thickness, carrying fluids at various pressures and flow rates; and
(b) 800°C to 500°C cooling time as an indicator of the weld zone microstructure and hardness, and therefore of the susceptibility to delayed cracking.

For example, **Figures 1.1(a)** and **1.1(b)**[1] display, in a quantitative manner, the general understanding that the effect of the water backing on cooling rate increases as the energy input increases or thickness decreases. From such data, one can estimate a critical thickness above which the water backing has no affect on the cooling rate.

Welding on live pipelines has been successfully performed for years, using mainly the shielded metal arc welding (SMAW) process. Over the past 25 years, failures have occurred in welds deposited on in-service pipelines, and these failures have been attributed to weldment hydrogen cracking, and inconsistent bead size or penetration profile. Numerous investigations have been completed to address the most significant in-service welding hazards, namely burn-through and hydrogen-induced cracking. Weld procedures designed to avoid burn-through and hydrogen cracking consider primarily the thermal cycle, while pipe chemistry and internal pressure are additional influencing parameters for delayed cracking and burn-through, respectively. The thermal cycle itself depends on the welding heat energy input, heat sink capacity of the pipeline (pipe wall thickness, fluid type and flow rate), and any preheat or post heat applied.

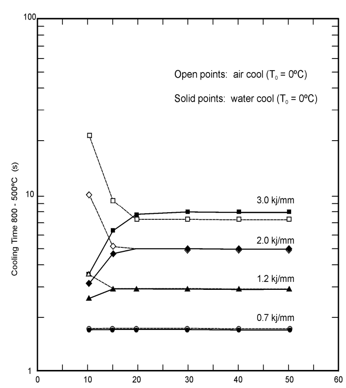

Figure 1.1(a): Cooling Time 800 to 500°C against Thickness for T-Joint (Equal Thickness)

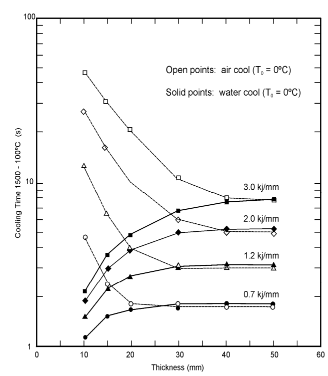

Figure 1.1(b): Cooling Time 1500 to 100°C against Thickness for T-Joint (Equal Thickness)

[1] Morrison, K.G.; "Repair Welding of Stiffeners to Hull Plating in Low Temperature Marine Environments without Preheat"; Fleet Technology Limited Report E83366C; November 1990

BMT and Graville Associates[2,3,4] developed and continue to refine an engineering tool for multi-pass weld hydrogen management which addresses many of the concerns related to hydrogen cracking. The current model considers a wide range of welding, environmental and material parameters influencing the risk of hydrogen cracking, and can also be applied to welding of the newer microalloyed, high strength steels used for major pipeline projects. This delayed cracking risk assessment approach is based upon a two-dimensional weld representation, assuming that hydrogen diffusion and heat flow are primarily normal to the weld axis. The inputs include a user-defined welding procedure, material description and weld cross-section, as shown in **Figure 1.2** for a six pass fillet welded sleeve welding procedure. Weld cracking susceptibility is based upon local hydrogen concentration, microstructure susceptibility (quantified in terms of hardness) and stress effects, thus developing a time history of cracking risk for all locations within the weldment. This model has been validated against lab trial results and continues to be improved.

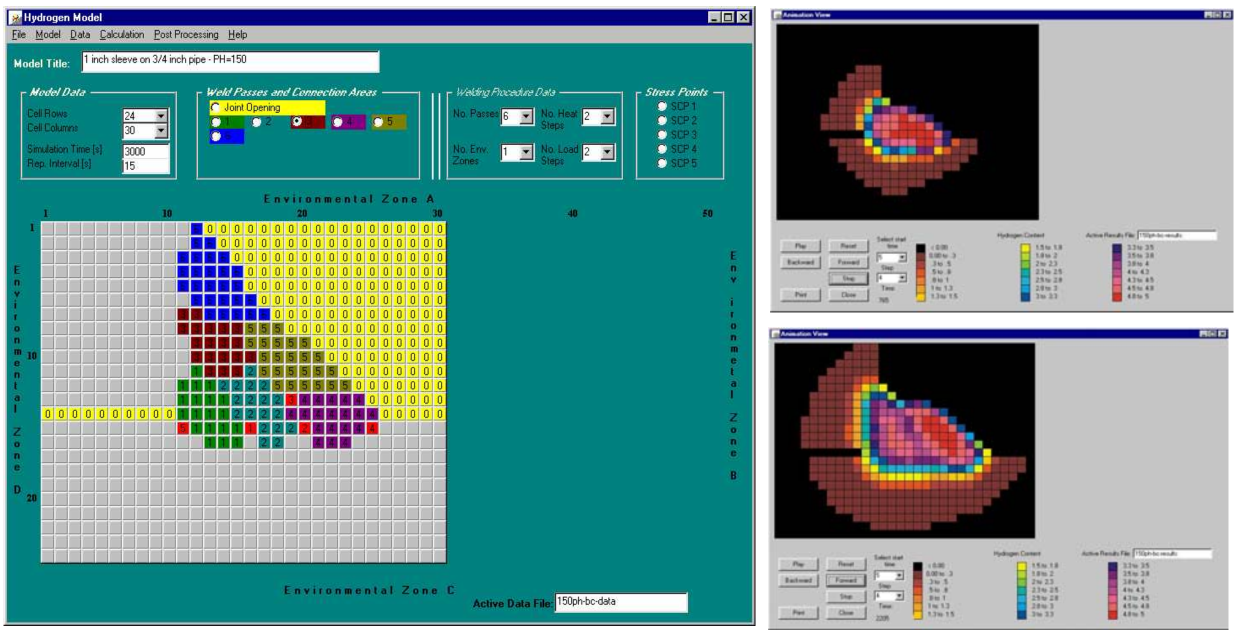

Figure 1.2: BMT Hydrogen Diffusion and Delayed Cracking Model

Other investigations have been experimental in nature and focused on weld zone cooling time and/or heat-affected zone hardness[5] as an indicator of the potential of hydrogen induced cold cracking (for example, see **Figure 1.3**[6]). Variables considered include heat input, pipe thickness and fluid flow characteristics. Analytic tools and graphical outputs are developed from these studies to help define ideal heat inputs for in-service welding.

[2] Dinovitzer, A., (1998), "Modelling Weld Hydrogen Diffusion and Predicting Delayed Cracking in Multi-Pass Welds", Fleet Technology Limited internal development report

[3] Dinovitzer, A., Graville, B., Glover, A., Pussegoda, N., "Multi-Pass Weld Hydrogen Management to Prevent Delayed Cracking", International Pipeline Conference, Calgary ,2000

[4] Graville, B.A., (1997), "The risk of delayed hydrogen cracking in pipeline welds", report P398/1 for Nova Gas Transmission Ltd., November

[5] Coe, F.R., "Welding Steels without Hydrogen Cracking", The Welding Institute, UK, 1973.

[6] Bruce, W.A.; "Hydrogen Cracking of Water-backed Welds"; International Conference on Advances in Welding Technology: Joining of High Performance Steels, Columbus, Ohio, November 1996

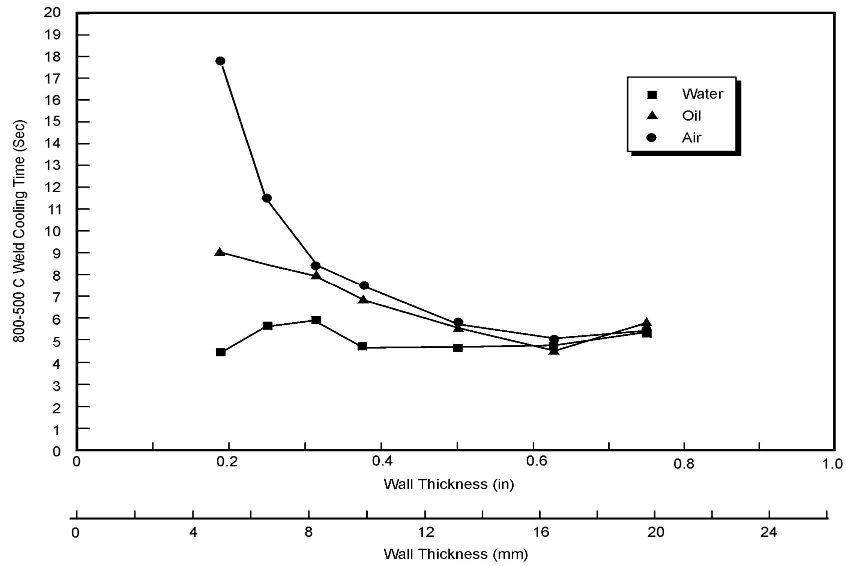

Figure 1.3: Wall Thickness vs. Weld Cooling Time for 40 kJ/in Weld

BMT has focused its numerical and experimental in-service welding investigations on three primary issues: the prevention of hydrogen cracking, the effectiveness of tempering on multi-pass weld hardness control and the development of welding procedures that ensure fault free high toughness welds. The prevention of delayed cracking involves the control of hydrogen, microstructure susceptibility, and tensile stresses. To understand the interaction of these factors, BMT has developed several tests to characterize the susceptibility of a base metal or weld metal to hydrogen cracking. These tests have been used along with other industry data to calibrate the BMT numerical model predicting the susceptibility of multi-pass weld procedures to hydrogen cracking. The constant deflection and slow bend tests, being standardized in a PRCI funded project are used to quantify susceptibility of materials and welding procedures to hydrogen cracking by identifying the relationship between applied stress and hydrogen concentration required for cracking[7]. This data has been used to develop a preliminary quantitative relationship between HAZ critical hardness, weld metal hydrogen content, local stress (**Figure 1.4**) that compares well with current industry standard hardness limits.

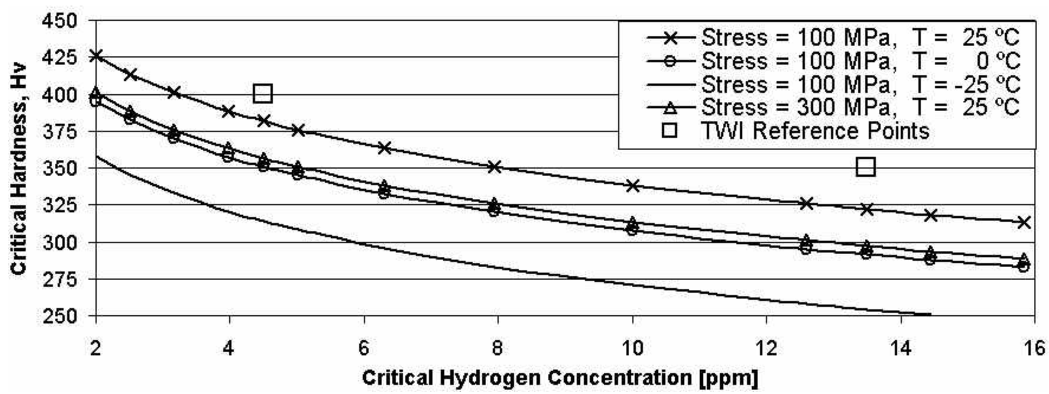

Figure 1.4: BMT Hydrogen Cracking Susceptibility Relationship

[7] Malik, Pussegoda, Graville, Glover, "Prediction of Maximum Time for Delayed Cracking in a Simulated Girth Weld Repair", International Pipeline Conference 1998.

This data is used in the BMT hydrogen cracking numerical model to identify hydrogen cracking risk, maximum cracking delay time and allows the user to investigate the effect of environmental, applied loading and welding procedure parameters on these results.

Experimentally, BMT has made extensive use of its welding expertise to evaluate welding equipment, consumables and procedures to produce sound welds with desired mechanical properties (e.g., fracture toughness). This work has been completed for a range of steels on plate and pipe in air and in the BMT in-service welding simulation flow loop facility.

2 PROJECT OBJECTIVES

The primary objective of this project is to define parameters and conditions associated with each advanced welding process that can preclude hydrogen cracking and burn-through in a reproducible manner.

A significant, process dependant, in-service welding concern that can be addressed by modern power sources is the reliable control of heat input and weld size that are often difficult to maintain in all position welding.

To increase in-service welding productivity, improve welder safety and assure weld integrity, alternative arc welding processes and other recent technological developments were evaluated. Welding process and procedure characteristics that aid in achieving these goals include:

(a) allowing higher deposition rate without burn-through. This can be achieved by virtue of a soft arc and reduced penetration, or by running a cold arc, i.e., by allowing a lower heat input for a given deposition rate;
(b) allowing lower heat input without causing hydrogen induced delayed cracking. This can be achieved through the use of processes/consumables with lower weld metal hydrogen potential. The arc efficiency of each process is another factor which can influence cooling rate, and hence the susceptibility of the weld zone microstructures to delayed cracking at a given energy input;
(c) having a reduced susceptibility to weld flaws;
(d) providing better and consistent control of the weld metal puddle;
(e) rugged and portable equipment for field use; and
(f) requiring reduced operator skill.

Five alternative welding processes were identified and evaluated that possessed one or more of the above desirable characteristics, compared to the SMAW process, and these were:

(a) Self-shielded flux cored arc welding (SS-FCAW):
   - higher productivity compared to SMAW;
   - controlled hydrogen, generally between that for low hydrogen SMAW electrodes and the GMAW process;
   - no shielding gas required and amenable to use in an outdoor environment without inducing weld flaws;
   - minimal skill requirement above and beyond that for the SMAW process; and
   - rugged equipment suitable for field use.

(b) Gas metal arc welding with Controlled Dip Transfer Technology, (Miller Electric's Regulated Metal Discharge (RMD)):
   - higher productivity compared to SMAW;
   - ability to achieve a higher deposition rate at a given energy input due to some flexibility in controlling the wire feed speed independent of the energy input;
   - lower weld metal hydrogen content; better and consistent control of the weld puddle and root bead profile;
   - out of position welding capability; may require higher operator skill level; and
   - equipment designed for field use, pipeline girth welds being a prime application.

(c) Pulsed Gas Metal Arc Welding (PGMAW) using state-of-the-art power sources with closed loop feedback control:
   - higher productivity compared to SMAW;
   - lower weld metal hydrogen content;
   - better and consistent control of the weld puddle, reduced susceptibility to flaws in all position welding;

- equipment suitable for use in field environment; and
- requires greater skill than that for the SMAW process.

(d) Gas Shielded Flux Cored Arc Welding (GS-FCAW):
- higher productivity compared to GMAW;
- low weld metal hydrogen content;
- consistent control of the weld puddle, reduced susceptibility to flaws in all position welding; equipment suitable for use in field environment; requires greater skill than the SMAW process, but less skill than GMAW;
- more tolerable of wind and drafts compared to GMAW (due to the protective slag covering).

(e) Pulsed Metal Cored Arc Welding (PMCAW):
- productivity between GS-FCAW and PGMAW, less susceptible to lack of fusion flaws compared to PGMAW, low weld metal hydrogen content;
- requires greater skill than the SMAW process but less than P-GMAW;
- electrodes can easily be manufactured to a specific composition.

Each of these semi-automatic processes has the potential to be used with mechanical tracking devices, and thus remove the variability in weld deposition and thus improve the safety and integrity of in-service welding. Mechanized welding also requires less welder skill to operate and apply welding procedures. The improved weld bead profiles that can be realized with mechanized welding also make these potential variants excellent candidates for temper bead welding procedures. Temper beads are used for high carbon equivalent pipe where weld parameters cannot on their own reduce heat-affected zone hardness to levels that would avoid hydrogen cracking.

3 WORK SCOPE

To assess if the alternative processes/variations do indeed offer some or all of the expected advantages, the alternative processes were subjected to mutual head to head experimental comparisons, as well as with the current practice, viz., shielded metal arc welding using low hydrogen electrodes. The comparison or performance trials focused on the prevention of hydrogen cracking, burn-through, and weld flaws. The results of the trials can be used to demonstrate the range of welding parameters that could be expected to produce sound welds for each process and develop comments on ease of welding, preparation requirements, and productivity. The evaluations were performed on instrumented pipe of both low and high strength pipe with a range of heat sink conditions, including static air and water backing, thus representing the extremes of expected in-service heat sink conditions that could be encountered during welding on thin wall live pipelines. A description of each task is provided below.

3.1 Task 1: Literature and Industry Practice Review: Establish the Current State-of-the-Art In Welding Process and Procedure Application for Hot Tapping and Repairs for the Linepipe Materials of Interest.

Work Scope: Pertinent documents were procured along with other pipeline research reports on this subject. A significant source of this information was from PRCI reports outlining the results of previous initiatives. All the gathered information was reviewed and a state-of-the-art summary was prepared that include:

(a) burn-through tendency and weld zone cooling rate as a function of the welding process, energy input, thickness and the backing medium; and
(b) practices for hot tapping and build-up repair in the field..

It was suggested from the onset that X52 and X80 be chosen for the evaluations, as these would demonstrate higher CE and strength, respectively, each having very different susceptibilities to cracking.

3.2 Task 2: Establish Practical Welding Parameter Ranges for Out-of-Position Welding

Work Scope: The intention of this task was to define the range of parameters that would be practical for in-service welding applications and not induce lack of fusion type of flaws. The consumables of interest for all evaluations were slightly over-matching and matching strength with respect to the X52 and X80 base materials, respectively.

Practical welding parameter ranges were established for buttering and for fillet welds of various sizes. The variables involved position of welding and the main pipe wall thickness. The highest and lowest ranges of heat inputs were established based on the following weld trial characteristics: weld bead visual appearances, weld pool fluidity and base metal wetting, weld depth of penetration and shape, and, susceptibility to interpass and lack of side wall fusion flaws.

3.3 Task 3: Examination the Potential for Burn-Through for the Selected Processes

Work Scope: Using the range of heat input limits established in Task 2, the critical material thicknesses and pressures for burn-through to occur were established with each welding processes of interest. This task was conducted with "still air" backing to simulate worst-case conditions. Thermocouples were placed on the opposite side of the pipe along the weld axis to measure the temperature of the base metal ligament between the root of the weld bead and the backside of the plate surface. These temperature measurements, along with macro sectioning and empirical correlations were used to numerically estimate the yield strength reduction (vs. increasing temperature) of the remaining base metal ligament and the susceptibility to significant bulging or blow out at various pipeline pressures.

3.4 Task 4: Examine Cooling Rates as a Function of Welding Process Arc Efficiency

Work Scope: The arc efficiency of each welding process type is known to have an effect on the cooling rate for a given heat input, therefore different results can be obtained when measuring the HAZ hardness and the susceptibility to cracking from one process to another. For example, the submerged arc welding is rated at approximately 95% arc efficiency and will have a slower cooling rate at a given heat input in comparison to the GMAW process, which is rated at approximately 75% arc efficiency. Although the arc efficiency differences for the SMAW, GMAW, and FCAW processes are small, they can still have a pronounced effect on the cooling rates and the resulting HAZ hardness, especially when welding on a live pipeline.

A series of bead on plate welds were conducted with each process over the range of heat inputs established in Task 2. Each plate was instrumented with a series of thermocouples attached to a multi-channel high-speed temperature data acquisition system, to examine the 1000 to 100°C and 800 to 500°C cooling times for each process. Samples were extracted from each weld to examine bead profiles, depth of penetration, and weld zone hardness. The results were compared to those obtained in Task 7 that simulated various operating and environmental in-service welding conditions (i.e., static air, flowing air, air-mist, and water backing) for each material of interest.

3.5 Task 5: Establish Diffusible Hydrogen Characteristics

Work Scope: The hydrogen potential of each process/consumable combination was characterized using AWS 4.3 standard of testing under mercury. Since welding parameters are known to influence the hydrogen entrapment, the diffusible hydrogen of each process was characterized at several welding parameter settings within the heat input range established in Task 2. The results from this task were used in correlation with Task 6 for determining delay times (i.e., time to peak hydrogen concentration and thus maximum time to cracking) with each process/consumable and base metal combination evaluated.

3.6 Task 6: Prediction of Delay Times for Hydrogen Cracking

Work Scope: BMT Fleet Technology Limited's hydrogen diffusion model was used to estimate the delay times for sample welds that are considered cracking susceptible (i.e., have a hardness of 300 HVN or more).

3.7 Task 7: Weld Zone Characterization for a Variety of Simulated Pipeline In-service Welding Conditions

Work Scope: Deposit a series of bead on pipe and fillet welds on pipe with flowing air, water-mist spray, and water backing using each welding process (at the predetermined highest and lowest heat inputs) and base materials of interest. Samples were extracted from each weld to examine the weld penetration depths and profiles, measure weld zone hardness, and to compare the results compared back those in Tasks 3 and 4. The intention of this task was to determine if susceptibility to burn-through could reduce with increasing heat sink capacity, at a given heat input level, and, if one or more processes could extend the safety envelope of in-service welding compared back to the SMAW process.

3.8 Task 8: Hot-tap Joint Simulation

Work Scope: Hot-tapping sleeve joints were simulated using pressure retaining sleeves provided by Williamson Industries. Modified mechanized welding equipment (by RMS Welding Systems) designed specifically for circumferential girth welding was used to complete the in-service hot tap sleeve welding simulations. Macros were removed from each position of welding for examination and hardness measurements as well for nick break tests in accordance with API 1104. The simulations were conducted in still air (rather than flowing water) to keep costs down of transporting either the BMT flow loop or mechanized welding equipment "to and from" the equipment manufacture's locations. Note that the primary objective of this task was to evaluate the equipment's ability to reproduce the procedures developed in the lab in each clock position of welding.

4 RESULTS

4.1 Task 1.1: Literature and Industry Practice Review

Research reports related to welding on in-service pipelines were gathered from project team members. Each report was reviewed and a state-of-the-art summary was produced from each, and is included in **Appendix A**. Most of the information discussed in these reports focuses on the use of the shielded metal arc welding (SMAW) process.

Although one of objectives in Task 1 was to review the application of state-of-the-art mechanized welding of sleeves to in-service pipelines, insufficient information was available from publicly published reports. The research reports reviewed included a series of experimental procedures for depositing welds on thin walled pipe and preventing the incidence of burn-through, using the SMAW process. The main variables used to establish burn-through limitations in these reports were the pipe wall thickness, electrode diameter, heat input, and flow rate and medium. A number of these procedures were duplicated in the lab to confirm their effectiveness to control burn-through on thin walled pipe, and are discussed in more detail in Tasks 3, 4, and 7 herein.

In developing a framework to establish optimal procedures for welding on "live" pipelines, three goals need to be achieved, that being:

(1) prevention of hydrogen cracking;
(2) prevention of burn-through; and
(3) prevention of weld flaws.

Of these, prevention of burn-through and of weld flaws depend on physical properties of the pipeline steel and welding parameters, and so any recommendations developed in this regard would be valid irrespective of the pipeline steel grade, since physical properties such as thermal conductivity are not altered by steel composition, at least within the range applicable to pipeline steels.

The incidence of hydrogen cracking, on the other hand, is strongly influenced by the composition and strength, and hence the grade of the steel. Older pipelines (e.g., 1950-60's vintage), were typically X52 grade, and steel composition used to be C-Mn type, with carbon in the range of 0.15 to 0.30%. Under fast cooling conditions of welding on live pipelines, the Heat Affected Zone (HAZ) in these steels can be quite hard (>350 VPN) thus increasing the potential for hydrogen cracking in the HAZ.

More recent pipelines have utilized X80 grade pipeline steels since they have lower carbon content (typically 0.05%) and thus represent better HAZ weldability in spite of their higher strength. However, research in recent years has suggested that critical hardness to prevent HAZ hydrogen cracking is lower in lower carbon steels and therefore any reliance on models predicting HAZ hardness as a function of composition and cooling rate must take this into account. Secondly, even if the potential for HAZ hydrogen cracking might be acceptably small, the necessary use of higher strength and therefore more highly alloyed weld metal increase the potential for weld metal cracking.

In the experimental program being undertaken here, including both these grades of pipeline steels (i.e., X52 and X80) will thus ensure that the hydrogen cracking resistant procedures recommended would have taken into account HAZ and weld metal susceptibilities as well as the effects of base metal and weld metal strengths.

4.2 Task 1.2: Pipe Selection

The grades, sizes, and thicknesses of X52 and X80 pipes obtained from industry for this study, including their composition and mechanical properties, are shown in **Table 4.1**. Although some of the pipes obtained are X70 grade, each of their yield strengths and carbon equivalents are within the range typical of X80, and should provide similar characteristics with respect to weldability.

Table 4.1: Base Metal Properties for Pipes Evaluated

Base Metal					Chemical Composition (%)																Mechanical Properties				
Grade	Manufacture	Diameter	Thickness	Heat Number	C	Mn	Si	S	P	Cr	Mo	Nb	V	Ni	Cu	Ti	Al	N	B	CE (Z245.2:1974)	UTS (ksi)	YS (ksi)	Elongation (%)	Charpy V-notch	
																								J	ºC
X52	LTV	NPS 10	6.4	293201	.05	1.04	.22			.04	.02	.044	.001	.03	.05					.16	75.7	69.7	35	61 (1/2 size)	-5
X52	NA	NPS 20	6.4	NA (era 1972)	.24	1.09	.033			.029				.025	.033					.43	78.3	58.5	32.5	12 (1/2 size)	-5
X52	LTV	NPS12	8	133062	.066	.72	.023	.021	.014	.042	.005	.037	.026	.01	.028					.14	70.2	62.4	37	NA	
X70	STELCO	NPS36	11	565879	.031	1.54	.021	.0042	.0024	.066	.19	.07	.034	.15	.34					.22	88	74.2	32	NA	
X80	STELCO	NPS 48	16.1	561831	.04	1.74	.37	.002	.014	.04	.31	.076	.004	.32	.28	.012	.029	.008		.27	106.8	86.2	40	168	-5
X70	SUMITOMO	NPS 40	19	2822519	.06	1.57	.14	.002	.011	.03	.17	.042	.04	.13	.14	.017	.029	.0034	.0001	.24	98	89	22.1	324	-5

4.3 Task 1.3: Welding Consumable Selection

Based on input from the project team and the consumable suppliers, welding consumables were selected for each grade of pipe. The electrodes selected were to provide suitable matching strength with the parent base metals, exhibit low diffusible hydrogen characteristics, and be able to operate and produce sound welds in each position of welding.

The project sponsors were consulted to determine if candidate off-the-shelf electrodes were available for the SMAW benchmark procedures, as well as the PGMAW, Self Shielded FCAW, and Controlled Dip Transfer Welding Process (i.e., RMD) that were examined. Based on their input, the electrodes shown in **Table 4.2** were utilized. Each electrode was selected based on its ability to provide matching strengths to the pipe grade as well as exhibit low diffusible hydrogen characteristics

.

Table 4.2: Welding Electrode Properties

Electrode						Chemical Composition (%)														Mechanical Properties				
Manufacture	**AWS Classification**	**Trade Name**	**Size**	**Lot Number**	**Pipe Grade Application**	**C**	**Mn**	**Si**	**S**	**P**	**Cu**	**Cr**	**Ni**	**Mo**	**V**	**Ti**	**Al**	**Co**	**Nb**	**UTS (ksi)**	**YS (ksi)**	**Elongation (%)**	**Charpy V-notch ft-lbs (2)**	**°F**
Hobart	E71T8-K6	Fabshield 71K6 (1)	5/64	H01629	X52	.04	.91	.06	.005	.012	<.01	.04	.74	.02	<.01		.72	.25		74	62	30	120	-40
Hobart	E81T8-Ni2 J	Fabshield 81N2 (1)	5/64	H02453	X80	.02	1.02	.05	.004	.011	<.01	.08	2.28	.02	<.01		.69	.35		88	76	26	96	-40
Hobart	E7018-1 H4R	718MC	3/32		X52	Not reported																		
Hobart	E7018-1 H4R	718MC (1)	1/8		X52	.05	1.07	.61	.012	.009		.02	.06	<.01	.01					79	66	30	81	-50
ESAB	E10018-G	Filarc 108MP (1)	1/8	1136191	X80	.07	1.98		.008	.006			.96		.02				.01	Not reported				
ESAB	MIL-10018-M1	Atomarc 10018-M1 (1)	1/8	4A321M02	X80	.035	1.18	.29	.010	.009		.02	1.95	.31	.01									
ESAB	ER70S-G	Spoolarc XTi (3)	.035		X80	.08	1.62	.64	.006	.012	.01					.045								
Bohler Thyssen	ER70S-6	Thyssen K-Nova (3)	.035		X52	.081	1.33	.61	.012	.008	.12	.04	.03	.005	.002	.021				88	81	24.5	87	-40
Bohler Thyssen	ER70S-6	Thyssen K-Nova (3)	.047		X52	.069	1.10	.50	.014	.007	.08	.05	.02	.009	.001	.021				82	69	26.2	53	-20

Notes:

(1) Chemical Composition from Weld Pad Analysis
(2) Average Absorbed Energy
(3) Chemical Composition from Wire Analysis

The project sponsors were consulted to determine if candidate off-the-shelf electrodes were also available for the PMCAW and gas shielded FCAW processes. Hobart Brothers recently had developed two metal cored electrode products for this application and the trade names are MC70 and MC100. Trans Canada Pipelines Limited (TCPL) had been concurrently evaluating the MC100 electrode for X80 grade pipe and their findings were sufficiently appealing to warrant further investigation in this test program. Previous testing by Hobart on their MC70 product demonstrated all weld metal mechanical properties of 78 ksi Yield Strength (YS), 91 ksi Ultimate Tensile Strength (UTS), and an average of 18 ft-lbs at -40°F, which are sufficient properties for X52 grade pipe. The MC100 product had demonstrated 95 ksi YS, 106 ksi UTS, and 41 ft-lbs at -40°F, which are sufficient properties for X80 grade pipe.

TCPL had also been examining gas shielded flux cored products from ESAB for various applications and these are the Dual Shield II 70T-12MJ H4 and Dual Shield II 80Ni1H4 electrodes. The Dual Shield II 70T-12MJH4 is an all position flux cored wire intended for applications with weld metal impact toughness requirements of more than 50 ft-lbs at -60°F, as well as Cracking Tip Opening Displacement (CTOD = industry accepted measurement of fracture toughness characterising a material's resistance to rapid crack extension) requirements of more than 20 mils at -40°F. The weld metal composition, strength, and diffusible hydrogen characteristics are reportedly similar to an E7018-1 shield metal arc welding (SMAW) electrode, and the typical properties as well as the AWS A5.1 requirements for an E7018-1 electrode are shown in **Table 4.3**. As shown in Table 3, both electrodes can produce welds with ultimate strength and elongation of the same order of magnitude. The apparent differences in toughness and yield strength are due to the different manner in which they are specified for each material.

Table 4.3: Dual Shield II 70T-12 Typical Properties and E7018-1 Requirements

Electrode	Composition (%)*						Mechanical Properties				
										Charpy V- Notch Impact	
	C	Mn	Si	P	S	Ni	Tensile Strength (Mpa)	Yield Strength (Mpa)	% Elongation	Temperature (°C)	Avg. Energy (J)
Dual Shield II 70T-12	0.05	1.16	0.31	0.008	0.012		580	531	28	-40	122
E7018-1 Requirements per AWS A5.1 Standard	NS	1.6 max.	0.75 max.	NS	NS	0.3	482 min.	399 min.	22 min.	-46	27 min.
NS = Not Specified											

The weld metal analysis of the Dual Shield II 80Ni1H4 is reportedly similar to an E8018-C3 low hydrogen SMAW electrode and produces excellent weld metal toughness in both the as-welded and stress relieved condition, and the typical properties as well as the AWS A5.5 requirements for E8018-C3 electrodes are shown in **Table 4.4**. As shown in Table 4.4, both electrodes can produce welds with ultimate strength, yield strength and elongation of the same order of magnitude. The apparent differences in toughness are due to the different manner in which it is specified for each material.

Table 4.4: Dual Shield II 80Ni1H4 Typical Properties and E8018C3 Requirements

Electrode	Composition (%)*						Mechanical Properties				
	C	Mn	Si	P	S	Ni	Tensile Strength (Mpa)	Yield Strength (Mpa)	% Elongation	Charpy V- Notch Impact Temperature (°C)	Charpy V- Notch Impact Avg. Energy (J)
Dual Shield II 80Ni1H4	0.048	1.18	0.32	0.015	0.009	0.91	600	545	28	-40	156
E8018-C3 Requirements per AWS A5.5 Standard	0.12 max.	0.40 to 1.25	0.80 max.	0.03 max.	0.03 max.	0.80 to 1.10	550 min.	470 to 550	24 min.	-40	27 min.
NS = Not Specified											

Both of the above flux cored products are considered low hydrogen that can produce <4ml of diffusible hydrogen per 100g of weld metal over a wide range of welding parameters. Low hydrogen electrodes are essential for reducing the risk for cracking under the conditions typical for in-service welding.

4.4 Task 2: Establish Practical Welding Parameter Ranges for Out-of-Position Welding

Each of the electrodes selected were used to produce fillet welds in each position of welding for a range of base metal thickness combinations. Each position of welding evaluated simulates those that would be experienced in the 5G position, i.e., the carrier pipe fixed in the horizontal position with welding progressing around its circumference, as shown in **Figure 4.1**.

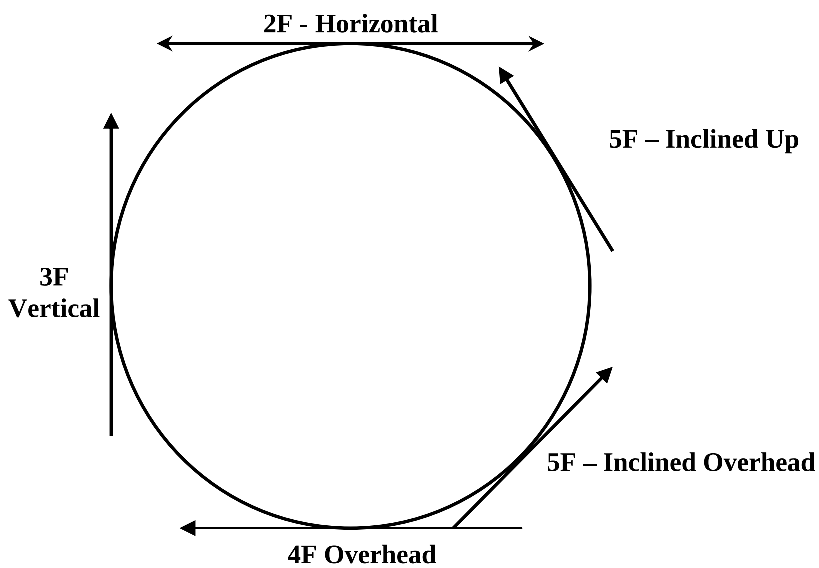

Figure 4.1: Welding Positions

This information was used to establish baseline welding conditions for the welding trials in later tasks. Mild steel plates were used for the welding parameter development trials instead of conventional pipeline materials as the steel grade, at least within the range of steels evaluated in this study, are not likely to have any influence on the process applications.

The simulated sleeve joint utilized a plate of "T" thickness (representing the parent pipe thickness) and a plate of at least "1.5T" (representing the sleeve thickness) which was selected based on input from TCPL, as shown in **Figure 4.2**. Parameters were developed for the 2F, 3F, 5F - 45º over-head, and 5F - 45º inclined positions.

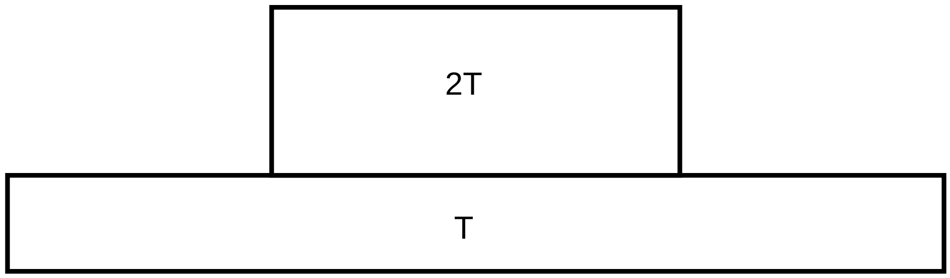

Figure 4.2: Sleeve Simulation Joint Configuration

The range of all parameters tested with the SMAW, PGMAW, self shielded FCAW, and RMD processes are tabulated in **Appendix B**. Note that BOP welds were rated as safe, marginal, and burn-thorough in the table in Appendix B, where:

(a) safe = heat input to avoid burn-through;
(b) marginal = HAZ extends to back side of plate however no melting on the backside of plate occurs; and
(c) burn-through = weld has penetrated the plate thickness or melting occurred on the back side of the plate.

These safe and marginal limits were verified in the burn-through susceptibility task based on back surface temperature measurements and weld penetration depths during welding.

The welding parameters that were developed in each position of welding with the PMCAW products and with C15 gas (15%CO_2 – bal. Argon) are shown in **Table 4.5**, using the Miller Axcess 450 power source with their Accu-Pulse technology. Several trials were conducted with various combinations of wire feed speed and pulse parameters to fine tune the arc and the final procedures are considered suitable for depositing single fillet welds (5 and 6mm leg size) in each position as well as for multi-pass welding to achieve larger fillet weld sizes. Cross-sections were extracted from each mock-up to evaluate the depth of penetration and soundness, and a sample weld cross section for MC70 and MC100 are shown in **Figure 4.3** and **4.4**, respectively, illustrating each position of welding for the smallest X52 and largest X80 pipe wall thicknesses being evaluated. Each cross-section exhibited acceptable bead profiles with equal leg lengths and suitable penetration to the root region. Note that the simulated sleeve thickness was at least 1.5 times the thickness of the thinner base plate.

Table 4.5: Hobart MC70 and MC100 Parameters

Base Plate Thickness (mm)	Single Fillet Weld Leg Size (mm)	Position	Wire Feed Speed (in/min)	Amperage (A)	Voltage (V)	Travel Speed (in/min)	Heat Input (kJ/mm)
X52 – MC70		2F					
6.4	5		200	140	20.5	13	0.52
8	6		240	165	20	10.5	0.74
X80 - MC100							
11	6		240	165	20	10.5	0.74
16.1	6		240	165	20	10.5	0.74
19.1	6		240	165	20	10.5	0.74
X52 – MC70		3F - up					
6.4	5		180	115	19.5	6	0.88
8	6		180	130	18.5	8	0.71
X80 – MC100							
11	6		180	130	18.5	8	0.71
16.1	6		180	130	18.5	8	0.71
19.1	6		180	130	18.5	8	0.71
X52 – MC70		4F					
6.4	5		180	135	20.5	10	0.65
8	6		180	135	19.5	8.5	0.73
X80 – MC100							
11	6		180	135	19.5	8.5	0.73
16.1	6		180	135	19.5	8.5	0.73
19.1	6		180	135	19.5	8.5	0.73
X52 – MC70		5F					
6.4	5		180	135	20.5	8	0.82
8	6		180	130	20	7.5	0.82
X80 – MC100							
11	6		180	130	20	7.5	0.82
16.1	6		180	130	20	7.5	0.82
19.1	6		180	130	20	7.5	0.82

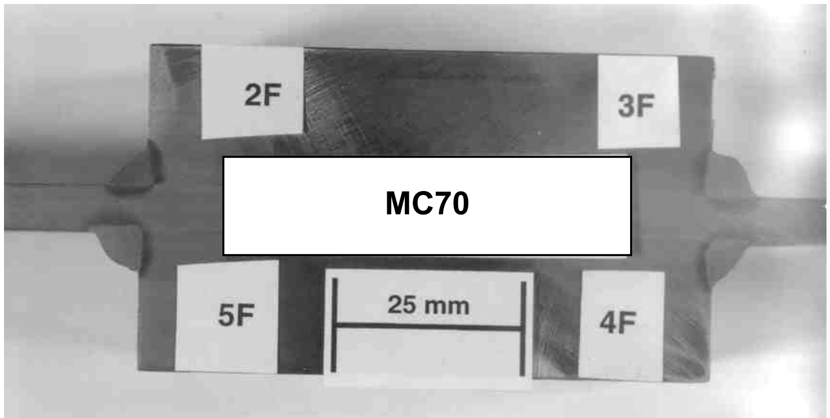

Figure 4.3: Weld Cross-sections for 6.4mm Pipe Wall X52 Simulations

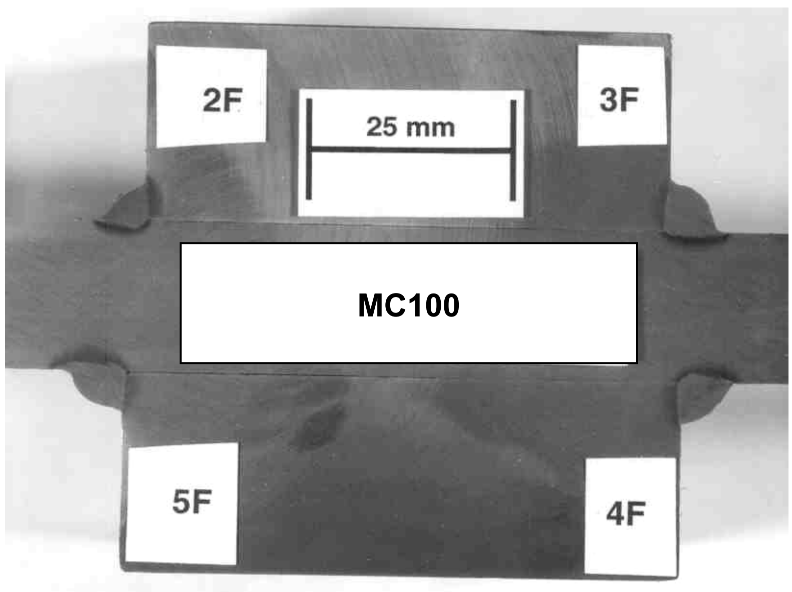

Figure 4.4: Cross-sections for 19mm Pipe Wall X80 Simulations

The welding parameters that were developed in each position of welding with the gas shielded FCAW products and C25 gas (25% CO_2 – bal. Argon) are shown in **Table 4.6** and **4.7**, using a conventional constant voltage (CV) power source. The final welding procedures are considered suitable for depositing single fillet welds (5 and 6mm leg size) in each position as well as for multi-pass welding to achieve larger fillet weld sizes. Cross-sections were extracted from each mock-up to evaluate the depth of penetration and soundness, and sample weld cross sections are shown in **Figure 4.5** and **4**.**6** illustrating each position of welding for the smallest X52 and largest X80 pipe wall thicknesses being evaluated. Each cross section exhibited acceptable bead profiles with equal leg lengths and suitable penetration to the root region.

Table 4.6: ESAB Dual Shield II 70T-12 Parameters

Base Plate Thickness (mm)	Single Fillet Weld Leg Size (mm)	Position	Wire Feed Speed (in/min)	Amperage (A)	Voltage (V)	Travel Speed (in/min)	Heat Input (kJ/mm)
6.4	5	2F	325	200	25.5	12	1.00
8	6		360	220	26.5	12	1.15
6.4	5	3F - up	325	205	25.5	9.5	1.30
8	6		330	210	26.5	8	1.64
6.4	5	4F	320	200	25	12	0.98
8	6		345	215	25.5	11	1.18
6.4	5	5F	320	200	24.5	10	1.16
8	6		345	215	25.5	8.5	1.52

Table 4.7: ESAB Dual Shield II 80 NiMH4 Parameters

Base Plate Thickness (mm)	Single Fillet Weld Leg Size (mm)	Position	Wire Feed Speed (in/min)	Amperage (A)	Voltage (V)	Travel Speed (in/min)	Heat Input (kJ/mm)
11	6	2F	360	215	26.5	11	1.22
16.1	6		360	215	26.5	11	1.22
19.1	6		360	215	26.5	11	1.22
11	6	3F-up	325	190	26	8	1.46
16.1	6		325	190	26	8	1.46
19.1	6		325	190	26	8	1.46
11	6	4F	345	210	25.5	9.5	1.33
16.1	6		345	210	25.5	9.5	1.33
19.1	6		345	210	25.5	9.5	1.33
11	6	5F	345	215	25.5	9.5	1.36
16.1	6		345	215	25.5	9.5	1.36
19.1	6		345	215	25.5	9.5	1.36

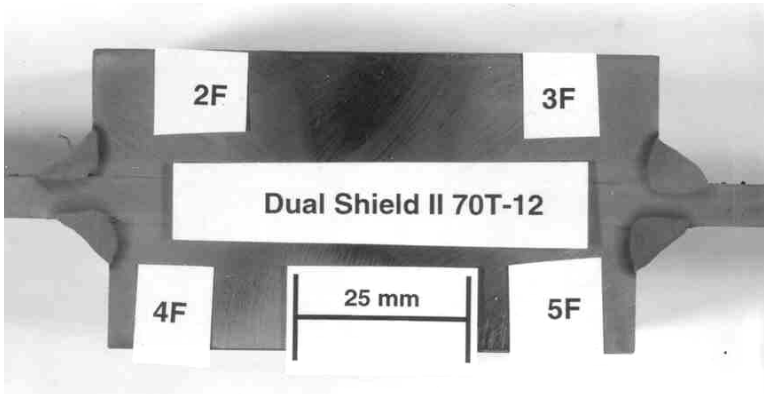

Figure 4.5: Weld Cross-sections for 6.4mm Pipe Wall X52 Simulations

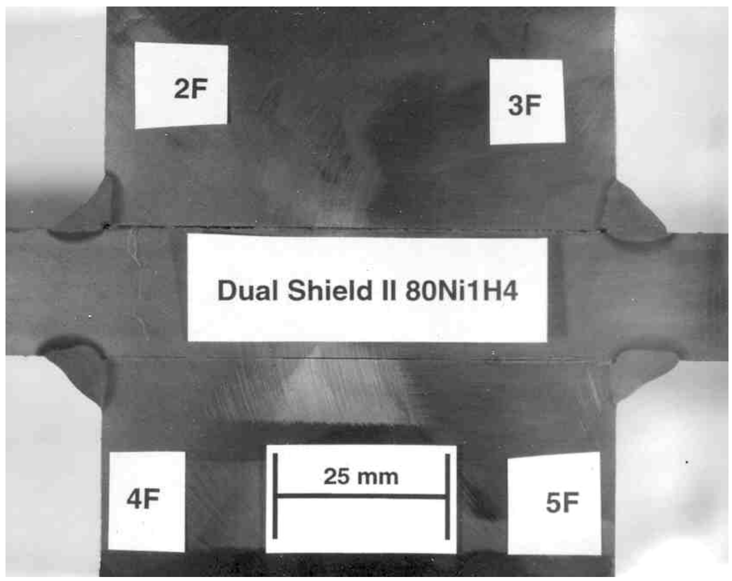

Figure 4.6: Cross-sections for 19mm Pipe Wall X80 Simulations

4.5 Task 3: Examination the Potential for Burn-Through for the Selected Processes

The objective of this task was to numerically predict the susceptibility of each welding process and procedure to burn-through over the entire range of practical heat inputs developed in Task 2. The primary factors determining the susceptibility to burn-through include the peak back surface temperature, depth of weld penetration and wall thickness, and pipeline operating pressure. Calculations based upon the "ASME B31G" formulation were used to determine the required operating pressure to cause a burn-through / bulging event with each of the welds deposited. The "ASME B31G" type calculations considered material with a peak temperature above 1000^{o}C as a corrosion feature and applied a temperature based material strength reduction to the remaining ligament.

Bead on pipe welds were deposited over the range of pipe thicknesses evaluated (i.e. 3.2, 6.4, 7.9, 11, 16.1, and 19mm) for the X52 and X80 materials. The 3.2mm wall thickness was achieved by slotting a 6.4mm wall X52 pipe, using a 20mm wide square bottom machining mill cutter, as shown in **Figure 4.7**, for simulating welds on thin walled pipe. The 3.2mm thicknesses were verified in each region using an ultrasonic thickness gauge. Each intended weld zone was instrumented with K-type thermocouples along the centreline axis of the welds, on both the back surface of the pipe and in the weld. This method is effective in acquiring the actual thermal history at both the back surface and at the weld fusion line (as shown in **Figure 4.8**), compared to thermocouple plunging. The thermocouples were attached to a high speed temperature acquisition system at a collection frequency of 25Hz.

Figure 4.7: Slotted Pipe to Achieve 3.2mm Thickness

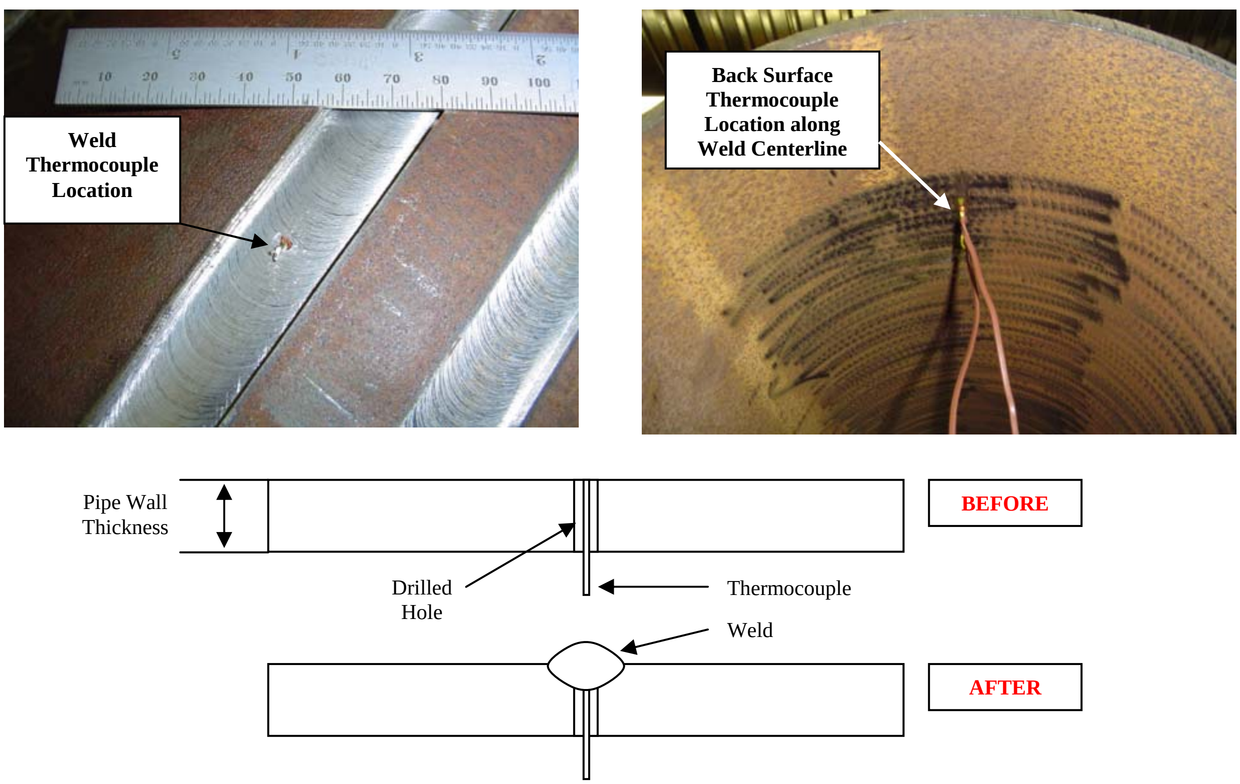

Figure 4.8: Thermocouple Set-up

All welding was initially performed in still air (no flow conditions) to simulate the worst case scenario for burn-through to occur, however the same welds were repeated at a later stage with water backing to determine if a higher heat sink capacity could extend the safety envelope for in-service welding with the alternative welding processes.

4.5.1 Weld Burn-through – Static Air (No Flow)

After fine tuning the welding procedures developed in Task 2, a series of bead on pipe welds were deposited using mechanized travel to achieve the predetermined heat input level, examples of welding with both wire fed and SMAW processes are shown in **Figures 4.9** and **4.10**, respectively.

Figure 4.9: Set-up for Controlled Welding with Semi-Automatic Processes

Figure 4.10: Set-up for Controlled Welding with SMAW Process

All welding data for bead on pipe welds for static air (no flow) conditions is shown in **Appendix C**. The thermocouple data was acquired at a scanning frequency of 25Hz. The thermocouple ID number is the same as the weld number. An example of the typical thermal history plots showing both weld and back surface temperature histories are shown in **Figure 4.11** and **4.12**, for welds A62 and A63, respectively. Note the increase in peak back surface temperature and as well as the longer weld cooling rate with increasing the heat input from 0.53kJ/mm to 1.29kJ/mm.

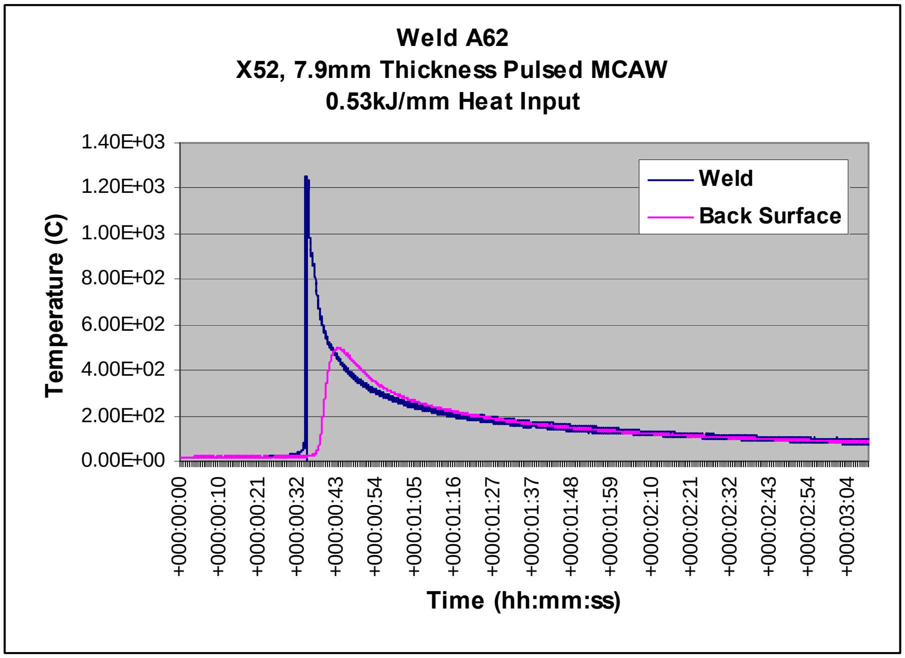

Figure 4.11: Thermal History of Weld and Back Surface

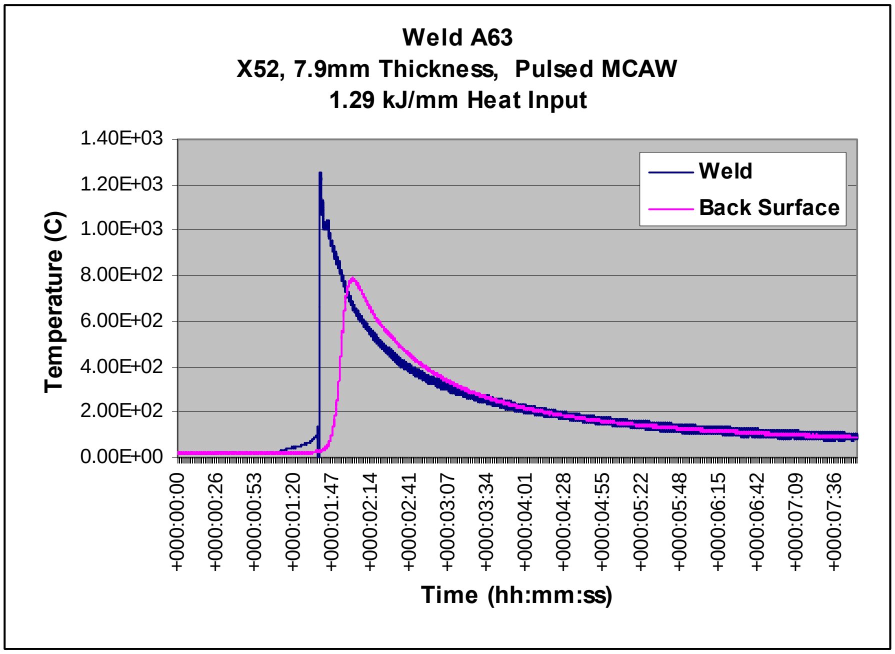

Figure 4.12: Thermal History of Weld and Back Surface

Each of peak back surface temperature measurements was plotted vs. welding process for heat inputs of .53 and 1.29 kJ/mm, and are shown in **Figure 4.13**. This data shows that for a given heat input, the PMCAW provides the greatest peak back surface temperature, followed by the GSFCAW, PGMAW, and SMAW process. The self shielded FCAW process demonstrates the highest peak back surface temperatures at the 1.29 kJ/mm level.

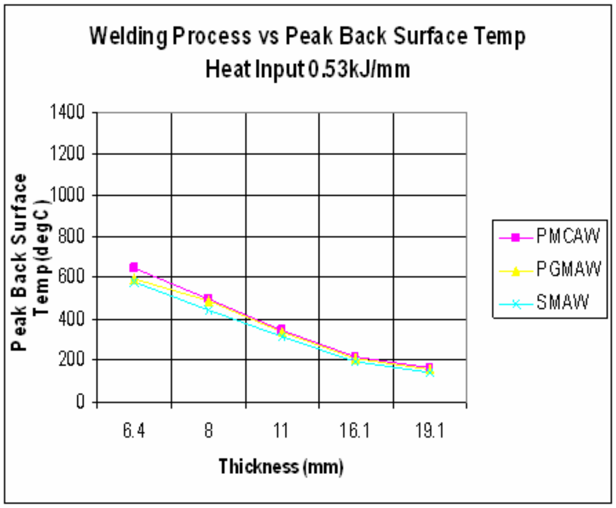

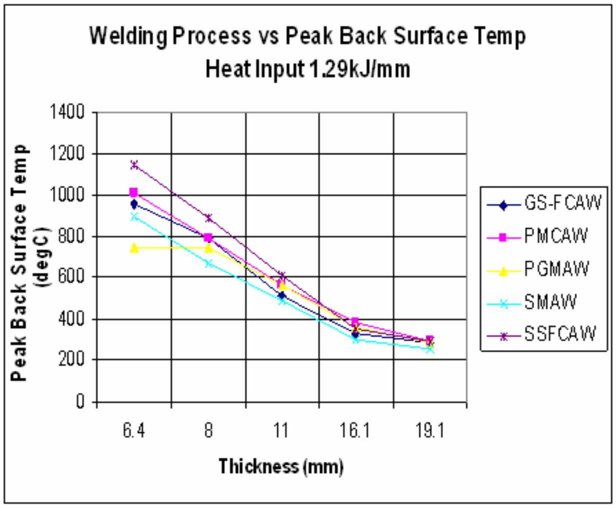

Figure 4.13: Peak Back Surface Temperatures vs. Heat Input and Process

Welds were cross-sectioned to measure the depths of penetration and to determine the remaining base metal ligament thickness between the root of the weld and the back surface of the pipe. Sample weld cross-sections for welds A62 and A63 using the P-MCAW process on 7.9mm X52 pipe at heat inputs of 0.53 kJ/mm and 1.29 kJ/mm, are shown in **Figures 4.14** and **4.15**, respectively. All remaining bead on pipe weld cross-sections for static air conditions are shown in **Appendix D**.

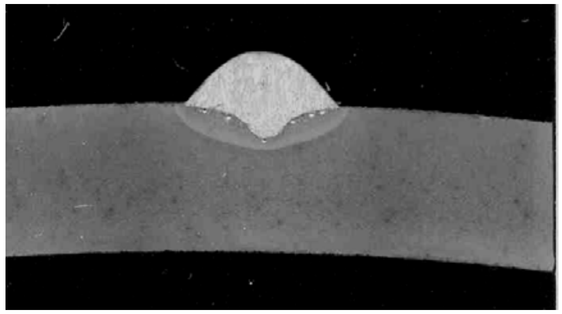

Figure 4.14: Weld A62 Macro, 0.53 kJ/mm, 2.5X Mag

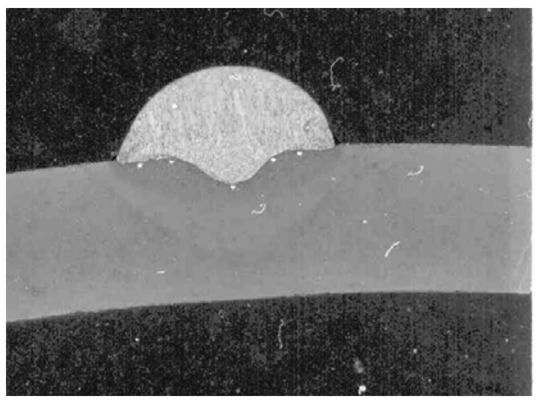

Figure 4.15: Weld A63 Macro, 1.29 kJ/mm, 2.5X Mag.

Since the weld temperature history of the weld fusion line and back surface were obtained, the thermal transients between these two regions could therefore be interpolated. This thermal history, along with the weld travel speed, was used to estimate a flaw size based on a zero strength at 1000ºC temperature limit correlation, as calculated in **Figure 4.16**.

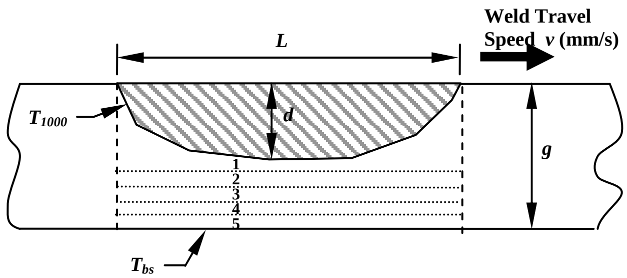

Welding Conditions

T_{1000} = Isotherm (1000^oC)
T_{bs} = Back surface temperature (^oC)
T_{1-5} = Interpolated temperature in layers 1 through 5
$\Delta T_{1000-1000}$ = Time between 1000^oC for heating and cooling cycles
d = "flaw" depth = depth to 1000^oC isotherm
g = plate thickness (mm)
L = "flaw" length = $v \times \Delta T_{1000-1000}$
v = weld travel speed (mm/s)

Calculations

P_{int} = Burst Pressure (MPa) $= \dfrac{2 \times \sigma_f \times g}{D_m}$

σ_f = hoop stress @ burst $= \bar{\sigma}_{flow}\left[\dfrac{1 - A/A_o}{1 - \left(A/A_o\right)\left(M_T\right)^{-1}}\right]$

D_m = mean pipe diameter (mm)
A = area of "flaw" $= L \times d$
A_o = area of plate $= L \times g$

$\bar{\sigma}_{flow}$ = average flow stress for remaining ligament $= \dfrac{\sigma^1_{flow} + \sigma^2_{flow} + \sigma^3_{flow} + \sigma^4_{flow} + \sigma^5_{flow}}{5}$

M_T = Folias Factor $= \left[1 + 0.6275\dfrac{L^2}{Dg} - 0.003375\dfrac{L_4}{D^2 g^2}\right]^{1/2}$ for $\dfrac{L^2}{Dg} \leq 50$

$= 0.032\dfrac{L^2}{Dg} + 3.3$ for $\dfrac{L^2}{Dg} > 50$

σ^i_{flow} = flow stress at layer i = $\sigma^i_{YS} + C^i_f$

σ^i_{YS} = Yield Stress at layer i = $\sigma_{YS}\left(1.38x10^{-9}\left(T_i^3\right) - 2.51x10^{-6}\left(T_i^2\right) + 1.85x10^{-4}\left(T\right) + 1.0\right)$
σ_{YS} = Room Temperature Yield Stress (MPa)
Ti = Temperature at layer i
C^i_f = flow stress correction = $68.95\left(1.38x10^{-9}\left(T_i^3\right) - 2.51x10^{-6}\left(T_i^2\right) + 1.85x10^{-4}\left(T\right) + 1.0\right)$

Figure 4.16: Methodology and Calculations for Determining Burn-through

The results of the burn-through calculations are presented in **Tables 4.8** and **4.9** where the information can be plotted as Burst Pressure over Maximum Operating Pressure (MOP = 72% pipe yield pressure). Note that the values in red are for welds where the back surface temperature (ID of pipe) during welding reached at least 1000°C and that the effective flow stresses to cause a burst event is essentially any pressure over 0 Mpa. This data can be used to estimate the susceptibility to burn-through with each welding process over a range of heat inputs and material thicknesses, at a given percentage of MOP, as shown in **Figures 4.17** and **4.18**, where any value below each curve for a given welding process is considered a safe region. In the examples shown, these curves illustrate that as heat input increases from 0.53 to 1.29 kJ/mm, the arc efficiency of the process has a greater influence on heat transfer, depth of penetration, and the susceptibility to burn-through. For example, the FCAW and P-GMAW processes have theoretically higher arc efficiencies (i.e., transfer heat from the arc to the base metal more efficiently) when compared to the SMAW process, and are therefore more susceptible to burn-through at a given heat input. As heat input increases from 0.53 kJ/mm to 1.29 kJ/mm, the arc efficiency characteristics become more apparent as demonstrated by the increasing separation of their curves with increasing heat input. This is consistent with what was illustrated previously in the peak back surface temperature plot in Figure 4.13. **Figure 4.19** illustrates the results of both the combined 0.53 and 1.29 kJ/mm heat inputs.

Because these burst pressure values are presented in non-dimensional form, ratio of burst pressure to maximum operating pressure (MOP), the results may be used to consider a range of pipe material grades and geometries.

Table 4.8: Burst Pressure Calculations

Test ID	Surface Temp	Temperature						Yield Stress						Flow Stress Correction						Flow Stress						Effective	Flaw Length	Effective Flaw	L^2/(Dt)	Folias Factor	Flaw Area	Plate Area	Hoop Stress	Internal Pressure
		0	1	2	3	4	5	0	1	2	3	4	5	0	1	2	3	4	5	0	1	2	3	4	5	Flow Stress		Depth		Mt	A	Ao	@ Burst	@ Burst
	oC	oC	oC	oC	oC	oC	oC	(MPa)	(MPa)	(MPa)	(MPa)	(MPa)	(MPa)	(MPa)	(MPa)	(MPa)	(MPa)	(MPa)	(MPa)	(MPa)	(MPa)	(MPa)	(MPa)	(MPa)	(MPa)	(MPa)	(mm)	(mm)			(mm2)	(mm2)	(MPa)	(MPa)
A1	938.5	1000	993.85	981.55	969.25	956.95	944.65	0.00	25.53	29.42	33.50	37.79	42.26	0.0	4.09	4.71	5.37	6.06	6.77	0.00	29.62	34.13	38.87	43.84	49.04	39.10	16.51	2.94	0.26	1.08	48.49	52.83	21.48	0.43
A2	1227.1	1000	1022.71	1068.13	1113.55	1158.97	1204.39	0.00	17.24	6.73	-0.38	-3.76	-3.09	0.0	2.76	1.08	-0.06	-0.60	-0.49	0.00	20.00	7.81	-0.44	-4.37	-3.58	0.00	17.92	4.86	0.31	1.09	87.02	57.34	0.00	0.00
A3	1255.3	1000	1025.53	1076.59	1127.65	1178.71	1229.77	0.00	16.50	5.14	-1.84	-3.99	-0.82	0.0	2.64	0.82	-0.30	-0.64	-0.13	0.00	19.14	5.97	-2.14	-4.63	-0.95	0.00	20.00	4.29	0.39	1.11	85.69	63.99	0.00	0.00
A4	486.6	1000	948.66	845.98	743.3	640.62	537.94	0.00	38.23	78.92	128.05	182.01	237.17	0.0	6.54	13.49	21.89	31.11	40.54	0.00	44.77	92.42	149.94	213.12	277.72	155.59	5.03	3.82	0.01	1.00	19.18	32.17	155.04	3.96
A5	587.1	1000	958.71	876.13	793.55	710.97	628.39	0.00	34.84	65.94	103.18	144.69	188.59	0.0	5.96	11.27	17.64	24.73	32.24	0.00	40.80	77.21	120.82	169.43	220.82	125.82	3.56	4.06	0.00	1.00	14.47	22.80	125.55	3.20
A6	655.7	1000	965.57	896.71	827.85	758.99	690.13	0.00	32.59	57.54	87.09	120.15	155.62	0.0	5.57	9.84	14.89	20.54	26.60	0.00	38.16	67.38	101.98	140.68	182.22	106.08	2.27	4.41	0.00	1.00	10.02	14.55	105.97	2.70
A7	908	1000	990.8	972.4	954	935.6	917.2	0.00	24.82	30.41	36.42	42.82	49.59	0.0	4.24	5.20	6.23	7.32	8.48	0.00	29.06	35.61	42.64	50.14	58.06	43.10	10.33	5.66	0.03	1.01	58.45	66.11	40.01	1.02
A8	579.6	1000	957.96	873.88	789.8	705.72	621.64	0.00	35.09	66.88	104.99	147.43	192.22	0.0	6.00	11.43	17.95	25.20	32.86	0.00	41.09	78.31	122.94	172.64	225.08	128.01	5.20	4.25	0.01	1.00	22.09	33.27	127.36	3.25
A9	898.1	1000	989.81	969.43	949.05	928.67	908.29	0.00	25.11	31.35	38.10	45.32	52.99	0.0	4.29	5.36	6.51	7.75	9.06	0.00	29.40	36.71	44.61	53.07	62.05	45.17	9.76	5.64	0.03	1.01	55.10	62.49	42.31	1.08
A10	446.7	1000	944.67	834.01	723.35	612.69	502.03	0.00	42.25	89.91	147.49	210.18	273.16	0.0	6.77	14.41	23.64	33.68	43.77	0.00	49.03	104.31	171.13	243.87	316.93	177.05	0.37	4.44	0.00	1.00	1.65	2.93	177.05	8.85
A11	671.5	1000	967.15	901.45	835.75	770.05	704.35	0.00	34.22	59.38	89.07	122.29	158.03	0.0	5.48	9.52	14.27	19.60	25.32	0.00	39.71	68.89	103.34	141.88	183.35	107.43	3.91	5.34	0.01	1.00	20.89	30.88	107.02	5.35
A14	315	1000	931.5	794.5	657.5	520.5	383.5	0.00	56.18	130.30	219.38	312.53	398.87	0.0	7.57	17.56	29.57	42.12	53.76	0.00	63.75	147.86	248.94	354.65	452.62	253.57	2.31	5.57	0.00	1.00	12.87	25.43	253.52	6.18
A15	486.1	1000	948.61	845.83	743.05	640.27	537.49	0.00	48.52	100.19	162.58	231.10	301.13	0.0	6.54	13.50	21.91	31.14	40.58	0.00	55.06	113.69	184.49	262.24	341.71	191.44	11.79	6.25	0.01	1.00	73.71	129.71	190.36	4.64
A16	195.7	1000	919.57	758.71	597.85	436.99	276.13	0.00	71.75	177.24	302.14	425.96	528.23	0.0	8.32	20.56	35.05	49.42	61.28	0.00	80.08	197.80	337.19	475.38	589.51	335.99	3.91	7.03	0.00	1.00	27.49	62.98	335.93	8.98
A17	304	1000	930.4	791.2	652	512.8	373.6	0.00	65.86	153.71	259.20	369.04	469.98	0.0	7.64	17.83	30.07	42.81	54.52	0.00	73.50	171.54	289.27	411.85	524.50	294.13	3.51	7.73	0.00	1.00	27.09	56.43	294.08	7.87
A18	139.4	1000	913.94	741.82	569.7	397.58	225.46	0.00	77.32	195.96	335.00	468.54	570.66	0.0	8.69	22.02	37.64	52.64	64.12	0.00	86.01	217.98	372.65	521.19	634.78	366.52	6.40	7.89	0.00	1.00	50.48	121.62	366.35	13.96
A19	257.8	1000	925.78	777.34	628.9	480.46	332.02	0.00	70.57	168.96	286.49	406.56	512.55	0.0	7.93	18.98	32.19	45.68	57.59	0.00	78.50	187.94	318.68	452.25	570.14	321.50	4.88	8.72	0.00	1.00	42.54	92.66	321.40	12.25
A20	589.4	1000	958.94	876.82	794.7	712.58	630.46	0.00	37.08	70.03	109.47	153.45	199.97	0.0	5.94	11.22	17.54	24.59	32.05	0.00	43.03	81.25	127.02	178.04	232.02	132.27	10.93	2.16	0.12	1.04	23.65	34.99	123.44	2.46
A21	915	1000	991.5	974.5	957.5	940.5	923.5	0.00	26.26	31.73	37.59	43.81	50.38	0.0	4.21	5.09	6.02	7.02	8.07	0.00	30.46	36.82	43.62	50.83	58.45	44.04	19.05	2.98	0.35	1.10	56.84	60.96	19.14	0.38
A22	1232.2	1000	1023.22	1069.66	1116.1	1162.54	1208.98	0.00	17.11	6.44	-0.67	-3.86	-2.78	0.0	2.74	1.03	-0.11	-0.62	-0.45	0.00	19.85	7.47	-0.78	-4.48	-3.22	0.00	22.82	4.04	0.50	1.15	92.21	73.02	0.00	0.00
A23	601.3	1000	960.13	880.39	800.65	720.91	641.17	0.00	34.37	64.17	99.79	139.53	181.71	0.0	5.88	10.97	17.06	23.85	31.06	0.00	40.25	75.14	116.85	163.39	212.78	121.68	6.00	4.46	0.01	1.00	26.76	38.39	120.72	3.08
A24	864.7	1000	986.47	959.41	932.35	905.29	878.23	0.00	26.10	34.61	43.99	54.16	65.06	0.0	4.46	5.92	7.52	9.26	11.12	0.00	30.56	40.53	51.50	63.42	76.19	52.44	13.76	5.58	0.06	1.02	76.73	88.07	46.81	1.19
A25	694.1	1000	969.41	908.23	847.05	785.87	724.69	0.00	33.45	56.55	83.68	114.02	146.75	0.0	5.36	9.06	13.41	18.27	23.52	0.00	38.81	65.62	97.09	132.29	170.27	100.82	8.99	2.20	0.08	1.02	19.76	28.77	95.86	1.91
A26	997.2	1000	999.72	999.16	998.6	998.04	997.48	0.00	23.75	23.92	24.08	24.25	24.42	0.0	3.81	3.83	3.86	3.89	3.91	0.00	27.55	27.75	27.94	28.14	28.34	27.94	11.34	3.19	0.12	1.04	36.15	36.29	2.60	0.05
A27	1136.4	1000	1013.64	1040.92	1068.2	1095.48	1122.76	0.00	19.72	12.64	6.72	2.02	-1.38	0.0	3.16	2.03	1.08	0.32	-0.22	0.00	22.88	14.67	7.80	2.35	-1.60	0.00	19.14	3.95	0.35	1.11	75.60	61.24	0.00	0.00
A28	597.3	1000	959.73	879.19	798.65	718.11	637.57	0.00	34.50	64.67	100.74	140.98	183.65	0.0	5.90	11.05	17.22	24.10	31.39	0.00	40.40	75.72	117.96	165.08	215.04	122.84	7.59	3.87	0.02	1.01	29.35	48.58	121.82	3.11
A29	747.3	1000	974.73	924.19	873.65	823.11	772.57	0.00	29.68	46.97	66.98	89.26	113.40	0.0	5.07	8.03	11.45	15.26	19.38	0.00	34.75	55.00	78.43	104.52	132.78	81.10	3.47	4.40	0.00	1.00	15.28	22.22	80.89	2.06
A30	486.1	1000	948.61	845.83	743.05	640.27	537.49	0.00	40.80	84.26	136.73	194.34	253.24	0.0	6.54	13.50	21.91	31.14	40.58	0.00	47.34	97.76	158.64	225.49	293.82	164.61	0.83	4.58	0.00	1.00	3.78	6.52	164.59	8.23
A31	746.7	1000	974.67	924.01	873.35	822.69	772.03	0.00	31.68	50.18	71.58	95.42	121.24	0.0	5.08	8.04	11.47	15.29	19.43	0.00	36.75	58.22	83.05	110.71	140.67	85.88	2.57	5.56	0.00	1.00	14.27	20.27	85.72	4.28
A32	341.5	1000	934.15	802.45	670.75	539.05	407.35	0.00	54.97	125.48	210.41	300.08	384.80	0.0	7.41	16.91	28.36	40.44	51.86	0.00	62.38	142.39	238.77	340.52	436.66	244.14	1.90	5.62	0.00	1.00	10.70	20.95	244.12	5.95
A33	564.6	1000	956.46	869.38	782.3	695.22	608.14	0.00	45.14	87.24	137.78	193.98	253.04	0.0	6.08	11.76	18.57	26.14	34.10	0.00	51.23	98.99	156.35	220.13	287.14	162.77	1.31	6.43	0.00	1.00	8.41	14.39	162.76	3.97
A34	214.5	1000	921.45	764.35	607.25	450.15	293.05	0.00	70.72	173.09	294.67	416.37	519.10	0.0	8.20	20.08	34.18	48.30	60.22	0.00	78.92	193.17	328.86	464.67	579.32	328.99	4.64	7.27	0.00	1.00	33.70	74.63	328.89	8.80
A35	359.6	1000	935.96	807.88	679.8	551.72	423.64	0.00	62.90	141.99	237.36	338.66	435.55	0.0	7.30	16.47	27.54	39.29	50.53	0.00	70.20	158.46	264.89	377.94	486.08	271.52	4.50	7.76	0.00	1.00	34.87	72.38	271.43	7.26
A36	158.4	1000	915.84	747.52	579.2	410.88	242.56	0.00	76.22	191.56	327.24	459.01	562.65	0.0	8.56	21.52	36.77	51.57	63.22	0.00	84.79	213.09	364.00	510.58	625.87	359.67	2.44	7.88	0.00	1.00	19.26	46.45	359.64	13.71
A37	286.8	1000	928.68	786.04	643.4	500.76	358.12	0.00	68.95	162.50	274.63	390.60	495.67	0.0	7.75	18.26	30.86	43.89	55.69	0.00	76.70	180.76	305.49	434.49	551.36	309.76	5.66	8.63	0.00	1.00	48.88	107.62	309.62	11.80
A38	1049.1	1000	1004.91	1014.73	1024.55	1034.37	1044.19	0.00	20.82	18.20	15.71	13.35	11.13	0.0	3.56	3.11	2.68	2.28	1.90	0.00	24.38	21.31	18.39	15.63	13.03	0.00	35.59	6.89	0.39	1.12	245.23	227.79	0.00	0.00
A39	1143.3	1000	1014.33	1042.99	1071.65	1100.31	1128.97	0.00	18.30	11.39	5.68	1.24	-1.84	0.0	3.13	1.95	0.97	0.21	-0.31	0.00	21.43	13.34	6.65	1.45	-2.15	0.00	35.06	7.85	0.38	1.11	275.06	224.36	0.00	0.00
A40	808	1000	980.8	942.4	904	865.6	827.2	0.00	29.66	43.10	58.31	75.08	93.21	0.0	4.75	6.91	9.34	12.03	14.94	0.00	34.41	50.01	67.65	87.11	108.15	69.47	5.33	6.64	0.01	1.00	35.40	42.14	68.22	3.41
A41	891.8	1000	989.18	967.54	945.9	924.26	902.62	0.00	26.98	34.09	41.80	50.08	58.88	0.0	4.32	5.46	6.70	8.03	9.44	0.00	31.30	39.55	48.50	58.10	68.32	49.16	3.98	7.21	0.01	1.00	28.69	31.45	48.19	2.41
A44	609.2	1000	960.92	882.76	804.6	726.44	648.28	0.00	43.27	80.15	124.19	173.36	225.64	0.0	5.83	10.80	16.74	23.36	30.41	0.00	49.10	90.95	140.93	196.72	256.05	146.75	5.82	8.06	0.00	1.00	46.92	64.03	146.33	3.56
A45	784.7	1000	978.47	935.41	892.35	849.29	806.23	0.00	36.17	54.39	75.20	98.25	123.21	0.0	4.88	7.33	10.13	13.24	16.61	0.00	41.05	61.72	85.33	111.49	139.82	87.88	20.60	8.84	0.04	1.01	182.08	226.60	83.45	2.03
A46	357.3	1000	935.73	807.19	678.65	550.11	421.57	0.00	63.02	142.47	238.25	339.92	437.03	0.0	7.31	16.53	27.64	39.43	50.70	0.00	70.33	159.00	265.89	379.36	487.73	272.46	22.40	9.35	0.03	1.01	209.44	360.62	269.51	7.21
A47	498.5	1000	949.85	849.55	749.25	648.95	548.65	0.00	55.74	113.97	184.25	261.60	341.07	0.0	6.47	13.22	21.37	30.35	39.57	0.00	62.20	127.19	205.62	291.95	380.64	213.52	27.44	10.36	0.04	1.01	284.29	441.74	209.06	5.59
A48	297.3	1000	929.73	789.19	648.65	508.11	367.57	0.00	68.37	160.18	270.35	384.77	489.34	0.0	7.68	18.00	30.38	43.23	54.98	0.00	76.05	178.18	300.72	428.00	544.32	305.45	11.83	10.53	0.01	1.00	124.53	224.73	304.60	11.61
A49	407.4	1000	940.74	822.22	703.7	585.18	466.66	0.00	62.36	136.43	225.91	322.34	417.27	0.0	7.01	15.33	25.38	36.22	46.88	0.00	69.37	151.76	251.29	358.56	464.15	259.02	7.01	11.02	0.00	1.00	77.28	133.28	258.74	9.86
A50	799.1	1000	979.91	939.73	899.55	859.37	819.19	0.00	28.08	41.35	56.41	73.06	91.08	0.0	4.80	7.07	9.64	12.49	15.57	0.00	32.88	48.41	66.06	85.55	106.64	67.91	5.77	4.86	0.01	1.00	28.04	36.96	67.23	1.72
A51	957.8	1000	995.78	987.34	978.9	970.46	962.02	0.00	23.38	25.84	28.39	31.03	33.75	0.0	4.00	4.42	4.85	5.30	5.77	0.00	27.38	30.25	33.24	36.33	39.52	33.34	26.15	5.96	0.21	1.06	155.88	167.33	18.35	0.47
A52	716.5	1000	971.65	914.95	858.25	801.55	744.85	0.00	32.69	53.80	78.45	105.98	135.75	0.0	5.24	8.62	12.57	16.98	21.76	0.00	37.93	62.43	91.02	122.97	157.51	94.37	6.89	5.53	0.02	1.01	38.10	55.13	93.18	4.72
A53	790.1	1000	979.01	937.03	895.05	853.07	811.09	0.00	30.24	45.13	62.08	80.86	101.18	0.0	4.85	7.23	9.95	12.96	16.21	0.00	35.09	52.36	72.03	93.81	117.39	74.14	5.55	5.89	0.01	1.00	32.72	44.43	73.38	3.72
A54	514.7	1000	951.47	854.41	757.35	660.29	563.23	0.00	47.28	95.40	153.43	217.49	283.70	0.0	6.37	12.86	20.68	29.31	38.23	0.00	53.65	108.26	174.11	246.80	321.93	180.95	35.95	6.35	0.13	1.04	228.29	395.44	172.02	4.19
A55	748.1	1000	974.81	924.43	874.05	823.67	773.29	0.00	37.61	59.47	84.74	112.89	143.38	0.0	5.07	8.01	11.42	15.21	19.32	0.00	42.68	67.48	96.16	128.11	162.71	99.43	31.65	7.81	0.10	1.03	247.19	348.13	92.66	2.26
A56	333.8	1000	933.38	800.14	666.9	533.66	400.42	0.00	64.27	147.40	247.46	352.83	451.84	0.0	7.46	17.10	28.71	40.93	52.42	0.00	71.72	164.49	276.17	393.76	504.26	282.08	24.49	7.63	0.03	1.01	186.99	394.35	279.70	7.48
A57	453.9	1000	945.39	836.17	726.95	617.73	508.51	0.00	58.00	122.76	201.01	286.35	372.35	0.0	6.73	14.24	23.32	33.22	43.20	0.00	64.73	137.00	224.33	319.57	415.55	232.24	25.60	8.29	0.03	1.01	212.26	412.21	229.72	6.14
A58	284.1	1000	928.41	785.23	642.05	498.87	355.69	0.00	69.10	163.10	275.74	392.10	497.27	0.0	7.76	18.33	30.98	44.06	55.87	0.00	76.86	181.42	306.72	436.16	553.15	310.86	5.03	8.83	0.00	1.00	44.40	96.06	310.75	11.91
A59	379.8	1000	937.98	813.94	689.9	565.86	441.82	0.00	63.85	142.28	236.94	338.14	436.18	0.0	7.17	15.99	26.62	37.99	49.01	0.00	71.02	158.26	263.56	376.13	485.19	270.83	27.26	9.17	0.04	1.01	250.01	520.72	267.91	10.27
A60	649.2	1000	964.92	894.76	824.6	754.44	684.28	0.00	32.80	58.32	88.58	122.43	158.71	0.0	5.61	9.97	15.14	20.93	27.13	0.00	38.41	68.29	103.72	143.35	185.84	107.92	6.60	4.46	0.01	1.00	29.48	42.27	106.89	2.73
A61	1008.1	1000	1000.81	1002.43	1004.05	1005.67	1007.29	0.00	21.96	21.51	21.06	20.62	20.18	0.0	3.75	3.68	3.60	3.52	3.45	0.00	25.71	25.18	24.66	24.14	23.63	0.00	17.16	6.48	0.09	1.03	111.10	109.81	0.00	0.00
A62	499.4	1000	949.94	849.82	749.7	649.58	549.46	0.00	40.32	82.38	133.14	189.01	246.44	0.0	6.46	13.20	21.34	30.29	39.49	0.00	46.78	95.58	154.47	219.31	285.93	160.41	6.16	4.87	0.01	1.00	29.99	49.31	159.28	8.07
A63	789.8	1000	978.98	936.94	894.9	852.86	810.82	0.00	30.25	45.16	62.15	80.95	101.31	0.0	4.85	7.24	9.96	12.97	16.24	0.00	35.10	52.40	72.11	93.93	117.55	74.22	14.58	6.12	0.08	1.03	89.17	116.64	68.69	3.48
A64	342.6	1000	934.26	802.78	671.3	539.82	408.34	0.00	54.92	125.28	210.04	299.56	384.21	0.0	7.40	16.88	28.31	40.37	51.78	0.00	62.32	142.17	238.35	339.93	435.99	243.75	9.03	5.68	0.01	1.00	51.30	99.28	243.09	5.92
A65	561.6	1000	956.16	868.48	780.8	693.12	605.44	0.00	45.27	87.72	138.71	195.39	254.89	0.0	6.10	11.82	18.69	26.33	34.35	0.00	51.37	99.54	157.41	221.72	289.24	163.86	5.51	6.61	0.00	1.00	36.44	60.63	163.62	3.99
A66	216.1	1000	921.61	764.83	608.05	451.27	294.49	0.00	70.63	172.74	294.04	415.54	518.30	0.0	8.19	20.04	34.11	48.21	60.13	0.00	78.82	192.78	328.15	463.75	578.43	328.39	6.60	7.43	0.00	1.00	49.05	106.32	328.19	8.78
A67	380.5	1000	938.05	814.15	690.25	566.35	442.45	0.00	61.80	137.66	229.21	327.11	422.00	0.0	7.17	15.97	26.59	37.95	48.96	0.00	68.97	153.63	255.80	365.06	470.96	262.88	15.29	8.27	0.01	1.00	126.49	246.18	261.86	7.00
A68	164.7	1000	916.47	749.41	582.35	415.29	248.23	0.00	75.86	190.11	324.66	455.81	559.88	0.0	8.52	21.36	36.48	51.21	62.91	0.00	84.38	211.47	361.14	507.03	622.79	357.36	5.72	8.17	0.00	1.00	46.73	109.32	357.22	13.69
A69	295	1000	929.5	788.5	647.5	506.5	365.5	0.00	68.49	160.69	271.29	386.05	490.73	0.0	7.70	18.05	30.48	43.38	55.14	0.00	76.19	178.74	301.77	429.42	545.87	306.40	12.45	8.94	0.01	1.00	111.31	237.72	305.73	11.72

Table 4.9: Weld Data and Burst Pressure Results

Weld	Process	Dia (mm)	Electrode	Amps (A)	Volts (V)	TS ipm	HI kJ/mm	Weld Pentration Depth (mm)	Pipe Details	Thickness (mm)	Pipe Diameter (mm)	Yield Strength (initial)	Max. Back Surface Temp (degC)	Fusion Line Time 1000oC - 1000oC	Calculated Bursting Pressure	Burst P/ Yield Pressure	Burst P/ MOP
A1	SMAW	2.4	718MC	90	21	13.0	0.35	0.8	NPS 12 , X52	3.2	324	430.25	938.5	3	0.43	0.04993	0.0359
A2	SMAW	2.4	718MC	90	21	8.5	0.53	1.21	NPS 12 , X52	3.2	324	430.25	1227.1	4.98	0.00	0.00000	-
A3	SMAW	2.4	718MC	90	21	6.0	0.74	2.16	NPS 12 , X52	3.2	324	430.25	1255.3	7.83	0.00	0.00000	-
A4	SMAW	2.4	718MC	90	21	12.5	0.35	1.3	NPS 20, X52	6.4	508	403.36	486.6	0.95	3.96	0.38437	0.2767
A5	SMAW	2.4	718MC	90	21	8.5	0.53	1.23	NPS 20, X52	6.4	508	403.36	587.1	0.99	3.20	0.31126	0.2241
A6	SMAW	2.4	718MC	90	21	6.0	0.74	1.51	NPS 20, X52	6.4	508	403.36	655.7	0.89	2.70	0.26271	0.1892
A7	SMAW	2.4	718MC	90	21	3.5	1.29	1.63	NPS 20, X52	6.4	508	403.36	908	7.05	1.02	0.09918	0.0714
A8	SMAW	3.2	718MC	120	20.5	11.0	0.53	1.69	NPS 20, X52	6.4	508	403.36	579.6	1.12	3.25	0.31575	0.2273
A9	SMAW	3.2	718MC	120	20.5	4.5	1.29	1.93	NPS 20, X52	6.4	508	403.36	898.1	5.12	1.08	0.10489	0.0755
A10	SMAW	3.2	718MC	120	20.5	11.0	0.53	1.32	NPS 12, X52	7.9	324	430.25	446.7	0.08	8.85	0.41150	0.2963
A11	SMAW	3.2	718MC	120	20.5	4.5	1.29	1.45	NPS 12, X52	7.9	324	430.25	671.5	2.05	5.35	0.24873	0.1791
A14	SMAW	3.2	AtomArc 10018-M1	120	20	10.5	0.53	1.6	NPS36, X70	11	914	511.61	315	0.52	6.18	0.49554	0.3568
A15	SMAW	3.2	AtomArc 10018-M1	120	20	4.5	1.29	1.63	NPS36, X70	11	914	511.61	486.1	6.19	4.64	0.37208	0.2679
A16	SMAW	3.2	AtomArc 10018-M1	120	20	10.5	0.53	1.39	NPS 48, X80	16.1	1220	594.35	195.7	0.88	8.98	0.56520	0.4069
A17	SMAW	3.2	AtomArc 10018-M1	120	20	4.5	1.29	1.715	NPS 48, X80	16.1	1220	594.35	304	1.84	7.87	0.49479	0.3562
A18	SMAW	3.2	AtomArc 10018-M1	120	20	10.5	0.53	1.43	NPS 40, X70	19	1016	613.66	139.4	1.44	13.96	0.59699	0.4298
A19	SMAW	3.2	AtomArc 10018-M1	120	20	4.5	1.29	1.8	NPS 40, X70	19	1016	613.66	257.8	2.56	12.25	0.52374	0.3771
A20	GMAW - RMD	1.2	K-NOVA	130	17	27.5	0.19	0.9	NPS 12 , X52	3.2	324	430.25	589.4	0.94	2.46	0.28690	0.2066
A21	GMAW - RMD	1.2	K-NOVA	130	17	15.0	0.35	1.71	NPS 12 , X52	3.2	324	430.25	915	3	0.38	0.04450	0.0320
A22	GMAW - RMD	1.2	K-NOVA	130	17	10.0	0.53	2.23	NPS 12 , X52	3.2	324	430.25	1232.2	5.39	0.00	0.00000	-
A23	GMAW - RMD	1.2	K-NOVA	170	17	13.0	0.53	2.03	NPS 20, X52	6.4	508	403.36	601.3	1.09	3.08	0.29929	0.2155
A24	GMAW - RMD	1.2	K-NOVA	170	17	5.5	1.29	2.53	NPS 20, X52	6.4	508	403.36	864.7	5.91	1.19	0.11605	0.0836
A25	P-GMAW	0.9	K-NOVA	70	18	15.5	0.19	0.56	NPS 12 , X52	3.2	324	430.25	694.1	1.37	1.91	0.22280	0.1604
A26	P-GMAW	0.9	K-NOVA	70	18	8.5	0.35	1.04	NPS 12 , X52	3.2	324	430.25	997.2	3.15	0.05	0.00605	0.0044
A27	P-GMAW	0.9	K-NOVA	70	18	5.5	0.53	1.2	NPS 12 , X52	3.2	324	430.25	1136.4	8.22	0.00	0.00000	-
A28	P-GMAW	0.9	K-NOVA	70	18	5.5	0.53	0.72	NPS 20, X52	6.4	508	403.36	597.3	3.26	3.11	0.30201	0.2174
A29	P-GMAW	0.9	K-NOVA	70	18	2.5	1.29	0.45	NPS 20, X52	6.4	508	403.36	747.3	3.28	2.06	0.20054	0.1444
A30	P-GMAW	0.9	K-NOVA	90	19	7.5	0.53	1.34	NPS 12, X52	7.9	324	430.25	486.1	0.26	8.23	0.38255	0.2754
A31	P-GMAW	0.9	K-NOVA	90	19	3.0	1.29	0.95	NPS 12, X52	7.9	324	430.25	746.7	2.02	4.28	0.19923	0.1434
A32	P-GMAW	0.9	ER70XTi	90	19	7.5	0.53	1.53	NPS36, X70	11	914	511.61	341.5	0.6	5.95	0.47715	0.3435
A33	P-GMAW	0.9	ER70XTi	90	19	3.0	1.29	1.18	NPS36, X70	11	914	511.61	564.6	1.03	3.97	0.31813	0.2291
A34	P-GMAW	0.9	ER70XTi	90	19	7.5	0.53	1.65	NPS 48, X80	16.1	1220	594.35	214.5	1.46	8.80	0.55337	0.3984
A35	P-GMAW	0.9	ER70XTi	90	19	3.0	1.29	1.24	NPS 48, X80	16.1	1220	594.35	359.6	3.54	7.26	0.45669	0.3288
A36	P-GMAW	0.9	ER70XTi	90	19	7.5	0.53	1.27	NPS 40, X70	19	1016	613.66	158.4	0.77	13.71	0.58607	0.4220
A37	P-GMAW	0.9	ER70XTi	90	19	3.0	1.29	1.36	NPS 40, X70	19	1016	613.66	286.8	4.46	11.80	0.50456	0.3633
A38	SS-FCAW	2.0	FABSHIELD 71K6	200	18	8.0	1.06	1.9	NPS 20, X52	6.4	508	403.36	1049.1	10.48	0.00	0.00000	-
A39	SS-FCAW	2.0	FABSHIELD 71K6	200	18	6.5	1.29	2.8	NPS 20, X52	6.4	508	403.36	1143.3	12.74	0.00	0.00000	-
A40	SS-FCAW	2.0	FABSHIELD 71K6	280	19	12.0	1.06	3.35	NPS 12, X52	7.9	324	430.25	808	1.05	3.41	0.15856	0.1142
A41	SS-FCAW	2.0	FABSHIELD 71K6	280	19	9.5	1.29	4	NPS 12, X52	7.9	324	430.25	891.8	0.99	2.41	0.11200	0.0806
A44	SS-FCAW	2.0	FABSHIELD 81N2	310	19	11.0	1.29	4.3	NPS36, X70	11	914	511.61	609.2	1.25	3.56	0.28601	0.2059
A45	SS-FCAW	2.0	FABSHIELD 81N2	310	19	7.0	1.99	3.82	NPS36, X70	11	914	511.61	784.7	6.96	2.03	0.16312	0.1174
A46	SS-FCAW	2.0	FABSHIELD 81N2	310	19	11.0	1.29	4.1	NPS 48, X80	16.1	1220	594.35	357.3	4.81	7.21	0.45345	0.3265
A47	SS-FCAW	2.0	FABSHIELD 81N2	310	19	7.0	1.99	4.64	NPS 48, X80	16.1	1220	594.35	498.5	9.27	5.59	0.35175	0.2533
A48	SS-FCAW	2.0	FABSHIELD 81N2	310	19	11.0	1.29	4.5	NPS 40, X70	19	1016	613.66	297.3	2.54	11.61	0.49636	0.3574
A49	SS-FCAW	2.0	FABSHIELD 81N2	310	19	7.0	1.99	4.28	NPS 40, X70	19	1016	613.66	407.4	2.37	9.86	0.42164	0.3036
A50	GS-FCAW	1.2	DS II 71T-12	200	25.5	11.00	1.06	1.015	NPS 20, X52	6.4	508	403.36	799.1	1.24	1.72	0.16668	0.1200
A51	GS-FCAW	1.2	DS II 71T-12	175	24.5	8.00	1.29	0.775	NPS 20, X52	6.4	508	403.36	957.8	7.72	0.47	0.04549	0.0327
A52	GS-FCAW	1.2	DS II 71T-12	200	25.5	11.00	1.06	1.17	NPS 12, X52	8	324	430.25	716.5	1.48	4.72	0.21658	0.1559
A53	GS-FCAW	1.2	DS II 71T-12	175	24.5	8.00	1.29	0.87	NPS 12, X52	8	324	430.25	790.1	1.64	3.72	0.17054	0.1228
A54	GS-FCAW	1.2	DSII 80T1-Ni1	225	26.5	11.00	1.29	1.56	NPS36, X70	11	914	511.61	514.7	7.72	4.19	0.33623	0.2421
A55	GS-FCAW	1.2	DSII 80T1-Ni1	225	26.5	7.00	1.99	1.48	NPS36, X70	11	914	511.61	748.1	10.68	2.26	0.18111	0.1304
A56	GS-FCAW	1.2	DSII 80T1-Ni1	225	26.5	11.00	1.29	1.28	NPS 48, X80	16.1	1220	594.35	333.8	5.26	7.48	0.47060	0.3388
A57	GS-FCAW	1.2	DSII 80T1-Ni1	225	26.5	7.00	1.99	1.14	NPS 48, X80	16.1	1220	594.35	453.9	8.64	6.14	0.38651	0.2783
A58	GS-FCAW	1.2	DSII 80T1-Ni1	225	26.5	11.00	1.29	1.655	NPS 40, X70	19.1	1016	613.66	284.1	1.08	11.91	0.50640	0.3646
A59	GS-FCAW	1.2	DSII 80T1-Ni1	225	26.5	7.00	1.99	1.165	NPS 40, X70	19.1	1016	613.66	379.8	9.2	10.27	0.43659	0.3143
A60	MCAW	1.2	MC70	140	20.5	13.00	0.52	1.705	NPS 20, X52	6.4	508	403.36	649.2	1.2	2.73	0.26501	0.1908
A61	MCAW	1.2	MC70	140	20.5	5.25	1.29	1.835	NPS 20, X52	6.4	508	403.36	1008.1	7.72	0.00	0.00000	-
A62	MCAW	1.2	MC70	140	20.5	13.00	0.52	1.735	NPS 12, X52	8	324	430.25	499.4	1.12	8.07	0.37021	0.2666
A63	MCAW	1.2	MC70	140	20.5	5.25	1.29	1.635	NPS 12, X52	8	324	430.25	789.8	6.56	3.48	0.15966	0.1150
A64	MCAW	1.2	MC100	140	20.5	13.00	0.52	1.64	NPS36, X70	11	914	511.61	342.6	1.64	5.92	0.47515	0.3421
A65	MCAW	1.2	MC100	140	20.5	5.25	1.29	1.605	NPS36, X70	11	914	511.61	561.6	2.48	3.99	0.31982	0.2303
A66	MCAW	1.2	MC100	140	20.5	13.00	0.52	1.895	NPS 48, X80	16.1	1220	594.35	216.1	1.2	8.78	0.55218	0.3976
A67	MCAW	1.2	MC100	140	20.5	5.25	1.29	1.955	NPS 48, X80	16.1	1220	594.35	380.5	6.88	7.00	0.44058	0.3172
A68	MCAW	1.2	MC100	140	20.5	13.00	0.52	1.62	NPS 40, X70	19.1	1016	613.66	164.7	1.04	13.69	0.58212	0.4191
A69	MCAW	1.2	MC100	140	20.5	5.25	1.29	1.74	NPS 40, X70	19.1	1016	613.66	295	5.6	11.72	0.49821	0.3587

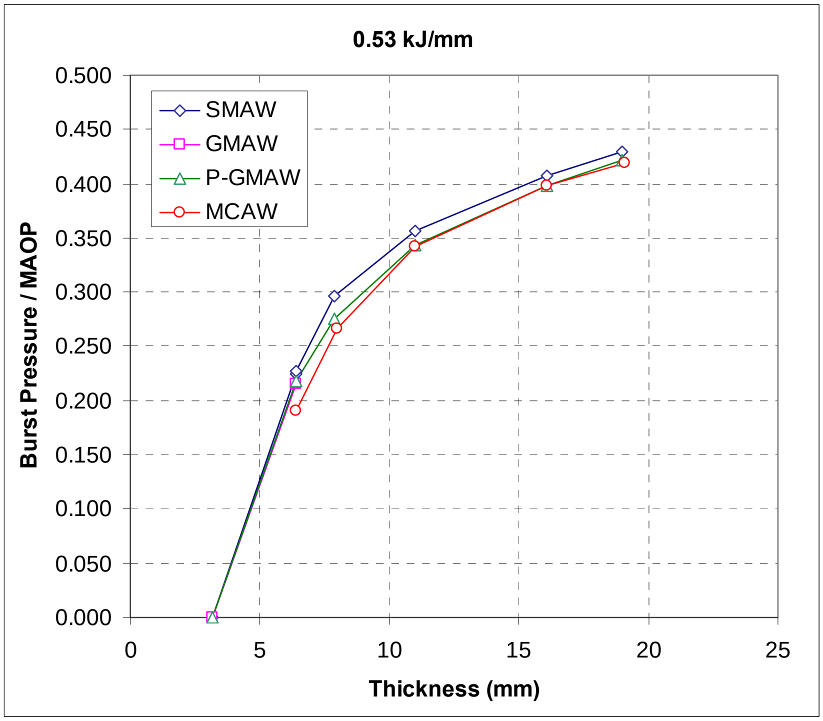

Figure 4.17: Burst Pressure/MOP (%) vs. Thickness and Weld Process – 0.53kJ/mm

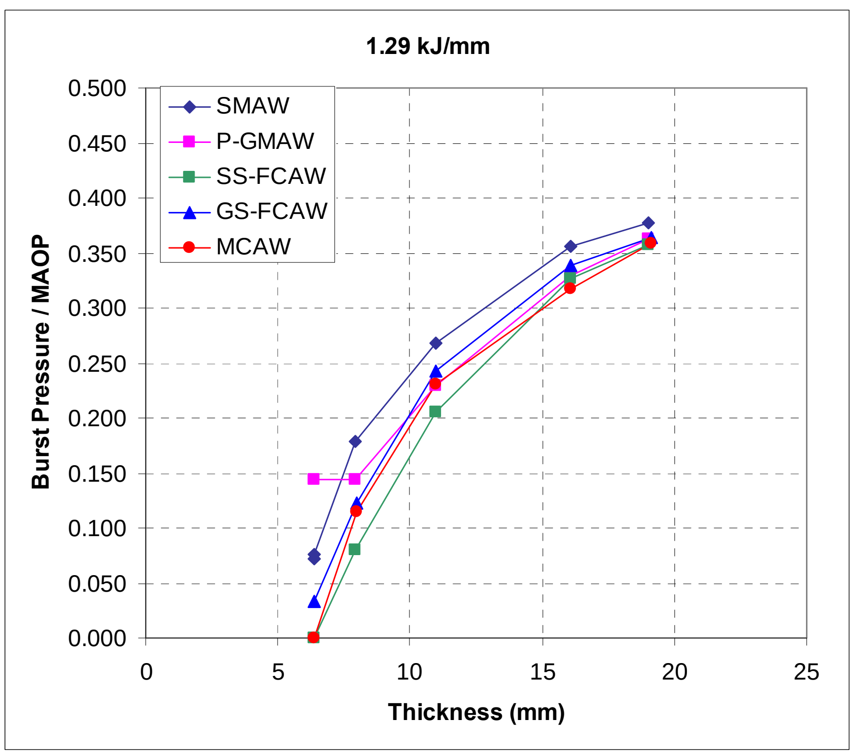

Figure 4.18: Burst Pressure/MOP (%) vs. Thickness and Weld Process - 1.29kJ/mm

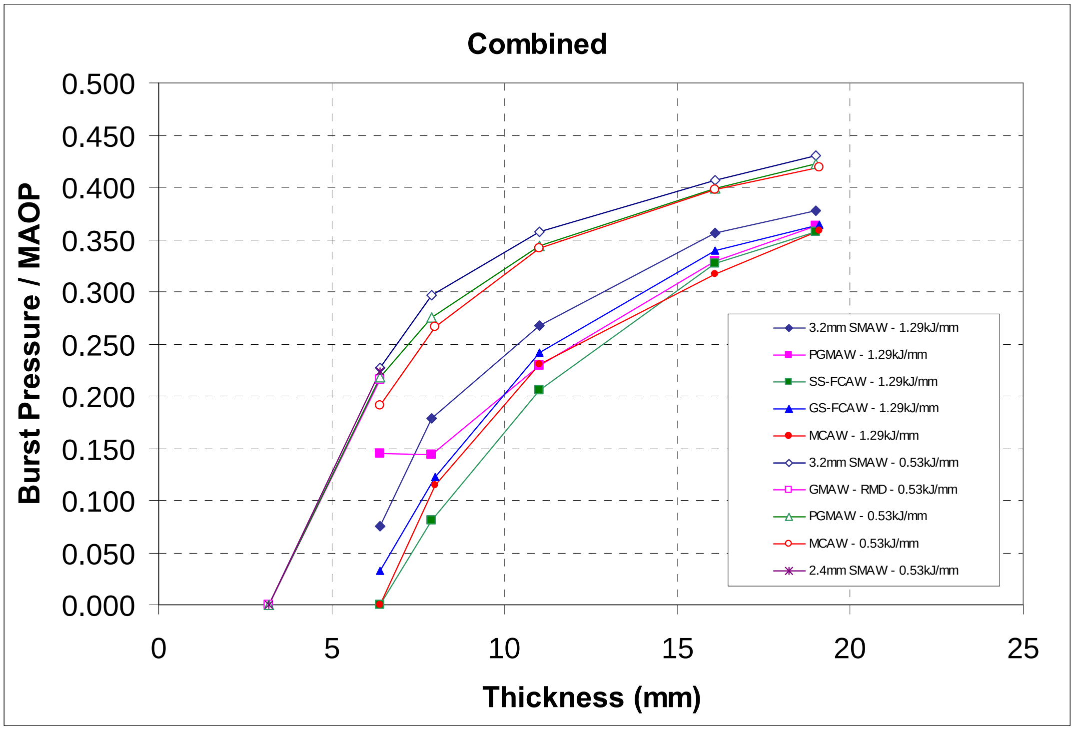

Figure 4.19: Burst Pressure/MOP (%) vs. Thickness and Weld Process, Combined Heat Inputs

4.5.2 Water Backed Burn-through Predictions

Although outside the scope of the original work plan, welds for static air deposited in the 6.4, 8, and 11mm thicknesses were reproduced with water backed conditions. This task was investigated to determine if the water backing would provide sufficient heat sink capacity to extend the limits of in-service welding. The set-up for welding with water backing for both bead on pipe and for fillet welding of sleeves is illustrated in **Figure 4.20**. It should be noted that the burn-through calculations are only based on the bead on pipe data and not for fillet welds.

All welding data for bead on pipe welds deposited with water backing is shown in **Appendix E**. The thermocouple data was acquired at a scanning frequency of 25Hz. The thermocouple ID number is the same as the weld number. An example of the typical thermal history plots showing both weld and back surface temperature histories are shown in **Figure 4.21** and **4.22**, for welds FW62 and FW63, respectively. All remaining bead on pipe weld cross-sections for water backed conditions are shown in **Appendix F**.

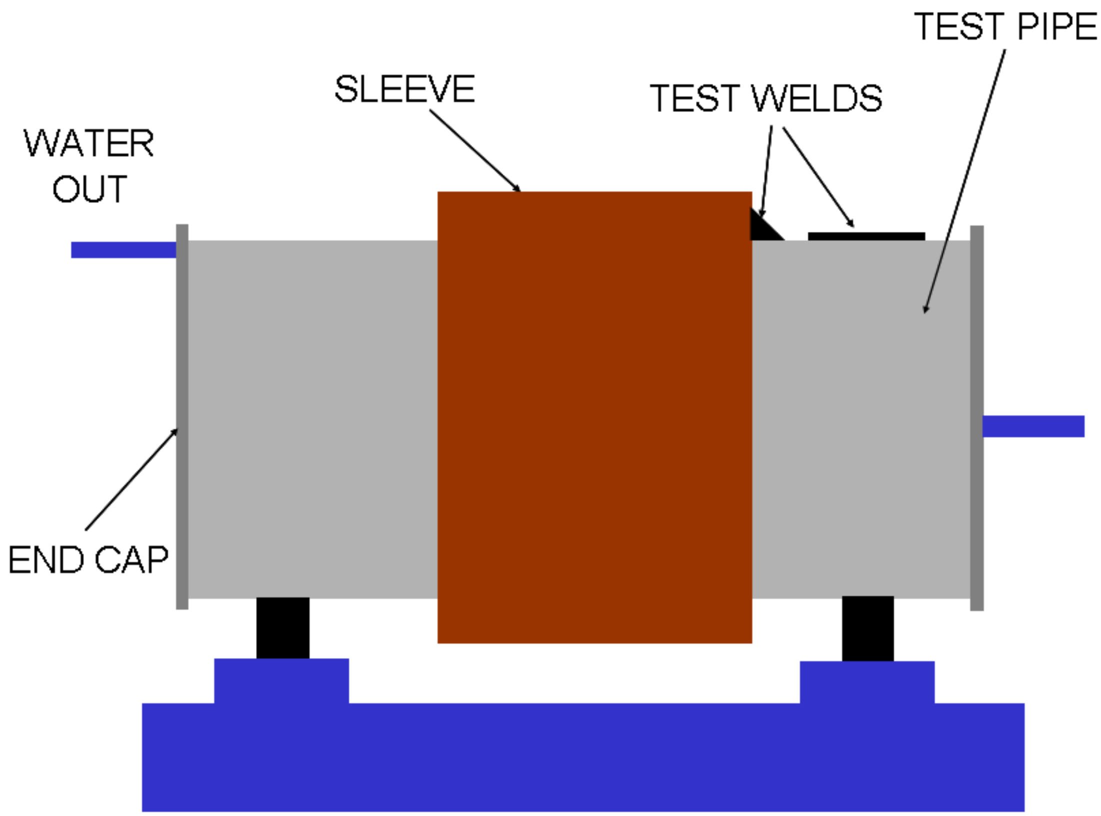

Figure 4.20: Water Backed Set-up

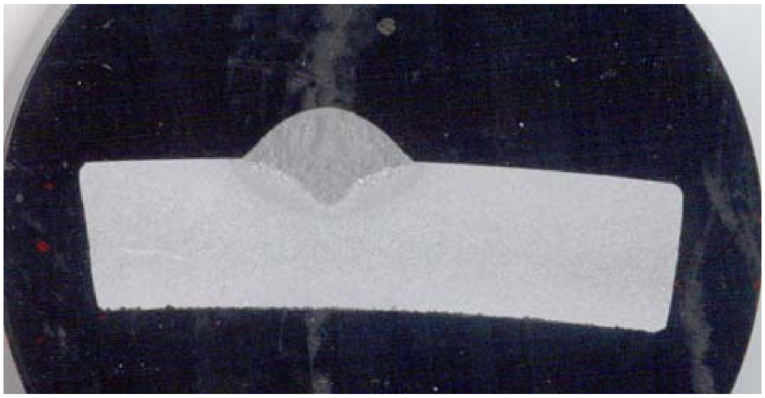

Figure 4.21: Weld FW62 Macro, 0.53 kJ/mm, 2.5X Mag

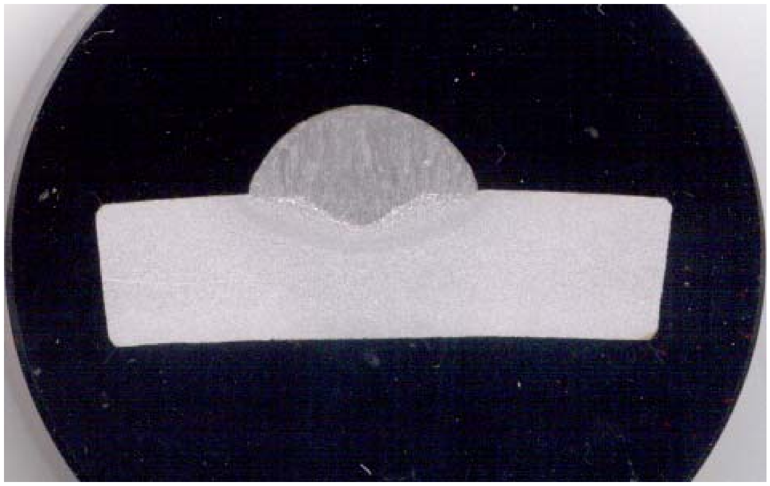

Figure 4.22: Weld FW63 Macro, 1.29 kJ/mm, 2.5X Mag.

The results of the burn-through calculations for water backed conditions are presented in **Tables 4.10** and **4.11** where the information can be plotted as Burst Pressure over Maximum Operating Pressure (MOP = 72% pipe yield pressure). Note that the values in red are for welds where the back surface temperature (ID of pipe) during welding reached at least 1000°C and that the effective flow stresses to cause a burst event is essentially any pressure over 0 Mpa. This data can be used to estimate the susceptibility to burn-through with each welding process over a range of heat inputs and material thicknesses, at a given percentage of MOP, as shown in **Figures 4.23** and **4.24**, where any value below each curve for a given welding process is considered a safe region. It should be noted that none of the welding procedures evaluated with water backing reached a peak back surface temperature of 1000°C, and therefore shows that the higher heat sink capacity of forced cooling provides a greater heat input window for safe in-service welding practice. **Figure 4.25** illustrates the results of both 0.53 and 1.29 kJ/mm heat inputs combined.

Table 4.10: Burst Pressure Calculations

Test ID	Surface Temp	Temperature						Yield Stress						Flow Stress Correction						Flow Stress						Effective	Flaw Length	Effective Flaw	L^2/(Dt)	Folias Factor	Flaw Area	Plate Area	Hoop Stress	Internal Pressure
		0	1	2	3	4	5	0	1	2	3	4	5	0	1	2	3	4	5	0	1	2	3	4	5	Flow Stress		Depth		Mt	A	Ao	@ Burst	@ Burst
	oC	oC	oC	oC	oC	oC	oC	(MPa)	(MPa)	(MPa)	(MPa)	(MPa)	(MPa)	(MPa)	(MPa)	(MPa)	(MPa)	(MPa)	(MPa)	(MPa)	(MPa)	(MPa)	(MPa)	(MPa)	(MPa)	(MPa)	(mm)	(mm)			(mm2)	(mm2)	(MPa)	(MPa)
FW4	482.6	1000	948.26	844.78	741.3	637.82	534.34	0.00	38.37	79.46	129.07	183.51	239.09	0.0	6.56	13.58	22.06	31.37	40.87	0.00	44.93	93.04	151.13	214.88	279.95	156.79	5.93	3.73	0.01	1.00	22.11	37.93	156.05	3.98
FW5	540	1000	954	862	770	678	586	0.00	36.42	71.93	114.67	162.04	211.43	0.0	6.23	12.30	19.60	27.70	36.14	0.00	42.64	84.22	134.27	189.74	247.58	139.69	5.18	3.99	0.01	1.00	20.65	33.16	139.10	3.55
FW6	600	1000	960	880	800	720	640	0.00	34.41	64.33	100.10	140.00	182.34	0.0	5.88	11.00	17.11	23.93	31.17	0.00	40.30	75.33	117.21	163.94	213.51	122.06	6.23	4.00	0.01	1.00	24.93	39.88	121.30	3.10
FW7	681.4	1000	968.14	904.42	840.7	776.98	713.26	0.00	31.77	54.50	81.28	111.23	143.50	0.0	5.43	9.32	13.89	19.01	24.53	0.00	37.20	63.82	95.17	130.25	168.03	98.89	4.63	4.36	0.01	1.00	20.19	29.63	98.46	2.51
FW8	657.9	1000	965.79	897.37	828.95	760.53	692.11	0.00	32.52	57.28	86.59	119.38	154.58	0.0	5.56	9.79	14.80	20.41	26.42	0.00	38.08	67.07	101.39	139.78	181.00	105.46	16.52	4.26	0.08	1.03	70.38	105.75	100.40	2.56
FW9	701.2	1000	970.12	910.36	850.6	790.84	731.08	0.00	31.13	52.20	76.89	104.49	134.29	0.0	5.32	8.92	13.14	17.86	22.96	0.00	36.46	61.12	90.03	122.35	157.25	93.44	2.59	4.67	0.00	1.00	12.12	16.60	93.28	2.38
FW10	531.9	1000	953.19	859.57	765.95	672.33	578.71	0.00	39.14	77.84	124.45	176.05	229.71	0.0	6.27	12.47	19.94	28.21	36.81	0.00	45.41	90.32	144.40	204.27	266.53	150.18	9.75	5.01	0.04	1.01	48.85	77.98	147.39	7.46
FW11	594	1000	959.4	878.2	797	715.8	634.6	0.00	36.92	69.42	108.30	151.66	197.60	0.0	5.92	11.12	17.36	24.30	31.67	0.00	42.84	80.54	125.65	175.97	229.26	130.85	8.49	5.54	0.03	1.01	46.97	67.89	128.37	6.50
FW12	510.4	1000	951.04	853.12	755.2	657.28	559.36	0.00	37.42	75.78	122.04	173.08	225.74	0.0	6.40	12.95	20.86	29.59	38.59	0.00	43.82	88.73	142.91	202.66	264.33	148.49	9.48	3.87	0.03	1.01	36.72	60.69	146.57	3.74
FW14	342.2	1000	934.22	802.66	671.1	539.54	407.98	0.00	54.94	125.36	210.18	299.75	384.43	0.0	7.40	16.89	28.33	40.40	51.81	0.00	62.34	142.25	238.50	340.14	436.23	243.89	8.22	5.69	0.01	1.00	46.77	90.46	243.35	5.93
FW15	465.6	1000	946.56	839.68	732.8	625.92	519.04	0.00	49.41	103.67	169.22	240.89	313.51	0.0	6.66	13.97	22.81	32.46	42.25	0.00	56.07	117.64	192.02	273.35	355.76	198.97	7.33	6.07	0.01	1.00	44.49	80.68	198.56	4.84
FW23	559.4	1000	955.94	867.82	779.7	691.58	603.46	0.00	35.76	69.44	109.90	154.86	202.02	0.0	6.11	11.87	18.79	26.47	34.53	0.00	41.88	81.31	128.69	181.33	236.56	133.95	11.45	4.10	0.04	1.01	46.99	73.26	131.04	3.34
FW24	770.2	1000	977.02	931.06	885.1	839.14	793.18	0.00	28.97	44.45	62.23	81.97	103.36	0.0	4.95	7.60	10.64	14.01	17.67	0.00	33.92	52.05	72.87	95.99	121.03	75.17	2.89	4.89	0.00	1.00	14.12	18.48	74.98	1.91
FW28	536.3	1000	953.63	860.89	768.15	675.41	582.67	0.00	36.54	72.41	115.58	163.41	213.23	0.0	6.25	12.38	19.76	27.93	36.45	0.00	42.79	84.78	135.34	191.35	249.68	140.79	4.10	3.99	0.01	1.00	16.37	26.23	140.41	3.58
FW29	752.2	1000	975.22	925.66	876.1	826.54	776.98	0.00	29.53	46.43	65.95	87.69	111.23	0.0	5.05	7.94	11.27	14.99	19.01	0.00	34.57	54.37	77.23	102.68	130.25	79.82	7.07	4.69	0.02	1.00	33.18	45.25	78.78	2.01
FW30	482.4	1000	948.24	844.72	741.2	637.68	534.16	0.00	40.94	84.78	137.73	195.83	255.13	0.0	6.56	13.59	22.07	31.38	40.89	0.00	47.50	98.37	159.80	227.21	296.01	165.78	6.51	4.67	0.02	1.01	30.39	52.07	164.61	8.33
FW31	755.6	1000	975.56	926.68	877.8	828.92	780.04	0.00	31.38	49.12	69.59	92.37	117.05	0.0	5.03	7.87	11.15	14.80	18.76	0.00	36.41	57.00	80.75	107.18	135.81	83.43	11.43	5.79	0.05	1.02	66.15	91.44	80.19	4.06
FW32	311.9	1000	931.19	793.57	655.95	518.33	380.71	0.00	56.32	130.86	220.43	313.98	400.48	0.0	7.59	17.64	29.71	42.32	53.97	0.00	63.91	148.50	250.14	356.30	454.45	254.66	4.76	5.50	0.00	1.00	26.21	52.39	254.48	6.20
FW33	473.6	1000	947.36	842.08	736.8	631.52	526.24	0.00	49.06	102.31	166.62	237.06	308.69	0.0	6.61	13.79	22.46	31.95	41.60	0.00	55.68	116.09	189.08	269.01	350.29	196.03	3.49	6.00	0.00	1.00	20.97	38.42	195.94	4.77
FW50	729.7	1000	972.97	918.91	864.85	810.79	756.73	0.00	30.23	48.94	70.71	94.99	121.28	0.0	5.17	8.37	12.09	16.24	20.73	0.00	35.40	57.31	82.79	111.23	142.01	85.75	0.00	4.62	0.00	1.00	0.00	0.00	85.75	2.19
FW51	766.4	1000	976.64	929.92	883.2	836.48	789.76	0.00	29.08	44.87	63.01	83.17	105.01	0.0	4.97	7.67	10.77	14.22	17.95	0.00	34.06	52.54	73.78	97.39	122.96	76.14	8.26	4.61	0.02	1.01	38.12	52.89	74.88	1.91
FW52	639.3	1000	963.93	891.79	819.65	747.51	675.37	0.00	35.33	63.48	96.92	134.32	174.33	0.0	5.66	10.17	15.53	21.52	27.94	0.00	41.00	73.65	112.45	155.84	202.27	117.04	9.55	5.29	0.04	1.01	50.49	76.37	114.62	5.80
FW53	752.1	1000	975.21	925.63	876.05	826.47	776.89	0.00	31.50	49.54	70.37	93.57	118.69	0.0	5.05	7.94	11.28	14.99	19.02	0.00	36.55	57.48	81.65	108.56	137.72	84.39	16.93	5.60	0.11	1.03	94.83	135.47	78.36	3.97
FW54	511.6	1000	951.16	853.48	755.8	658.12	560.44	0.00	47.41	95.92	154.42	218.96	285.60	0.0	6.39	12.93	20.81	29.51	38.49	0.00	53.80	108.85	175.23	248.47	324.09	182.09	15.37	6.23	0.02	1.01	95.69	169.04	180.37	4.39
FW55	606.6	1000	960.66	881.98	803.3	724.62	645.94	0.00	43.37	80.56	124.97	174.55	227.23	0.0	5.85	10.86	16.84	23.52	30.62	0.00	49.22	91.41	141.81	198.08	257.86	147.68	15.41	6.53	0.02	1.01	100.63	169.50	146.11	3.56
FW60	663.8	1000	966.38	899.14	831.9	764.66	697.42	0.00	32.33	56.58	85.24	117.32	151.78	0.0	5.53	9.67	14.57	20.05	25.95	0.00	37.86	66.25	99.81	137.37	177.73	103.80	10.79	4.22	0.04	1.01	45.48	69.03	101.64	2.59
FW61	856.9	1000	985.69	957.07	928.45	899.83	871.21	0.00	26.33	35.39	45.40	56.30	68.01	0.0	4.50	6.05	7.76	9.62	11.62	0.00	30.83	41.44	53.17	65.93	79.63	54.20	10.76	5.23	0.04	1.01	56.28	68.84	51.66	1.32
FW62	483.7	1000	948.37	845.11	741.85	638.59	535.33	0.00	40.89	84.60	137.38	195.31	254.46	0.0	6.55	13.56	22.02	31.30	40.78	0.00	47.44	98.16	159.39	226.61	295.24	165.37	8.26	5.19	0.03	1.01	42.85	66.04	162.92	8.25
FW63	702.6	1000	970.26	910.78	851.3	791.82	732.34	0.00	33.16	55.50	81.68	110.95	142.56	0.0	5.31	8.89	13.09	17.78	22.85	0.00	38.48	64.40	94.77	128.73	165.40	98.36	14.67	5.77	0.08	1.03	84.69	117.35	92.36	4.68
FW64	254.2	1000	925.42	776.26	627.1	477.94	328.78	0.00	59.00	141.53	240.08	340.59	429.01	0.0	7.95	19.07	32.36	45.90	57.82	0.00	66.95	160.61	272.44	386.49	486.83	274.66	5.23	5.06	0.00	1.00	26.46	57.51	274.46	6.69
FW65	508	1000	950.8	852.4	754	655.6	557.2	0.00	47.57	96.52	155.56	220.67	287.80	0.0	6.41	13.01	20.97	29.74	38.79	0.00	53.98	109.53	176.53	250.41	326.58	183.40	9.22	6.12	0.01	1.00	56.49	101.46	182.80	4.45

Table 4.11: Weld Data and Burst Pressure Results

Weld	Process	Dia (mm)	Electrode	Amps (A)	Volts (V)	TS ipm	HI kJ/mm	Weld Pentration Depth (mm)	Pipe Details	Thickness (mm)	Pipe Diameter (mm)	Yield Strength (initial)	Max. Back Surface Temp (degC)	Fusion Line Time 1000oC - 1000oC	Calculated Bursting Pressure	Burst P/ Yield Pressure	Burst P/ MOP
FW4	SMAW	2.4	718MC	90	21	12.5	0.35	1.15	NPS 20, X52	6.4	508	403.36	482.6	1.12	3.98	0.38689	0.2786
FW5	SMAW	2.4	718MC	90	21	8.5	0.53	1.36	NPS 20, X52	6.4	508	403.36	540	1.44	3.55	0.34485	0.2483
FW6	SMAW	2.4	718MC	90	21	6.0	0.74	1	NPS 20, X52	6.4	508	403.36	600	2.44	3.10	0.30073	0.2165
FW7	SMAW	2.4	718MC	90	21	3.5	1.29	1.16	NPS 20, X52	6.4	508	403.36	681.4	3.16	2.51	0.24409	0.1757
FW8	SMAW	3.2	718MC	120	20.5	11.0	0.53	1.13	NPS 20, X52	6.4	508	403.36	657.9	3.56	2.56	0.24892	0.1792
FW9	SMAW	3.2	718MC	120	20.5	4.5	1.29	1.78	NPS 20, X52	6.4	508	403.36	701.2	1.36	2.38	0.23125	0.1665
FW10	SMAW	3.2	718MC	120	20.5	11.0	0.53	1.82	NPS 12, X52	8	324	430.25	531.9	2.1	7.46	0.34257	0.2466
FW11	SMAW	3.2	718MC	120	20.5	4.5	1.29	2.5	NPS 12, X52	8	324	430.25	594	4.45	6.50	0.29837	0.2148
FW12	P-GMAW	0.9	K-NOVA	100	20.5	14.0	0.35	1.29	NPS 20, X52	6.4	508	403.36	510.4	1.6	3.74	0.36337	0.2616
FW14	SMAW	3.2	AtomArc 10018-M1	120	20	10.5	0.53	1.65	NPS36, X70	11	914	511.61	342.2	1.85	5.93	0.47565	0.3425
FW15	SMAW	3.2	AtomArc 10018-M1	120	20	4.5	1.29	1.45	NPS36, X70	11	914	511.61	465.6	3.85	4.84	0.38811	0.2794
FW23	GMAW - RMD	1.2	K-NOVA	170	17	13.0	0.53	1.5	NPS 20, X52	6.4	508	403.36	559.4	2.08	3.34	0.32488	0.2339
FW24	GMAW - RMD	1.2	K-NOVA	170	17	5.5	1.29	1.61	NPS 20, X52	6.4	508	403.36	770.2	1.24	1.91	0.18588	0.1338
FW28	P-GMAW	0.9	K-NOVA	100	20.5	5.5	0.53	1.4	NPS 20, X52	6.4	508	403.36	536.3	1.76	3.58	0.34810	0.2506
FW29	P-GMAW	0.9	K-NOVA	100	20.5	2.5	1.29	1.25	NPS 20, X52	6.4	508	403.36	752.2	6.68	2.01	0.19531	0.1406
FW30	P-GMAW	0.9	K-NOVA	100	20.5	7.5	0.53	1.45	NPS 12, X52	8	324	430.25	482.4	2.05	8.33	0.38258	0.2755
FW31	P-GMAW	0.9	K-NOVA	100	20.5	3.0	1.29	1.26	NPS 12, X52	8	324	430.25	755.6	9	4.06	0.18638	0.1342
FW32	P-GMAW	0.9	ER70XTi	100	20.5	7.5	0.53	1.51	NPS36, X70	11	914	511.61	311.9	1.5	6.20	0.49741	0.3581
FW33	P-GMAW	0.9	ER70XTi	100	20.5	3.0	1.29	1.26	NPS36, X70	11	914	511.61	473.6	2.75	4.77	0.38299	0.2758
FW50	GS-FCAW	1.2	DS II 71T-12	200	25.5	11.00	1.06	1.32	NPS 20, X52	6.4	508	403.36	729.7	0.00001	2.19	0.21259	0.1531
FW51	GS-FCAW	1.2	DS II 71T-12	175	24.5	8.00	1.29	0.79	NPS 20, X52	6.4	508	403.36	766.4	2.44	1.91	0.18565	0.1337
FW52	GS-FCAW	1.2	DS II 71T-12	200	25.5	11.00	1.06	1.53	NPS 12, X52	8	324	430.25	639.3	2.05	5.80	0.26640	0.1918
FW53	GS-FCAW	1.2	DS II 71T-12	175	24.5	8.00	1.29	0.76	NPS 12, X52	8	324	430.25	752.1	5	3.97	0.18212	0.1311
FW54	GS-FCAW	1.2	DSII 80T1-Ni1	225	26.5	11.00	1.29	1.34	NPS36, X70	11	914	511.61	511.6	3.3	4.39	0.35256	0.2538
FW55	GS-FCAW	1.2	DSII 80T1-Ni1	225	26.5	7.00	1.99	0.85	NPS36, X70	11	914	511.61	606.6	5.2	3.56	0.28559	0.2056
FW60	MCAW	1.2	MC70	140	20.5	13.00	0.52	0.97	NPS 20, X52	6.4	508	403.36	663.8	1.96	2.59	0.25198	0.1814
FW61	MCAW	1.2	MC70	140	20.5	5.25	1.29	1.15	NPS 20, X52	6.4	508	403.36	856.9	4.84	1.32	0.12807	0.0922
FW62	MCAW	1.2	MC70	140	20.5	13.00	0.52	2.47	NPS 12, X52	8	324	430.25	483.7	1.5	8.25	0.37866	0.2726
FW63	MCAW	1.2	MC70	140	20.5	5.25	1.29	2.03	NPS 12, X52	8	324	430.25	702.6	6.6	4.68	0.21466	0.1546
FW64	MCAW	1.2	MC100	140	20.5	13.00	0.52	1.08	NPS36, X70	11	914	511.61	254.2	0.95	6.69	0.53647	0.3863
FW65	MCAW	1.2	MC100	140	20.5	5.25	1.29	1.17	NPS36, X70	11	914	511.61	508	4.15	4.45	0.35730	0.2573

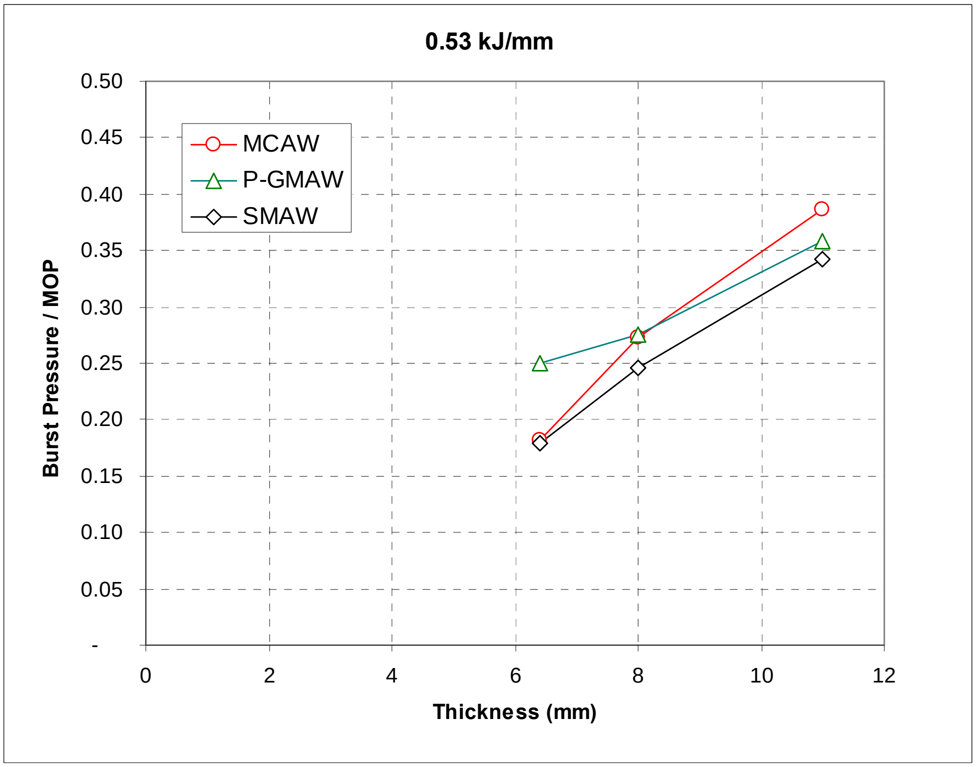

Figure 4.23: Burst Pressure/MOP (%) vs. Thickness and Weld Process - 0.53kJ/mm

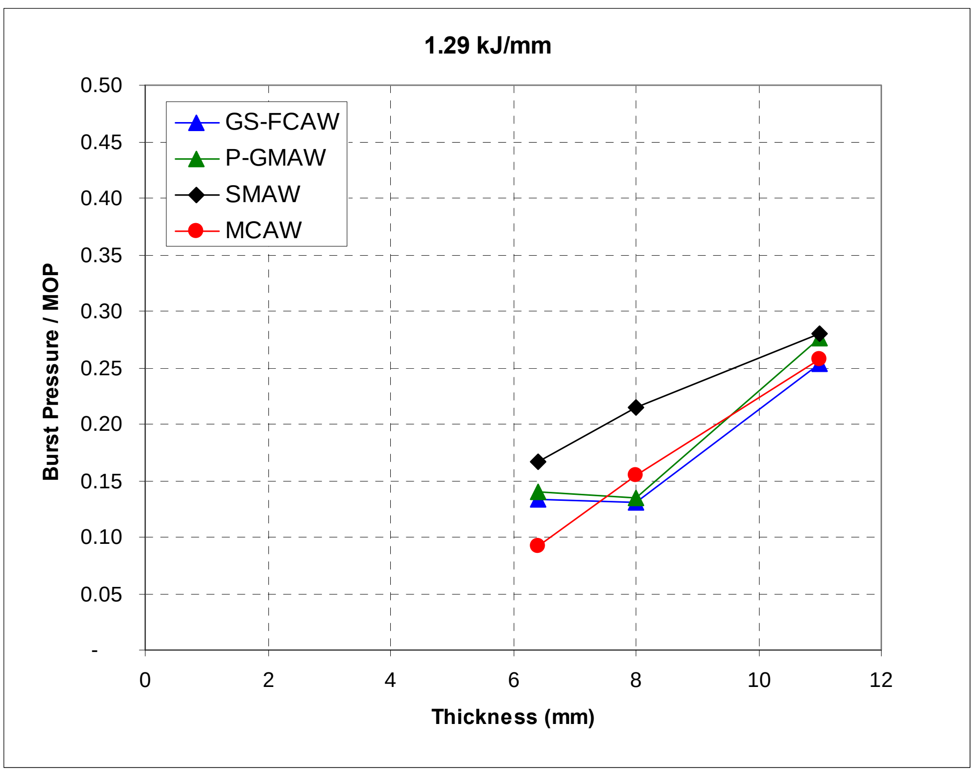

Figure 4.24: Burst Pressure/MOP (%) vs. Thickness and Weld Process - 1.29kJ/mm

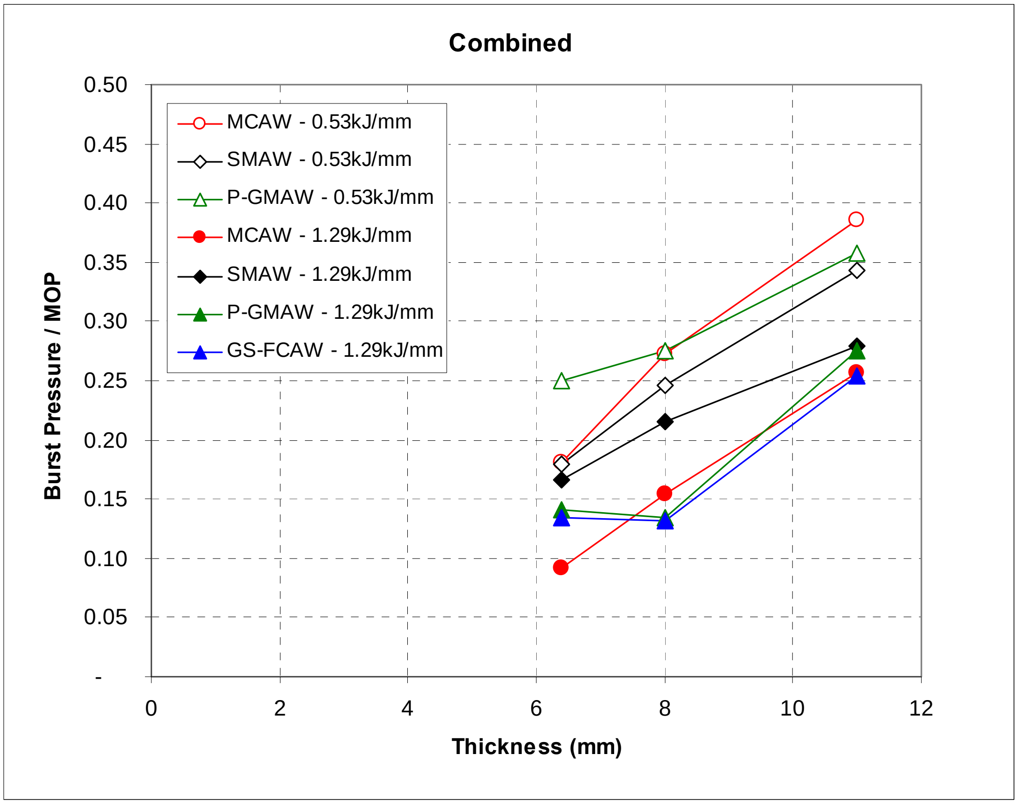

Figure 4.25: Burst Pressure / MOP (%) vs. Thickness and Weld Process – 0.53 and 1.29kJ/mm

4.6 Task 4: Examine Cooling Rates as a Function of Welding Process Arc Efficiency

The weld temperature history, calculated cooling rates, HAZ and weld metal hardness measurements, and maximum back surface temperatures from each of the welds under static air (no flow conditions) are shown in **Table 4.12**. Only the alloyed weld metals were measured for hardness as mild steel "weld metals" are typically not as sensitive to delayed cracking compared to those highly alloyed weld metals typically used in low CE high strength pipeline materials.

To acquire the required data, each test weld deposited on pipe measured a length of six (6) inches and the travel speed was maintained at a predetermined rate with mechanized travel. Using the methods outlined previously, thermocouples were used to acquire the thermal data from both the weld and back surface temperature for each weld deposited. The collected weld thermal data can be used to plot the cooling rate of each process over a range of thickness, as shown in **Figures 4.26** and **4.27**.

Table 4.12: Cooling Data and Hardness Results – Static Air

Weld ID	Pipe Thickness	Grade	C.E	Process	Heat Input	Cooling Rate		Location – Ocular Reading – CGHAZ - Pipe Side					Ocular Reading – CG-HAZ Sleeve			Ocular Reading – Weld				Location – Hardness (Hv5) – CGHAZ - Pipe Side					Hardness (Hv5) – CG-HAZ Sleeve			Hardness (Hv5) – Weld				Peak Hardness (Hv5)			Average Hardness (Hv5)		
	(mm)				(kJ/mm)	ΔT 800-500C (s)	Slope at 540C (degC / sec)	1	2	3	4	5	1	2	3	1	2	3	4	1	2	3	4	5	1	2	3	1	2	3	4	CGHAZ Pipe	CGHAZ Sleeve	Weld	CGHAZ Pipe	CGHAZ Sleeve	Weld
A1	3.2	X52	0.16	SMAW	0.35	6.06	-38	218	217	215	216	214								195	197	201	199	202								202			199		
A2	3.2	X52	0.16	SMAW	0.53	9.2	-20	221	218	213	217	220								190	195	204	197	192								204			196		
A3	3.2	X52	0.16	SMAW	0.74	14.59	-18	215	217	210	213	214								201	197	210	204	202								210			203		
A4	6.4	X52	0.43	SMAW	0.35	2.56	-59.5	155	164	175	172	166								386	345	303	313	336								386			337		
A5	6.4	X52	0.43	SMAW	0.53	6.56	-29.5	188	176	199	182	182								262	299	234	280	280								299			271		
A6	6.4	X52	0.43	SMAW	0.74	12.3	-22.5	199	200	201	200	202								234	232	229	232	227								234			231		
A7	6.4	X52	0.43	SMAW	1.29	22.36	-19.5	209	205	207	205	204								212	221	216	221	223								223			219		
A8	6.4	X52	0.43	SMAW	0.53	6.57	-17.5	214	227	226	231	232								202	180	182	174	172								202			182		
A9	6.4	X52	0.43	SMAW	1.29	25.54	-12	223	226	224	224	223								186	182	185	185	186								186			185		
A10	8	X52	0.14	SMAW	0.53	5.02	-52.5	215	215	213	216	215								201	201	204	199	201								204			201		
A11	8	X52	0.14	SMAW	1.29	23.29	-14.5	221	223	223	223	211								190	186	186	186	208								208			191		
A12	6.4	X52	0.43	P-GMAW	0.35	4.63	-46	157	180	181	167	172								376	286	283	332	313								376			318		
A14	11	X70	0.22	SMAW	0.53	3.34	-63	182	182	181	180	180				177	182	180	184	280	280	283	286	286				296	280	286	274	286		296	283		284
A15	11	X70	0.22	SMAW	1.29	10.88	-6	194	193	199	194	194				187	196	195	192	246	249	234	246	246				265	241	244	252	249		265	244		250
A16	16.1	X80	0.27	SMAW	0.53	2.66	-92	172	171	174	171	171				175	180	180	179	313	317	306	317	317				303	286	286	289	317		303	314		291
A17	16.1	X80	0.27	SMAW	1.29	10.04	-23	173	179	178	180	179				184	191	190	190	310	289	293	286	289				274	254	257	257	310		274	293		260
A18	19.1	X70	0.24	SMAW	0.53	2.5	-88.5	175	175	180	178	176				176	183	176	181	303	303	286	293	299				299	277	299	283	303		299	297		290
A19	19.1	X70	0.24	SMAW	1.29	9.35	-29.5	190	190	193	199	198				184	186	188	191	257	257	249	234	237				274	268	262	254	257		274	247		265
A20	3.2	X52	0.16	GMAW - RMD	0.19	2.55	-80.5	211	211	213	209	206								208	208	204	212	218								218			210		
A21	3.2	X52	0.16	GMAW - RMD	0.35	5.96	-43	212	211	212	212	213								206	208	206	206	204								208			206		
A22	3.2	X52	0.16	GMAW - RMD	0.53	8.49	-20	212	213	213	214	211								206	204	204	202	208								208			205		
A23	6.4	X52	0.43	GMAW - RMD	0.53	5.89	-28.5	180	181	187	192	193								286	283	265	252	249								286			267		
A24	6.4	X52	0.43	GMAW - RMD	1.29	30.59	-0.5	209	209	211	214	211								212	212	208	202	208								212			209		
A25	3.2	X52	0.16	P-GMAW	0.19	2.9	-68	211	213	214	211	212								208	204	202	208	206								208			206		
A26	3.2	X52	0.16	P-GMAW	0.35	7.14	-36.5	211	212	217	213	217								208	206	197	204	197								208			203		
A27	3.2	X52	0.16	P-GMAW	0.53	14.13	-20	217	212	215	215	215								197	206	201	201	201								206			201		
A28	6.4	X52	0.43	P-GMAW	0.53	8.01	-23.5	222	181	195	192	193								188	283	244	252	249								283			243		
A29	6.4	X52	0.43	P-GMAW	1.29	24.46	-8.89	209	212	208	215	216								212	206	214	201	199								214			206		
A30	8	X52	0.14	P-GMAW	0.53	7.63	-37	213	216	219	217	217								204	199	193	197	197								204			198		
A31	8	X52	0.14	P-GMAW	1.29	27.49	-8	229	224	227	225	222								177	185	180	183	188								188			183		
A32	11	X70	0.22	P-GMAW	0.53	2.83	-37	186	182	181	180	182				186	186	189	188	268	280	283	286	280				268	268	260	262	286		268	279		264
A33	11	X70	0.22	P-GMAW	1.29	23.02	-8.34	198	198	197	197	198				203	204	204	207	237	237	239	239	237				225	223	223	216	239		225	237		222
A34	16.1	X80	0.27	P-GMAW	0.53	4.14	-66.5	173	169	172	173	173				179	184	185	181	310	325	313	310	310				289	274	271	283	325		289	313		279
A35	16.1	X80	0.27	P-GMAW	1.29	12.62	-25	182	182	183	182	185				198	199	185	198	280	280	277	280	271				237	234	271	237	280		271	278		245
A36	19.1	X70	0.24	P-GMAW	0.53	3.11	-86	181	184	179	178	176				175	175	180	178	283	274	289	293	299				303	303	286	293	299		303	288		296
A37	19.1	X70	0.24	P-GMAW	1.29	7.22	-32	193	197	194	188	189				196	194	198	198	249	239	246	262	260				241	246	237	237	262		246	251		240
A38	6.4	X52	0.43	SS-FCAW	1.06	31.44	-8.5	215	214	216	217	217								201	202	199	197	197								202			199		
A39	6.4	X52	0.43	SS-FCAW	1.29	37.09	-8.5	212	219	217	217	219								206	193	197	197	193								206			197		
A40	8	X52	0.14	SS-FCAW	1.06	18.9	-13.5	225	225	229	225	221								183	183	177	183	190								190			183		
A41	8	X52	0.14	SS-FCAW	1.29	27.73	-6	223	228	228	226	230								186	178	178	182	175								186			180		
A44	11	X70	0.22	SS-FCAW	1.29	22.71	-14.5	197	196	199	200	200				204	203	203	204	239	241	234	232	232				223	225	225	223	241		225	236		224
A45	11	X70	0.22	SS-FCAW	1.99	39.91	-2.5	202	202	204	202	204				206	211	205	208	227	227	223	227	223				218	208	221	214	227		221	225		215
A46	16.1	X80	0.27	SS-FCAW	1.29	7.68	-23	180	179	180	184	180				191	190	192	196	286	289	286	274	286				254	257	252	241	289		257	284		251
A47	16.1	X80	0.27	SS-FCAW	1.99	17.51	-8	192	190	192	191	196				202	203	199	200	252	257	252	254	241				227	225	234	232	257		234	251		230
A48	19.1	X70	0.24	SS-FCAW	1.29	4.99	-24.4	192	196	196	196	195				191	197	193	198	252	241	241	241	244				254	239	249	237	252		254	244		245
A49	19.1	X70	0.24	SS-FCAW	1.99	16.2	-15	201	201	201	204	205				203	203	206	206	229	229	229	223	221				225	225	218	218	229		225	226		222
A50	6.4	X52	0.43	GS-FCAW	1.06	21.12	-7.2	208	209	217	209	210								214	212	197	212	210								214			209		
A51	6.4	X52	0.43	GS-FCAW	1.29	35.24	-6.375	210	208	210	208	213								210	214	210	214	204								214			211		
A52	8	X52	0.14	GS-FCAW	1.06	16.16	-10.625	222	223	226	224	221								188	186	182	185	190								190			186		
A53	8	X52	0.14	GS-FCAW	1.29	24.04	-9.875	226	225	226	225	225								182	183	182	183	183								183			183		
A54	11	X70	0.22	GS-FCAW	1.29	7.56	-77.25	199	201	198	198	198				200	202	201	200	234	229	237	237	237				232	227	229	232	237		232	235		230
A55	11	X70	0.22	GS-FCAW	1.99	37.88	-3.75	211	212	209	210	210				209	211	212	212	208	206	212	210	210				212	208	206	206	212		212	209		208
A56	16.1	X80	0.27	GS-FCAW	1.29	6.01	-37.5	183	182	181	182	185				194	197	197	201	277	280	283	280	271				246	239	239	229	283		246	278		238
A57	16.1	X80	0.27	GS-FCAW	1.99	15.62	-6	195	188	192	187	191				202	202	203	203	244	262	252	265	254				227	227	225	225	265		227	255		226
A58	19.1	X70	0.24	GS-FCAW	1.29	6.38	-34.5	190	197	197	194	191				194	194	202	202	257	239	239	246	254				246	246	227	227	257		246	247		237
A59	19.1	X70	0.24	GS-FCAW	1.99	13.42	-25.5	202	204	203	204	206				211	210	209	211	227	223	225	223	218				208	210	212	208	227		212	223		210
A60	6.4	X52	0.43	MCAW	0.53	7.28	-25.75	198	191	203	190	195								237	254	225	257	244								257			243		
A61	6.4	X52	0.43	MCAW	1.29	41.4	-6.5	215	214	222	219	220								201	202	188	193	192								202			195		
A62	8	X52	0.14	MCAW	0.53	4.6	-13.32	218	219	223	220	218								195	193	186	192	195								195			192		
A63	8	X52	0.14	MCAW	1.29	28.52	-9.375	228	227	231	231	228								178	180	174	174	178								180			177		
A64	11	X70	0.22	MCAW	0.53	3	-73.125	189	187	188	186	187				175	176	177	178	260	265	262	268	265				303	299	296	293	268		303	264		298
A65	11	X70	0.22	MCAW	1.29	16.08	-12.875	207	205	206	205	209				191	194	195	194	216	221	218	221	212				254	246	244	246	221		254	218		248
A66	16.1	X80	0.27	MCAW	0.53	2.92	-95	175	175	175	176	174				175	173	178	186	303	303	303	299	306				303	310	293	268	306		310	303		293
A67	16.1	X80	0.27	MCAW	1.29	6.93	-66	187	194	185	188	189				188	188	190	191	265	246	271	262	260				262	262	257	254	271		262	261		259
A68	19.1	X70	0.24	MCAW	0.53	2.76	-88.875	182	181	185	177	194				179	178	176	177	280	283	271	296	246				289	293	299	296	296		299	275		294
A69	19.1	X70	0.24	MCAW	1.29	6.64	-36.625	197	195	196	198	196				196	190	190	189	239	244	241	237	241				241	257	257	260	244		260	240		254

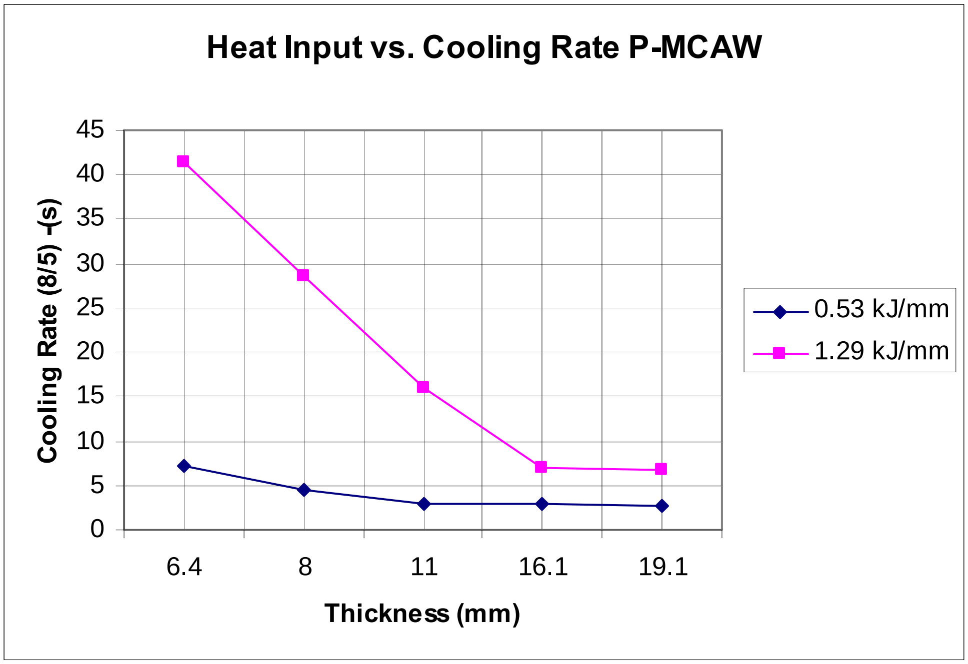

Figure 4.26: Cooling Rate vs. Heat Input, P-MCAW Process

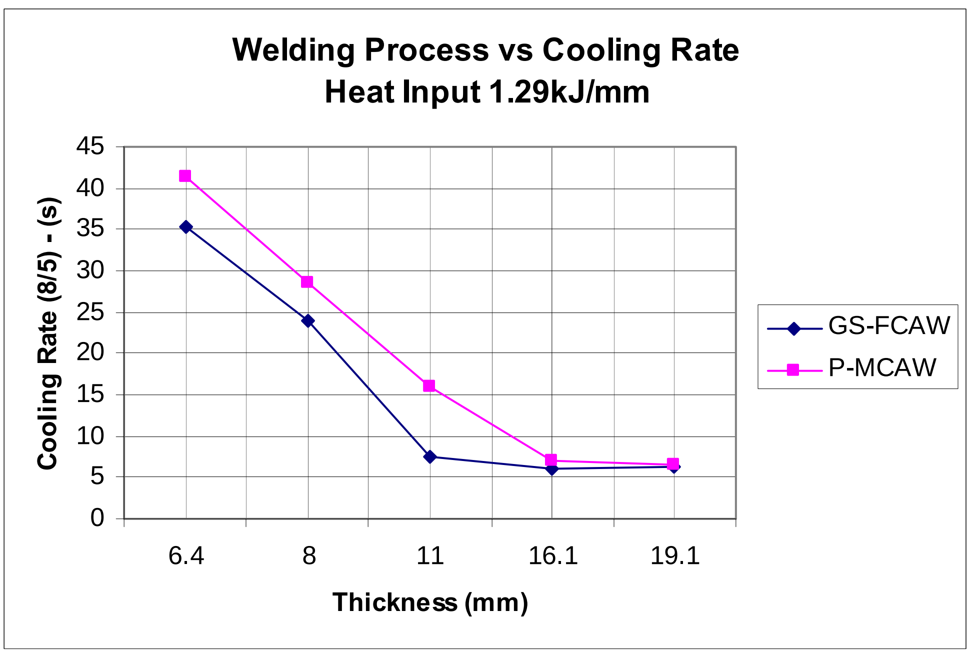

Figure 4.27: Cooling Rate vs. Welding Process, Heat Input 1.29 kJ/mm

Figure 4.27 shows that at a constant heat input of 1.29 kJ/mm, the P-MCAW process produces a slower cooling rate for a given thickness compared to the GS-FCAW process. This again is an effect of arc efficiency and could be advantageous in terms of using a specific process to produce softer weld zone microstructures that are less susceptible to delayed hydrogen cracking.

The hardness results when plotted vs. heat input and process (shown in **Figures 4.28** to **4.32**), show a general trend of decreasing hardness with increasing heat input as expected, however there is an even more interesting trend that shows the SMAW process results in the highest hardness at a given heat input level, with a downward trend in hardness vs. process at a given heat input level proceeding from the PGMAW to FCAW to PMCAW processes. This indicates that the processes with the higher arc efficiencies (i.e., transfer more heat from the arc to the base material) result in lower CGHAZ hardnesses regardless of material type and thickness. Based on these results, the SMAW process has the lowest arc efficiency (as demonstrated by the highest hardness) and the PMCAW has the highest arc efficiency (as demonstrated by the lowest hardness). As demonstrated in Figure 4.27, the MCAW process produced slower cooling rates vs. the FCAW process for a given heat input which in theory should provide a softer HAZ hardness. The plots in Figures 4.29 to 4.32 prove this theory is correct.

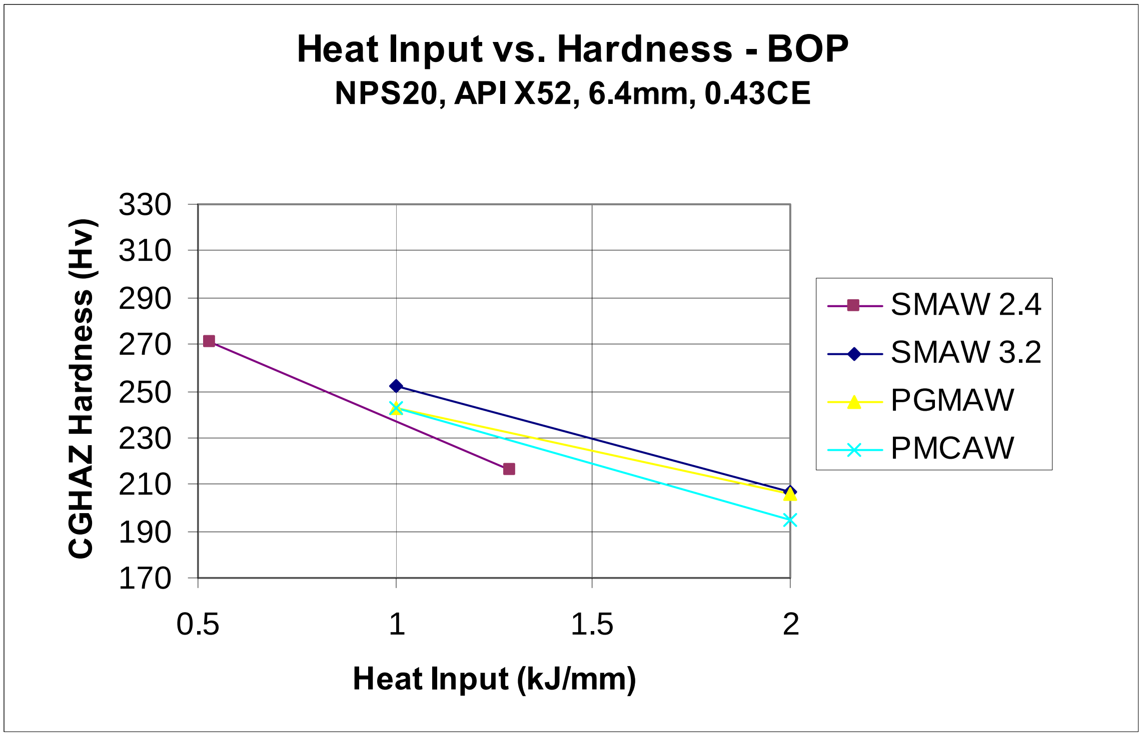

Figure 4.28: Heat Input vs. Hardness, 6.4mm

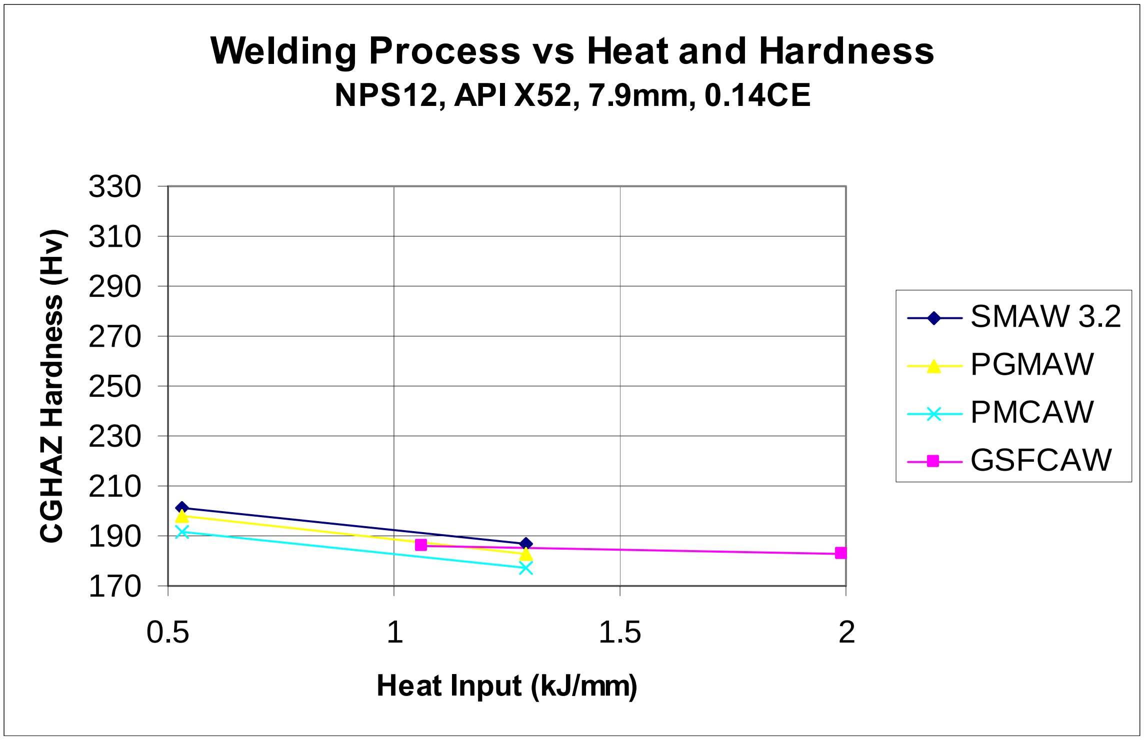

Figure 4.29: Heat Input vs. Hardness, 7.9mm

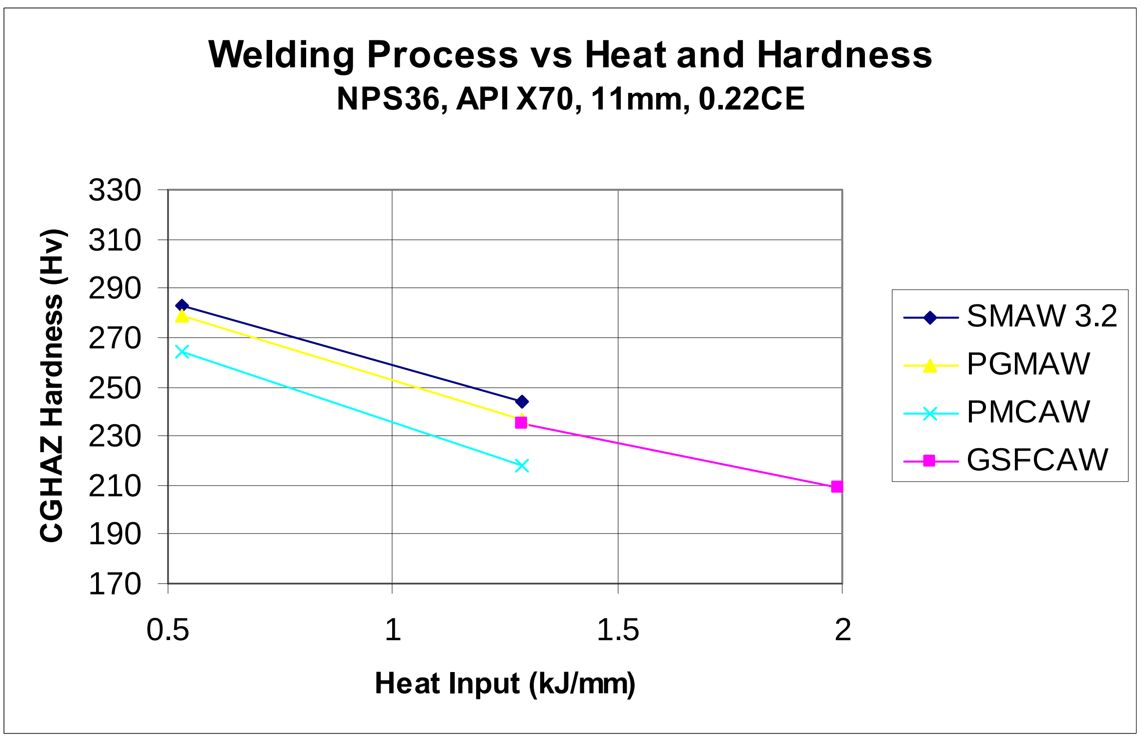

Figure 4.30: Heat Input vs. Hardness, 11mm

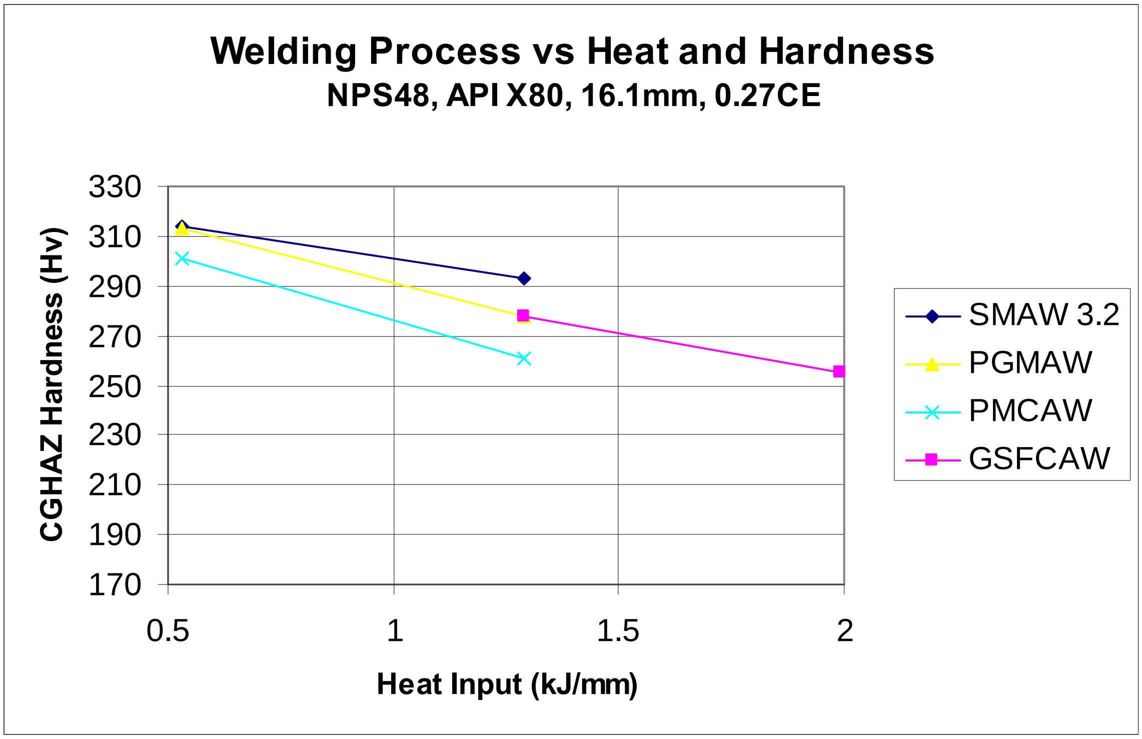

Figure 4.31: Heat Input vs. Hardness, 16.1mm

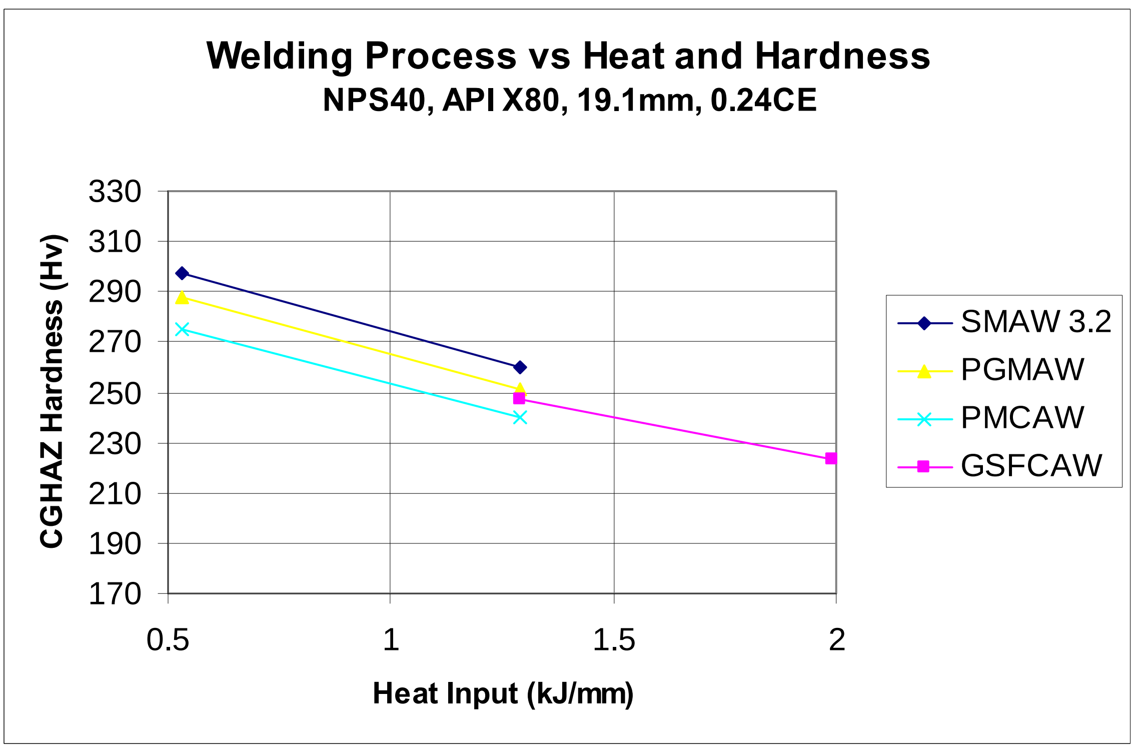

Figure 4.32: Heat Input vs. Hardness, 19.1mm

4.7 Task 5: Establish Diffusible Hydrogen Characteristics

This task was used to determine the diffusible hydrogen characteristics of each of the electrodes received for this study. The data was then used to investigate the times to peak hydrogen concentration in Task 6, that involves predicting delay times for welds that are considered susceptible to hydrogen cracking (i.e., those welds that have a hardness of 300 VHN or higher).

All low hydrogen mild steel SMAW electrodes received were baked at 400ºC for one (1) hour at a maximum layer depth of 25mm. The electrodes were immediately transferred into an electrode storage oven set at 120ºC. Each of the mild steel SMAW electrodes, except the 2.4mm diameter, were tested for diffusible hydrogen as per AWS A4.3 Standard using the under mercury method, in the as-received and baked condition. The results are shown in **Table 4.13**. No real trend was visible between the electrodes that were tested in the as-received and baked conditions, however a significant trend was apparent between increase of welding amperage and hydrogen. One possible reason for this hydrogen increase is that as amperage increases with the SMAW process using a constant current power source, the voltage across the arc and the arc length will increase. It is possible that this arc length increase allows for more moisture to be picked up and transferred across the arc in the form of hydrogen into the weld pool.

All other electrode/process combinations were subjected to diffusible hydrogen testing in the as-received condition to estimate the hydrogen potential and susceptibility to delayed cracking in Task 6, and the results are shown in **Figure 4.33**. The 10% $C0_2$ – 90% Argon shielding gas used for the GMAW processes was analyzed for moisture and the results indicated a 1ppm moisture concentration. Gas moisture and other factors have a direct correlation with available hydrogen, and 1ppm is considered to be on the low side of the range of most industrial gases which typically contain 5 to 10ppm concentrations.

Table 4.13: Diffusible Hydrogen Comparison between As-received and Conditioned Low Hydrogen Electrodes

Electrode	Condition	Amperage (A)	Average Diffusible Hydrogen (ml/100g)
2.4mm Hobart 718MC (E7018-1)	as received	90	2.93
3.2mm Hobart 718MC (E7018-1)	as-received	90	4.27
	baked	90	4.12
	as-received	160	6.03
	baked	160	6.73
4.0mm Hobart 718MC (E7018-1)	as-received	130	4.03
	baked	130	3.93
	as-received	220	5.28
	baked	220	6.2

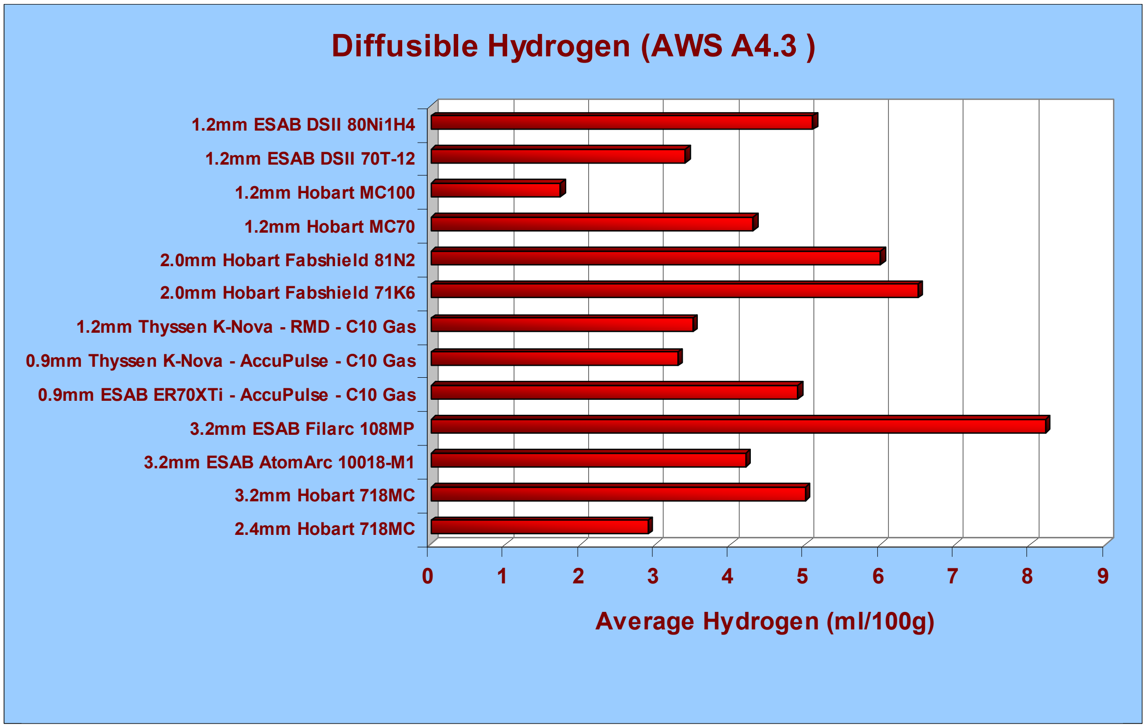

Figure 4.33: Diffusible Hydrogen Comparisons of Each Electrode Evaluated

4.8 Task 6: Establish Delay Time Predictions

It is well publicized that welds with a HAZ hardness of 350 VHN and higher, and with sufficient available hydrogen, are susceptible to hydrogen induced cold cracking, also known as delayed hydrogen cracking. Delay time is the amount of time that passes from the end of weld completion to the time that available (local) hydrogen reaches its highest concentration in the most susceptible cracking region (i.e., highest stress concentration zone in the hard HAZ). For the purpose of this project, select welds that exhibit a hardness of 300VHN and higher, were modelled to determine their time to peak hydrogen. The 300VHN boundary is selected to include the uncertainty of the 350HVN when applying this criterion to modern low carbon steels, noting that the 350VHN is based on C-Mn steels.

The delay time to peak hydrogen was determined using the BMT Fleet Technology Limited Hydrogen Cracking Susceptibility and Delay Time Prediction software. A typical example of a weld model used in the modeling software is shown in **Figure 4.34**. The weld profile (taken from an actual weld cross section) in this case is identified by green cells marked 1 and the dimensions were measured from the cross section of the bead-on-pipe weld A68 (P-MCAW weld using MC100 filler metal on 19.1mm thick X80 pipe, heat input of 0.53 kJ/mm)). The grey cells represent parent/base metal. The cells identified by 0 (yellow) are open space. A cell is 0.5mm x 0.5mm.

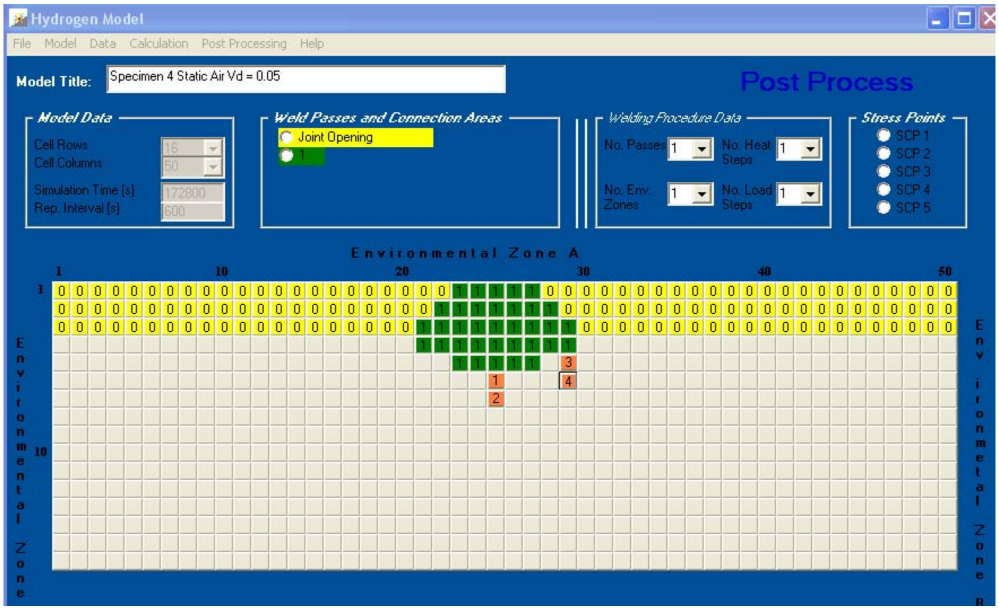

Figure 4.34: BMT Fleet Technology Limited Hydrogen Cracking Susceptibility and Delay Time Prediction Model

The hydrogen diffusion through the weld model is calculated using a finite difference technique, based on the thermal history and the apparent hydrogen diffusivity. The thermal history is calculated based on an analytical solution to the moving point heat source equation, and the apparent hydrogen diffusivity is calculated based on the trap density input for each weld model.

A diffusion analysis was conducted in this case for static air (no flow conditions). The analyses were carried out for a total hydrogen level equal to unity (H_{total} = 1.0). Two trap densities were considered for each model, v_d = 0.05 and v_d = 0.10. These trap densities span those that have been experimentally determined from apparent diffusivity for single pass welds encompassing SMAW and GMAW welds.[[8],[9]]

The hydrogen levels for four cells located in the HAZ (orange cells 1 and 2 (root location), and, 3 and 4 (weld toe location) in **Figure 4.35**) were monitored for a time period of 48 hours. A typical result, in terms of the hydrogen level versus time, is presented in **Figure 4.36** (for Specimen A68 in a static air environment). The time to peak hydrogen in Figure 4.36 represents a 1mm wide HAZ band where delayed cracking is most likely as it covers the hard HAZ. The important output from these plots is the maximum delay to peak hydrogen in the 1mm HAZ band and not the level of hydrogen, as the focus of this task is guidance for determination of optimal inspection times after welding. Thus, in this example for weld A68 the time to peak hydrogen concentration at the cell 2 location takes approximately 10.25 hours, and therefore the likelihood for hydrogen cracking is minimal after that time period has lapsed assuming a Vd = 0.1.

To assess the likelihood of delayed cracking before this delay time, knowledge of the susceptibility of the microstructure (hardness level is one of the parameters), and tensile stress (applied and residual) is required in addition to the actual peak hydrogen level, therefore the actual susceptibility of this weld to delayed cracking is uncertain.

---

[8] L. N. Pussegoda et al: "Delayed Cracking in Simulated Naval Platform Repair Welds", Trends in Welding Research-Proc. 6th Int. Conf.", ASM International, (2002), pp. 581-585.

[9] L. N. Pussegoda et al: "Determination of critical hydrogen curves from loe bend tests", Proc. IPC 2004 (IPC 04-0414).

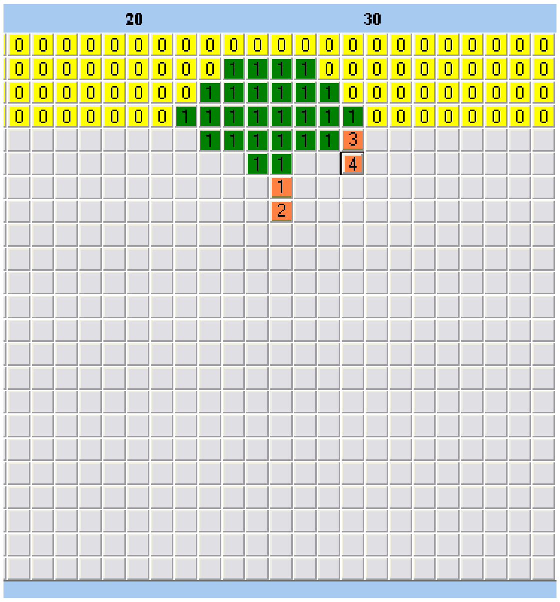

Figure 4.35: Cells Monitored in Model

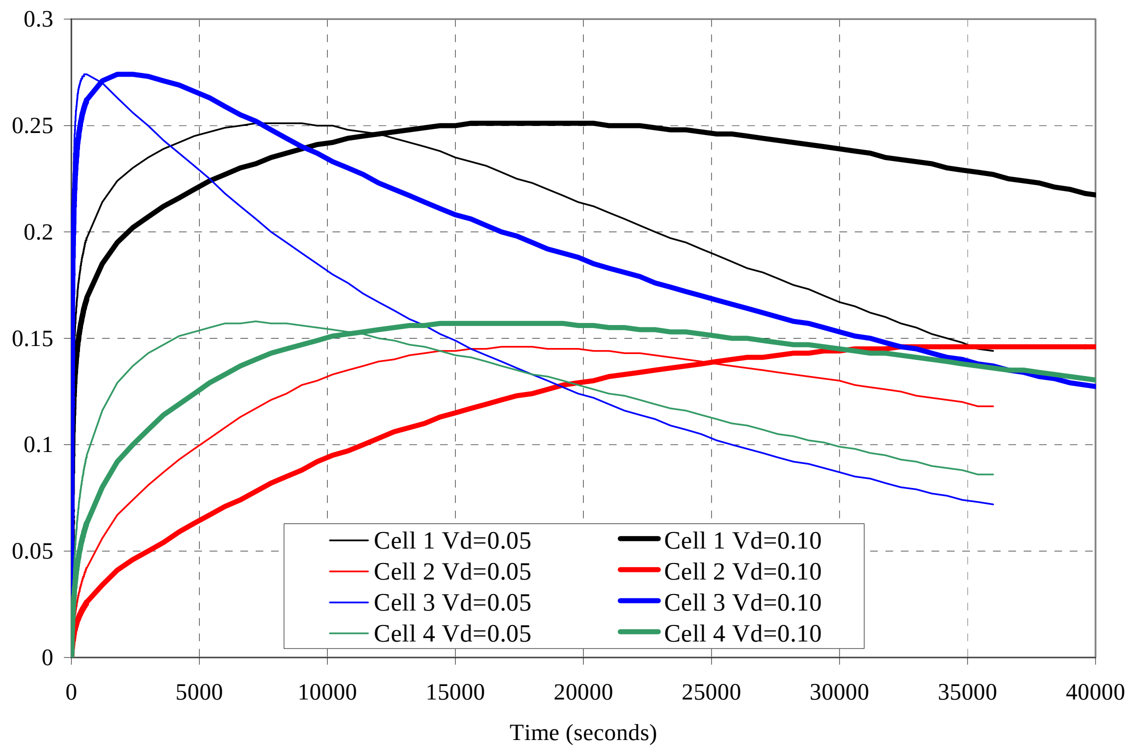

Figure 4.36: Hydrogen Concentration vs. Time (Specimen A68, Welded in Static Air)

The complete modeling results of the delay times in the welds that were considered highest susceptible to hydrogen cracking (CGHAZ above 300VHN), are shown in **Table 4.14**. These welds were produced in the NPS20 X52 pipe that had the highest carbon equivalent of 0.43 CE. Also note that the flowing air and water mist spray delay time results are based on the thermal history and hardness results achieved in Task 7. The columns identified as time to peak hydrogen are the delay times for V_d = 0.05 and 0.1, respectively.

Several of the welds deposited with static air and with water backing were plotted against each other as a comparison, and these are shown in **Figures 4.37** to **4.44**. These illustrate that the addition of the heat sink from the water containment results in a significance difference in delay time. The primary reason for this is the rapid cooling of the weld to the pipe temperature while in-service. One of the main controlling factors for the diffusion of hydrogen is temperature, therefore if the weld cools quicker to the pipeline operating temperature, then it will take longer for the hydrogen to migrate to a specific point within the weld zone, and thus a require a longer delay time.

Table 4.14: Delay Time Prediction Results

								Time 1000C to 100C					
						Cooling Rate		Experimental	Model	Vd = 0.05		Vd = 0.1	
	Weld	Thickness	Carbon Equivalent	Process	Heat Input	800-500	Slope at 540	T1000-100	T1000-100	Time to Peak H	Peak H	Time to Peak H	Peak H
Scenerio	#	mm	C.E.		(KJ/mm)	(s)	(oC/s)	(s)	(s)	(hrs)		(hrs)	
Air	A12	6.4	0.43	P-GMAW	0.35	4.63	-46	113.03	98.8	1.25	0.182	3.417	0.187
	A4	6.4	0.43	SMAW	0.35	2.56	-59.5	101.43	75.9	0.417	0.202	1.417	0.204
	A5	6.4	0.43	SMAW	0.53	6.56	-29.5	150.05	123.1	0.333	0.190	1.417	0.193
	A56	16.1	0.43	GS-FCAW	0.35	4.63	-46	195.03	279	2.830	0.22	7.000	0.220
	A64	11	0.22	MCAW	0.53	2.56	-59.5	136.64		5.000	0.154	10.580	0.154
	A66	16.1	0.27	MCAW	0.53	6.56	-29.5	86.08		4.470	0.147	10.080	0.147
	A68	19.1	0.24	MCAW	0.53	2.76	-88.9	52.88		4.830	0.146	10.250	0.146
Flowing Air	FA12	6.4	0.43	P-GMAW	0.35	4.41	-52	89.8	88.8	1.417	0.181	3.417	0.187
	FA28	6.4	0.43	P-GMAW	0.53	7.76	-25.5	150.88	127.5	0.667	0.224	2.417	0.228
	FA4	6.4	0.43	SMAW	0.35	4.27	-62.5	81.77	66.9	0.500	0.200	1.417	0.204
	FA5	6.4	0.43	SMAW	0.53	5.17	-38	105.17	108.2	0.583	0.188	1.750	0.194
Water Mist Spray	WMS12	6.4	0.43	P-GMAW	0.35	4.07	-55	71.06	52.9	2.167	0.182	5.250	0.187
	WMS28	6.4	0.43	P-GMAW	0.53	7.85	-26	100.91	70.6	1.667	0.223	3.750	0.229
	WMS4	6.4	0.43	SMAW	0.35	2.53	-80	61.29	44.0	1.000	0.198	2.333	0.204
	WMS5	6.4	0.43	SMAW	0.53	5.5	-37.5	90.22	61.1	1.333	0.189	3.250	0.194
	WMS6	6.4	0.43	SMAW	0.74	11.04	-23.5	107.45	77.1	1.667	0.213	4.250	0.218
	WMS8	6.4	0.43	SMAW	0.53	5.16	-31	72.46	61.1	1.750	0.213	4.417	0.218
Water	W12	6.4	0.43	P-GMAW	0.35	3.14	-64.8	33.8	47.4	Not Investigated		5.40	0.188
	W4	6.4	0.43	SMAW	0.35	3.2	-63.3	28.8	39.4			2.50	0.206
	W5	6.4	0.43	SMAW	0.53	4.1	-50.8	37.9	55.8			3.33	0.195
	W64	11	0.22	SMAW	0.35	2	-81.1	59.25	54.2			15.00	0.154

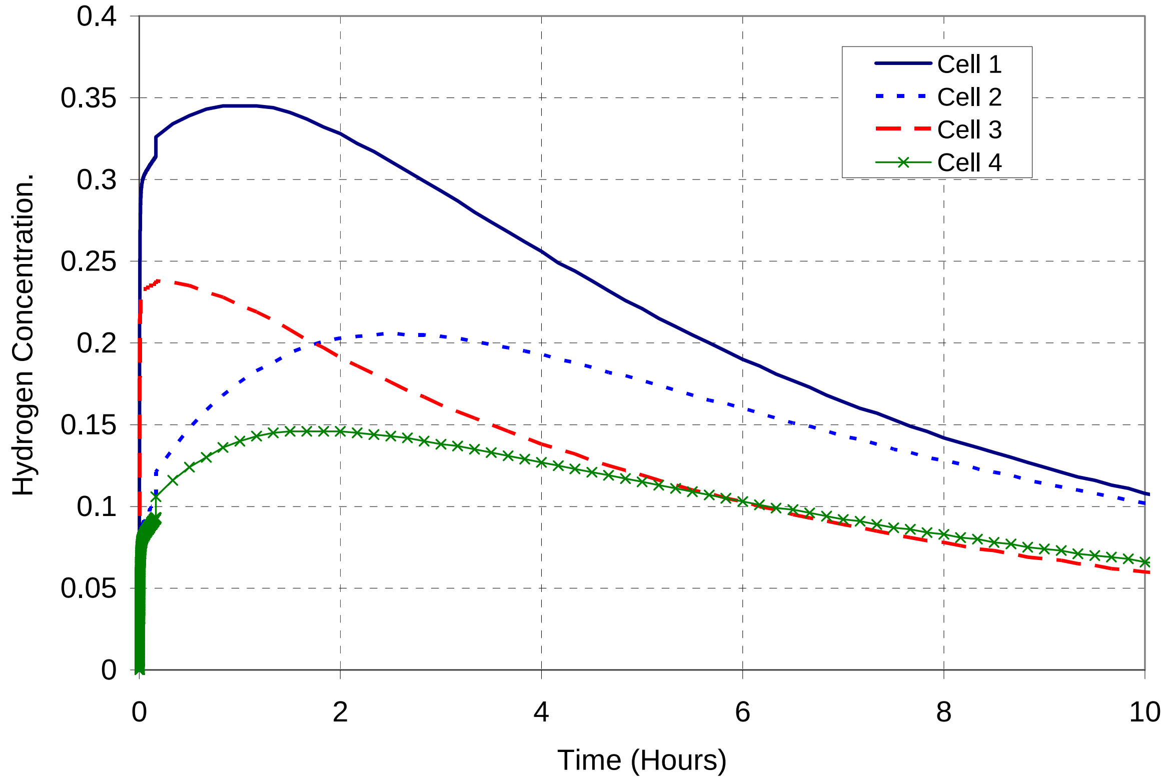

Figure 4.37: Specimen W4 – Static Water – Hydrogen vs. Time History

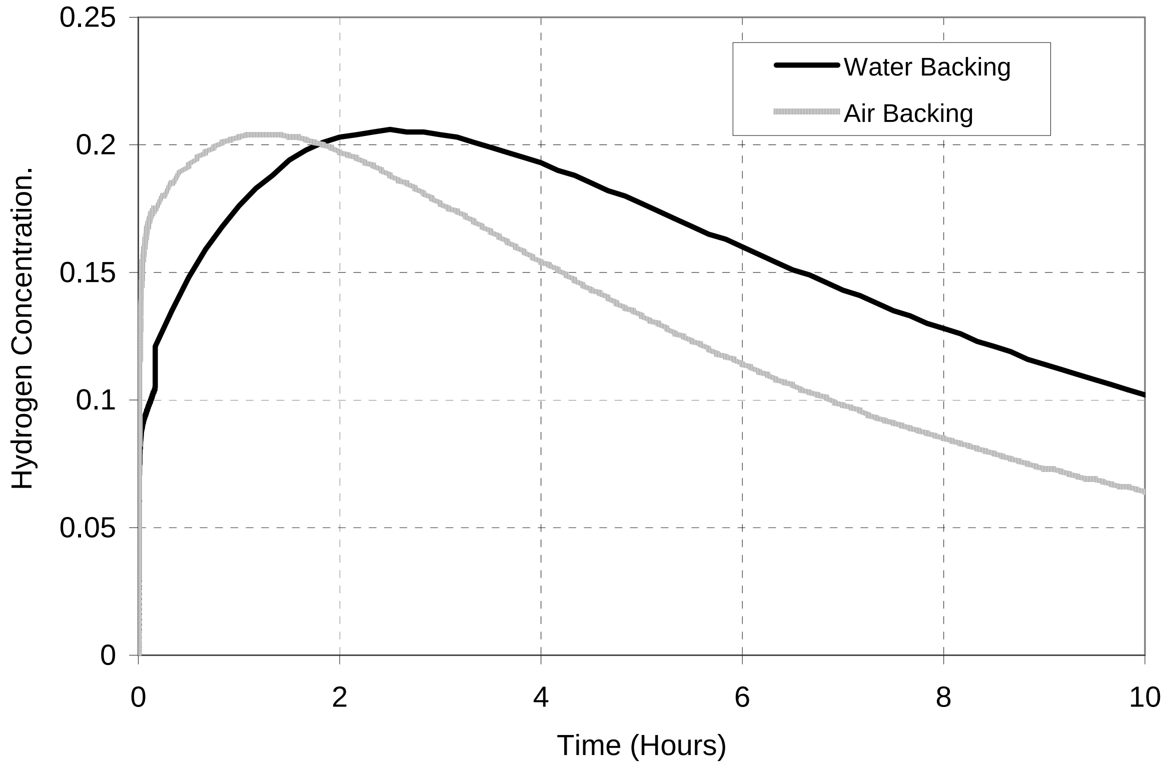

Figure 4.38: Specimen A4 & W4 – Comparison of Hydrogen Time Histories – Static Air and Static Water – Cell 2

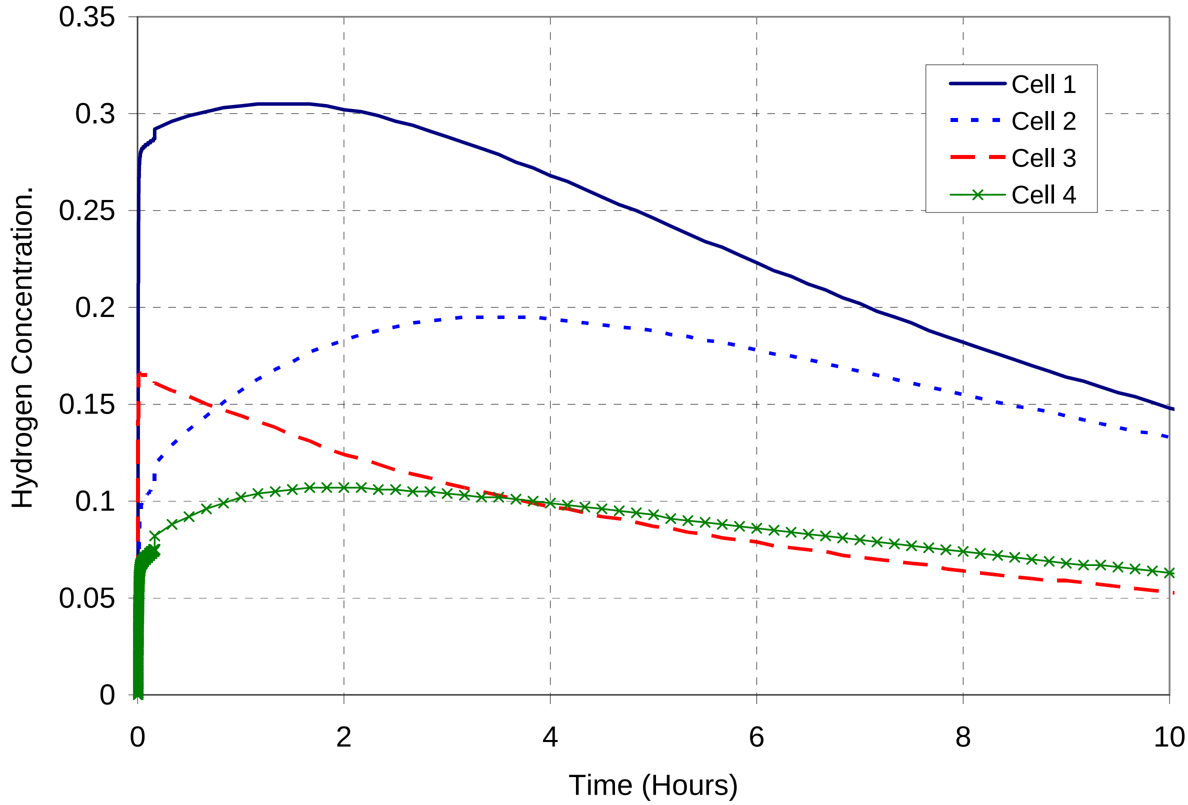

Figure 4.39: Specimen W5 – Static Water – Hydrogen vs. Time History

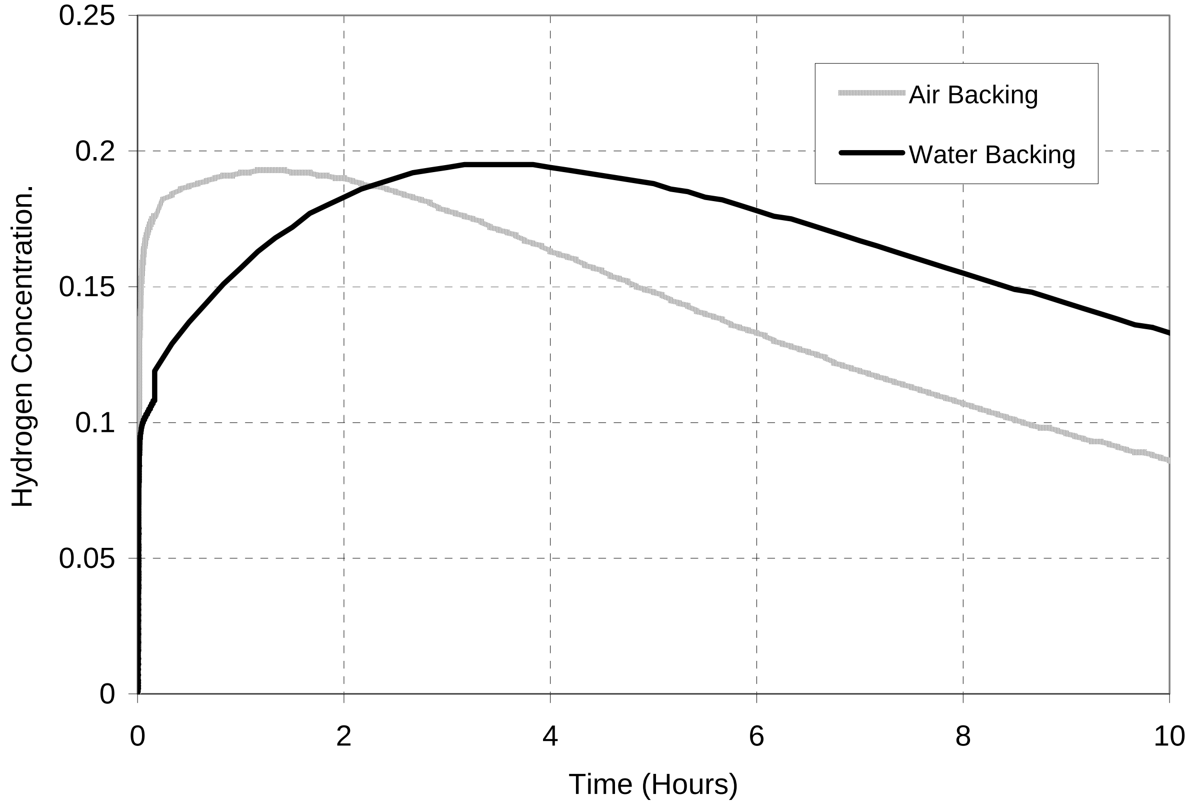

Figure 4.40: Specimen A5 & W5 – Comparison of Hydrogen Time Histories – Static Air and Static Water – Cell 2

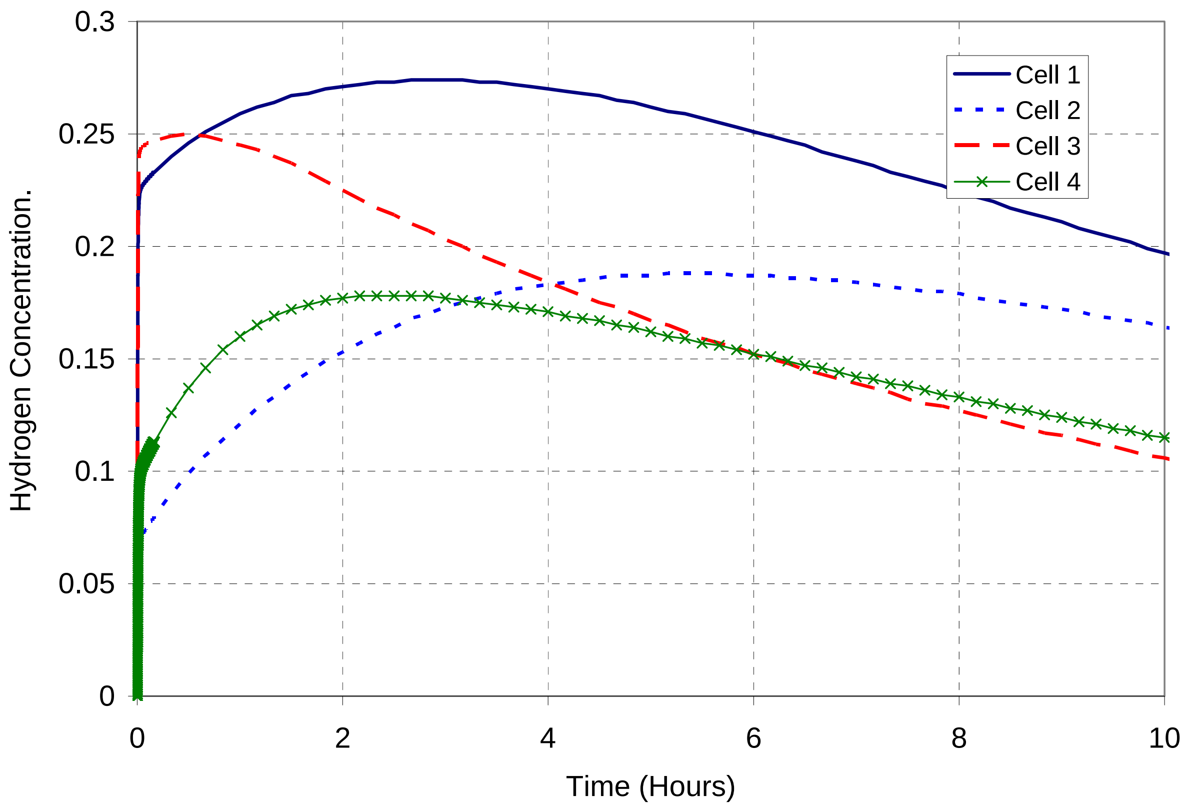

Figure 4.41: Specimen W12 – Static Water – Hydrogen vs. Time History

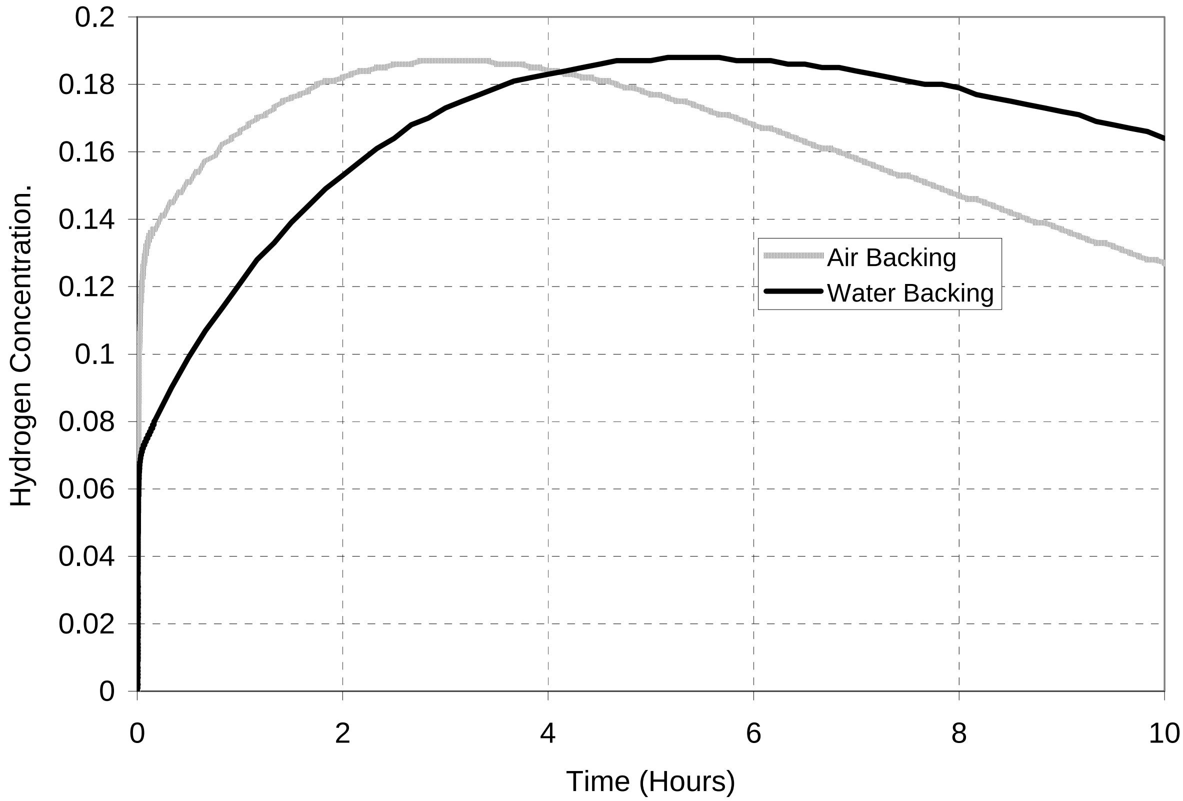

Figure 4.42: Specimen A12 & W12 – Comparison of Hydrogen Time Histories – Static Air and Static Water – Cell 2

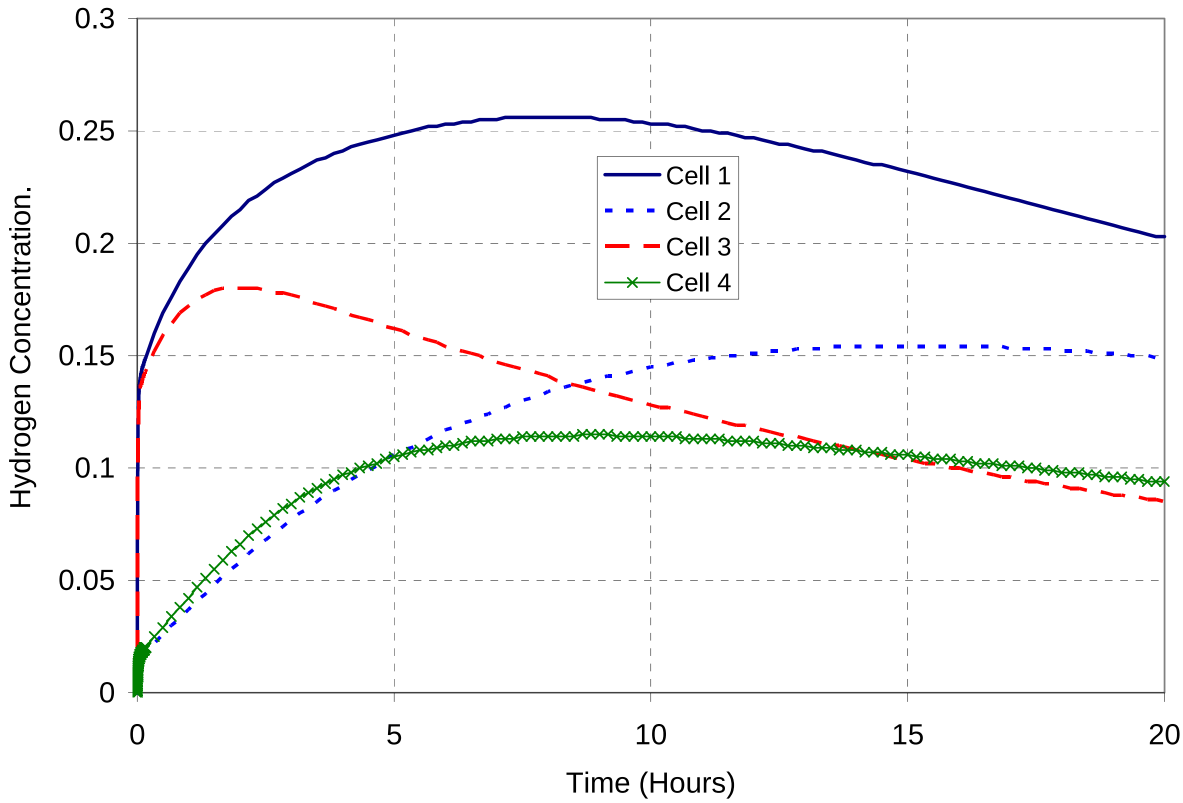

Figure 4.43: Specimen W64 – Static Water – Hydrogen vs. Time History

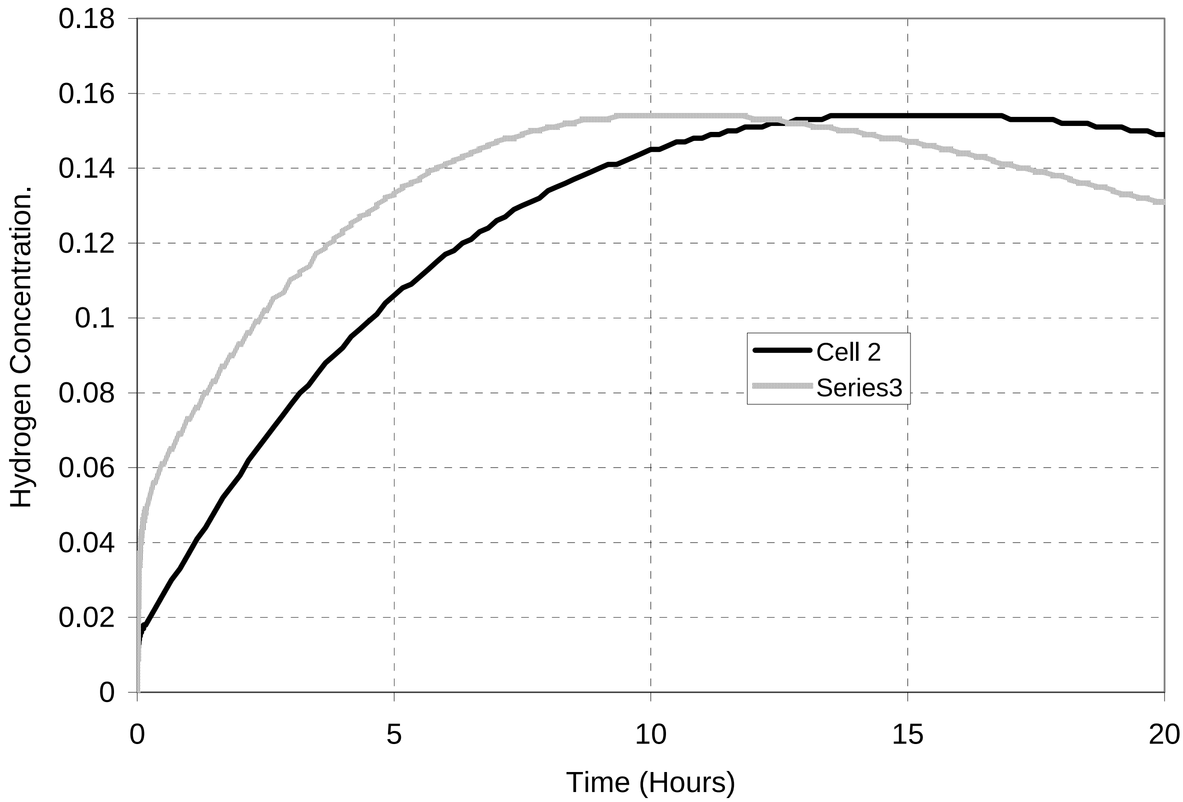

Figure 4.44: Specimen A64 & W64 – Comparison of Hydrogen Time Histories – Static Air and Static Water – Cell 2

4.9 Task 7: Weld Zone Characterization for Various Repair Scenarios

The intention of this task was to determine if susceptibility to burn-through could reduce with increasing heat sink capacity, at a given heat input level, and, if one or more processes could extend the safety envelope of in-service welding when compared back to the SMAW process.

4.9.1 Flowing Air – Bead on Pipe Welds

Each weld deposited measured a length of six (6) inches and the travel speed was maintained with mechanized travel. A 20-inch diameter fan was used to force air into the end of the pipe for the flowing air experiments to simulate environmental heat sink effects on weld cooling rates. The air speed was adjusted to achieve a consistent air speed at the back surface of each test weld at 15 MPH at ambient temperature. The air speed was measured using a calibrated anemometer and the speed is consistent with past work performed for PRCI (PRCI report ref L51713e). A hole was drilled at the mid-length of the intended test weld along the centreline, and a K-type thermocouple was inserted from the inside and exposed to the outside diameter surface. A thermocouple was also attached to the inside surface and approximately at the mid-length of the weld to measure peak back surface temperatures. Each test weld was deposited over the exposed thermocouple and was consumed by the weld metal. The weld temperature history, calculated cooling rates, and HAZ and weld metal hardness measurements from each of the welds with flowing air conditions, are shown in **Table 4.15**. All welding data is provided in **Appendix G**. A typical temperature-time plot achieved from a test weld on flowing air conditions is provided as **Figure 4.45**.

Table 4.15: Cooling Rate and Hardness Results – Flowing Air Conditions

Weld ID	Pipe Thickness (mm)	Grade	C.E	Process	Heat Input (kJ/mm)	Cooling Rate ΔT 800-500C (s)	Cooling Rate Slope at 540C (degC / sec)	Location – Ocular Reading: CGHAZ - Pipe Side 1	2	3	4	5	CG-HAZ Sleeve 1	2	3	Weld 1	2	3	4
FA1	3.2	X52	0.16	SMAW	0.35	5.57	-37.5	211	215	215	216	220							
FA2	3.2	X52	0.16	SMAW	0.53	7.73	-31	220	217	211	211	215							
FA3	3.2	X52	0.16	SMAW	0.74	10.4	-20.5	215	215	210	216	217							
FA4	6.4	X52	0.43	SMAW	0.35	4.27	-62.5	168	170	166	170	166							
FA5	6.4	X52	0.43	SMAW	0.53	5.17	-38	179	176	183	178	172							
FA6	6.4	X52	0.43	SMAW	0.74	12.52	-20	182	178	195	188	189							
FA7	6.4	X52	0.43	SMAW	1.29	20.94	-11	203	206	209	188	210							
FA8	6.4	X52	0.43	SMAW	0.53	7.78	-31.5	196	203	184	187	190							
FA9	6.4	X52	0.43	SMAW	1.29	26.86	-14.5	214	212	208	210	212							
FA10	8	X52	0.14	SMAW	0.53	4.72	-40	213	212	213	213	212							
FA11	8	X52	0.14	SMAW	1.29	13.91	-14	218	220	220	223	225							
FA12	6.4	X52	0.43	P-GMAW	0.35	4.41	-52	172	181	183	173	177							
FA14	11	X70	0.22	SMAW	0.53	3.78	-64.5	184	183	182	181	181				181	182	185	183
FA15	11	X70	0.22	SMAW	1.29	9.67	-26	194	193	194	196	193				193	189	192	194
FA16	16.1	X80	0.27	SMAW	0.53	2.95	-74	170	174	174	184	170				171	176	173	177
FA17	16.1	X80	0.27	SMAW	1.29	7.22	-34.5	181	177	179	180	181				191	192	184	192
FA18	19.1	X70	0.24	SMAW	0.53	2.44	-98	178	185	184	176	179				173	180	172	173
FA19	19.1	X70	0.24	SMAW	1.29	10.13	-23	190	190	193	195	188				193	194	193	191
FA20	3.2	X52	0.16	GMAW - RMD	0.19	2.4	-86.5	214	210	211	212	212							
FA21	3.2	X52	0.16	GMAW - RMD	0.35	5.13	-45.5	211	213	209	210	212							
FA23	6.4	X52	0.43	GMAW - RMD	0.53	5.95	-32	184	199	199	198	187							
FA24	6.4	X52	0.43	GMAW - RMD	1.29	25.32	-3	209	210	213	205	211							
FA25	3.2	X52	0.16	P-GMAW	0.19	3.39	-27	246	214	216	212	218							
FA26	3.2	X52	0.16	P-GMAW	0.35	6.9	-37	218	216	212	216	219							
FA27	3.2	X52	0.16	P-GMAW	0.53	10.97	-23	249	215	216	216	217							
FA28	6.4	X52	0.43	P-GMAW	0.53	7.76	-25.5	196	177	193	186	182							
FA29	6.4	X52	0.43	P-GMAW	1.29	26.79	-8	214	204	211	206	207							
FA30	8	X52	0.14	P-GMAW	0.53	6.51	-28	219	216	219	215	221							
FA31	8	X52	0.14	P-GMAW	1.29	23.38	-9	225	225	225	224	229							
FA32	11	X70	0.22	P-GMAW	0.53	3.49	-68.5	180	179	180	182	181				193	190	191	189
FA33	11	X70	0.22	P-GMAW	1.29	22.26	-11	200	201	198	196	198				207	207	205	206
FA34	16.1	X80	0.27	P-GMAW	0.53	3.23	-65.5	175	170	172	172	173				183	188	185	183
FA35	16.1	X80	0.27	P-GMAW	1.29	7.87	-37.5	188	182	184	181	182				198	196	194	198
FA36	19.1	X70	0.24	P-GMAW	0.53	2.82	-71.5	176	176	179	176	177				175	168	1881	182
FA37	19.1	X70	0.24	P-GMAW	1.29	9.69	-22.5	193	192	192	190	187				192	192	197	198
FA38	6.4	X52	0.43	SS-FCAW	1.06	23.73	-12	219	214	214	214	218							
FA39	6.4	X52	0.43	SS-FCAW	1.29	33.79	-5.5	213	213	212	210	215							
FA40	8	X52	0.14	SS-FCAW	1.06	17.49	-9	222	223	222	224	226							
FA41	8	X52	0.14	SS-FCAW	1.29	25.19	-9	221	228	229	228	224							
FA44	11	X70	0.22	SS-FCAW	1.29	20.21	-13.5	197	197	200	200	199				202	203	203	205
FA45	11	X70	0.22	SS-FCAW	1.99	39.3	-4.47	204	204	204	203	202				198	210	194	210
FA46	16.1	X80	0.27	SS-FCAW	1.29	8.21	-20	182	184	185	185	184				198	200	196	197
FA47	16.1	X80	0.27	SS-FCAW	1.99	17.34	-9	193	188	190	189	194				199	203	208	210
FA48	19.1	X70	0.24	SS-FCAW	1.29	8.82	-43.5	194	192	196	193	192				190	194	191	198
FA49	19.1	X70	0.24	SS-FCAW	1.99	15.55	-17	203	198	199	201	201				205	203	205	202

Weld ID	Location – Hardness (Hv5): CGHAZ - Pipe Side 1	2	3	4	5	CG-HAZ Sleeve 1	2	3	Weld 1	2	3	4	Peak Hardness (Hv5) CGHAZ Pipe	Peak Hardness (Hv5) CGHAZ Sleeve	Peak Hardness (Hv5) Weld	Average Hardness (Hv5) CGHAZ Pipe	Average Hardness (Hv5) CGHAZ Sleeve	Average Hardness (Hv5) Weld
FA1	208	201	201	199	192								208			200		
FA2	192	197	208	208	201								208			201		
FA3	201	201	210	199	197								210			201		
FA4	329	321	336	321	336								336			329		
FA5	289	299	277	293	313								313			294		
FA6	280	293	244	262	260								293			268		
FA7	225	218	212	262	210								262			226		
FA8	241	225	274	265	257								274			252		
FA9	202	206	214	210	206								214			208		
FA10	204	206	204	204	206								206			205		
FA11	195	192	192	186	183								195			190		
FA12	313	283	277	310	296								313			296		
FA14	274	277	280	283	283				283	280	271	277	283		283	279		278
FA15	246	249	246	241	249				249	260	252	246	249		260	246		252
FA16	321	306	306	274	321				317	299	310	296	321		317	306		306
FA17	283	296	289	286	283				254	252	274	252	296		274	288		258
FA18	293	271	274	299	289				310	286	313	310	299		313	285		305
FA19	257	257	249	244	262				249	246	249	254	262		254	254		250
FA20	202	210	208	206	206								210			207		
FA21	208	204	212	210	206								212			208		
FA23	274	234	234	237	265								274			249		
FA24	212	210	204	221	208								221			211		
FA25	153	202	199	206	195								206			191		
FA26	195	199	206	199	193								206			198		
FA27	150	201	199	199	197								201			189		
FA28	241	296	249	268	280								296			267		
FA29	202	223	208	218	216								223			214		
FA30	193	199	193	201	190								201			195		
FA31	183	183	183	185	177								185			182		
FA32	286	289	286	280	283				249	257	254	260	289		260	285		255
FA33	232	229	237	241	237				216	216	221	218	241		221	235		218
FA34	303	321	313	313	310				277	262	271	277	321		277	312		272
FA35	262	280	274	283	280				237	241	246	237	283		246	276		240
FA36	299	299	289	299	296				303	329	3	280	299		329	297		228
FA37	249	252	252	257	265				252	252	239	237	265		252	255		245
FA38	204	204	206	210	201								210			205		
FA39	188	186	188	185	182								188			186		
FA40	188	186	188	185	182								188			186		
FA41	190	178	177	178	185								190			182		
FA44	239	239	232	232	234				227	225	225	221	239		227	235		224
FA45	223	223	223	225	227				237	210	246	210	227		246	224		226
FA46	249	262	257	260	246				237	232	241	239	262		241	255		237
FA47	246	252	241	249	252				234	225	214	210	252		234	248		221
FA48	246	252	241	249	252				257	246	254	237	252		257	248		248
FA49	225	237	234	229	229				221	225	221	227	237		227	231		223

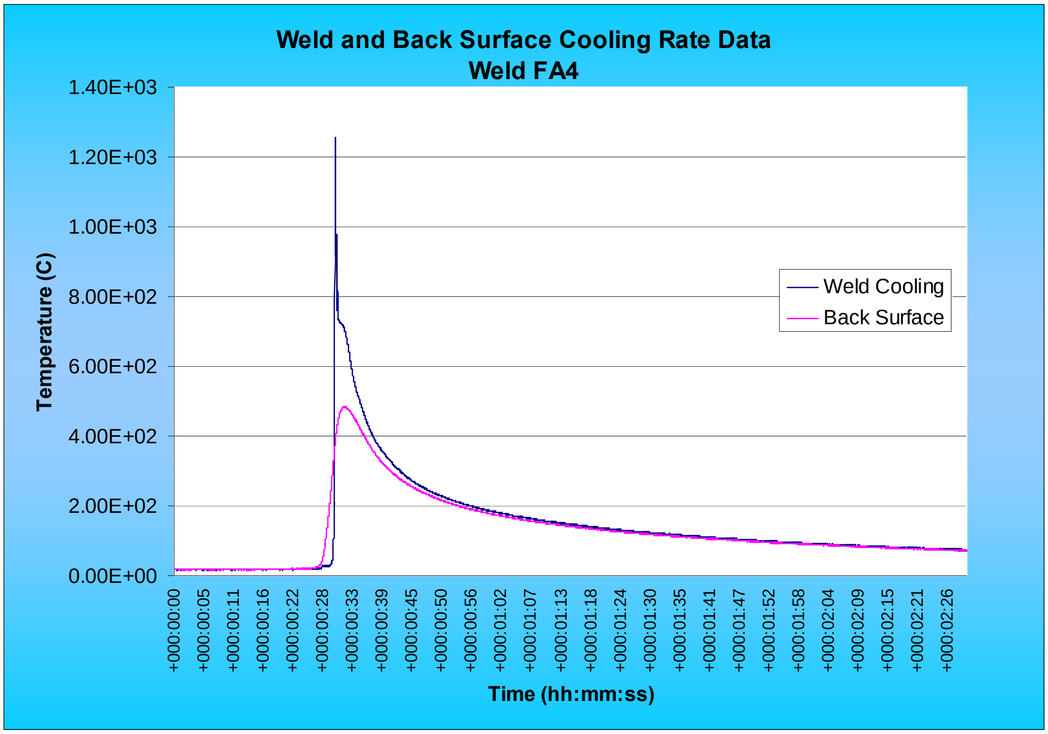

Figure 4.45: Weld and Back Surface Cooling Rate, Flowing Air Heat Sink Conditions

The sections that were removed from the mid-length of each bead on pipe each (outside the contamination zone from the melted thermocouple) for HAZ hardness measurements for flowing air conditions are shown in **Appendix H**.

Trends were plotted between heat input and HAZ hardness for each weld / process over the range of materials evaluated. **Figure 4.46** is a plot for welds deposited on NPS 20 grade X52 with a CE of 0.43 under flowing air conditions with each process. This plot shows that for a given heat input the differences in weld process arc efficiency has a direct influence on weld cooling rate and thus HAZ hardness. For example, the SS-FCAW process is a higher arc efficiency process compared to SMAW, and therefore transfers heat more efficiently at a given heat input in comparison. This higher arc efficiency at a given heat input results in slower weld cooling rates and a lower HAZ hardness.

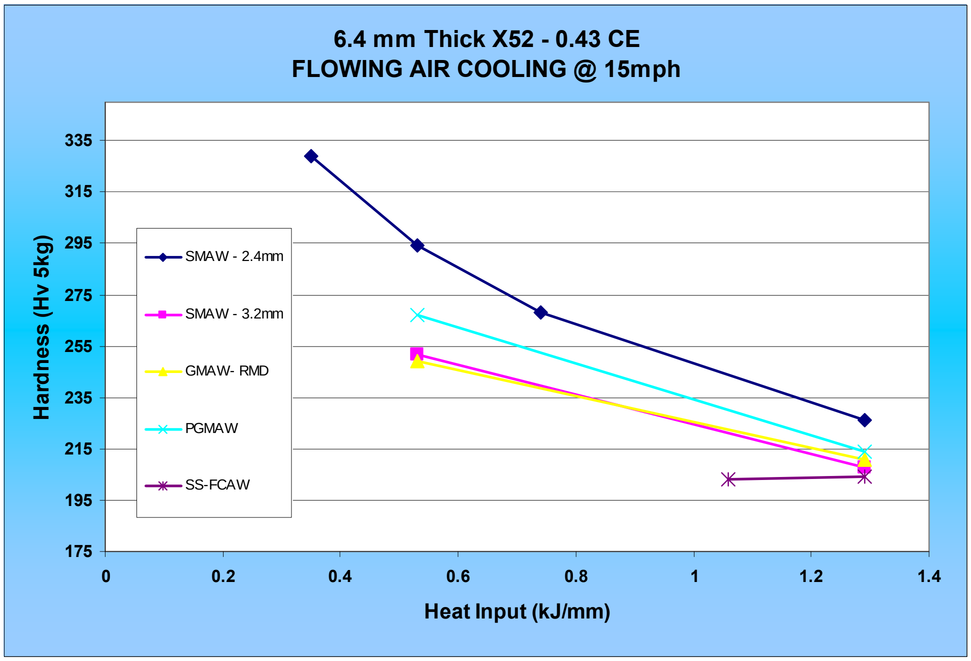

Figure 4.46: Heat Input vs. HAZ Hardness, Flowing Air Conditions

4.9.2 Water Mist Spray – Bead on Pipe Welds

Each weld deposited measured a length of six (6) inches and the travel speed was maintained with mechanized travel. A water mist nozzle system (consisting of spray nozzle, feed water, and compressed air), was used to simulate natural gas heat sink conditions and its affect on weld cooling rates over a range of material thicknesses, types, and welding procedures. To ensure consistency from one test to another, the air pressure and water feed rate to the spray nozzle was controlled by calibrated metering valves. The air pressure was adjusted to achieve an average flow rate of 5.5 meters per second (m/sec) at the back surface of each test weld, and the air speed was measured using an anemometer. The water pressure was adjusted to achieve a fine mist and wide spray pattern from the spray nozzle for maximum pipe wall coverage. To ensure the same spray pattern was used for all test welds, the indexed metering valves were locked to achieve a consistent air pressure and water flow rate. To determine if the flowing water mist spray would provide sufficient heat sink to achieve the cooling conditions of a in-service flowing natural gas pipelines, heat sink capacity spot heating tests were conducted to determine the 250°C to 100°C cooling times (procedure as specified in PRCI report L51713e) on the NPS 20 x 6.4mm wall X52 pipe. The results of spot heating tests provided an average cooling time of 23 sec from 250°C to 100°C. The linear flow rate and resulting heat sink cooling capacity measurements are within the range of tests from past research for PRCI (PRCI report ref. L51713e), conducted on the High Pressure Loop at the GRI Metering Research Facility, on a simulated 6.4mm wall natural gas pipeline flowing at a volumetric flow rate of 16.9 mmscfd.

A hole was drilled at the mid-length of the intended test weld location and along its centreline, and a K-type thermocouple was inserted from the inside diameter and exposed to the outside diameter surface. The temperature of the flowing water mist spray was measured with a thermocouple attached to the back surface of the test weld before welding commenced, and the temperature ranged from 10 to 12°C for all welds deposited. The test weld was deposited over the exposed thermocouple and was consumed by the weld metal. The weld temperature history, calculated cooling rates, and HAZ and weld metal hardness measurements from each of the welds deposited with flowing water mist spray, are shown in **Table 4.16**. All welding data is provided in **Appendix I**. A typical temperature-time plot achieved from a test weld, and the back surface, with flowing water mist spray conditions is provided as **Figure 4.47**.

Table 4.16: Cooling Rate and Hardness Data vs. Process – Water Mist Spray Conditions

Weld ID	Pipe Thickness	Grade	C.E	Process	Heat Input	Cooling Rate		Location																													
								Ocular Reading												Hardness (Hv5)																	
						ΔT 800-500C	Slope at 540C	CGHAZ - Pipe Side					CG-HAZ Sleeve			Weld				CGHAZ - Pipe Side					CG-HAZ Sleeve			Weld				Peak Hardness (Hv5)			Average Hardness (Hv5)		
	(mm)				(kJ/mm)	(s)	(degC / sec)	1	2	3	4	5	1	2	3	1	2	3	4	1	2	3	4	5	1	2	3	1	2	3	4	CGHAZ Pipe	CGHAZ Sleeve	Weld	CGHAZ Pipe	CGHAZ Sleeve	Weld
WMS1	3.2	X52	0.16	SMAW	0.35	4.72	-51	214	216	218	218	216								202	199	195	195	199								202			198		
WMS2	3.2	X52	0.16	SMAW	0.53	7.05	-31	211	212	214	214	216								208	206	202	202	199								208			204		
WMS3	3.2	X52	0.16	SMAW	0.74	11.98	-23	212	213	213	212	217								206	204	204	206	197								206			204		
WMS4	6.4	X52	0.43	SMAW	0.35	2.53	-80	155	152	159	150	156								386	401	367	412	381								412			389		
WMS5	6.4	X52	0.43	SMAW	0.53	5.5	-37.5	186	180	182	176	184								268	286	280	299	274								299			281		
WMS6	6.4	X52	0.43	SMAW	0.74	11.04	-23.5	194	197	178	175	196								246	239	293	303	241								303			264		
WMS7	6.4	X52	0.43	SMAW	1.29	20.17	-17	205	212	209	202	203								221	206	212	227	225								227			218		
WMS8	6.4	X52	0.43	SMAW	0.53	5.16	-31	167	174	182	182	185								332	306	280	280	271								332			294		
WMS9	6.4	X52	0.43	SMAW	1.29	16.75	-2.5	204	208	212	214	212								223	214	206	202	206								223			210		
WMS10	8	X52	0.14	SMAW	0.53	3.59	-57	211	216	215	214	212								208	199	201	202	206								208			203		
WMS11	8	X52	0.14	SMAW	1.29	15.74	-17.5	227	226	222	221	221								180	182	188	190	190								190			186		
WMS12	6.4	X52	0.43	P-GMAW	0.35	4.07	-55	175	177	200	178	183								303	296	232	293	277								303			280		
WMS14	11	X70	0.22	SMAW	0.53	3.21	-66.5	182	186	184	182	182				183	187	187	184	280	268	274	280	280				277	265	265	274	280		277	276		270
WMS15	11	X70	0.22	SMAW	1.29	12.56	-11.5	202	195	196	197	200				197	199	200	194	227	244	241	239	232				239	234	232	246	244		246	237		238
WMS16	16.1	X80	0.27	SMAW	0.53	3.19	-66.5	172	173	171	172	174				180	181	179	183	313	310	317	313	306				286	283	289	277	317		289	312		284
WMS17	16.1	X80	0.27	SMAW	1.29	5.36	-57	184	184	185	183	183				190	192	192	192	274	274	271	277	277				257	252	252	252	277		257	274		253
WMS18	19.1	X70	0.24	SMAW	0.53	2.72	-60.5	174	181	181	181	180				179	181	186	183	306	283	283	283	286				289	283	268	277	306		289	288		279
WMS19	19.1	X70	0.24	SMAW	1.29	6.62	-34	188	191	193	193	190				193	193	191	191	262	254	249	249	257				249	249	254	254	262		254	254		252
WMS20	3.2	X52	0.16	GMAW - RMD	0.19	1.91	-91.5	212	208	210	206	207								206	214	210	218	216								218			213		
WMS21	3.2	X52	0.16	GMAW - RMD	0.35	4.41	-17.5	212	207	210	210	210								206	216	210	210	210								216			211		
WMS22	3.2	X52	0.16	GMAW - RMD	0.53	6.84	-31.5	211	215	210	216	210								208	201	210	199	210								210			206		
WMS23	6.4	X52	0.43	GMAW - RMD	0.53	6.25	-32	191	184	196	181	196								254	274	241	283	241								283			259		
WMS24	6.4	X52	0.43	GMAW - RMD	1.29	27.81	-8.5	209	211	205	208	207								212	208	221	214	216								221			214		
WMS25	3.2	X52	0.16	P-GMAW	0.19	3	-71.5	217	211	211	212	213								197	208	208	206	204								208			205		
WMS26	3.2	X52	0.16	P-GMAW	0.35	6.31	-46	208	205	211	206	208								214	221	208	218	214								221			215		
WMS27	3.2	X52	0.16	P-GMAW	0.53	10.15	-48	215	213	217	213	215								201	204	197	204	201								204			201		
WMS28	6.4	X52	0.43	P-GMAW	0.53	7.85	-26	176	178	190	192	190								299	293	257	252	257								299			271		
WMS29	6.4	X52	0.43	P-GMAW	1.29	25.58	-11	222	212	179	176	177								188	206	289	299	296								299			256		
WMS30	8	X52	0.14	P-GMAW	0.53	5.46	-39.5	220	215	217	213	217								192	201	197	204	197								204			198		
WMS31	8	X52	0.14	P-GMAW	1.29	26.72	-6	222	232	227	224	223								188	172	180	185	186								188			182		
WMS32	11	X70	0.22	P-GMAW	0.53	3.48	-77.5	183	181	184	184	186				185	190	185	191	277	283	274	274	268				271	257	271	254	283		271	275		263
WMS33	11	X70	0.22	P-GMAW	1.29	12.84	-17	195	194	196	196	198				203	206	206	204	244	246	241	241	237				225	218	218	223	246		225	242		221
WMS34	16.1	X80	0.27	P-GMAW	0.53	2.75	-97	173	172	173	173	175				183	180	181	180	310	313	310	310	303				277	286	283	286	313		286	309		283
WMS35	16.1	X80	0.27	P-GMAW	1.29	9.09	-20	186	177	187	179	186				195	201	197	199	268	296	265	289	268				244	229	239	234	296		244	277		237
WMS36	19.1	X70	0.24	P-GMAW	0.53	1.71	-106	177	178	177	173	175				176	168	181	174	296	293	296	310	303				299	329	283	306	310		329	299		304
WMS37	19.1	X70	0.24	P-GMAW	1.29	7.41	-40.5	188	188	189	186	190				193	191	192	190	262	262	260	268	257				249	254	252	257	268		257	262		253
WMS38	6.4	X52	0.43	SS-FCAW	1.06	26.44	-8	211	208	211	207	209								208	214	208	216	212								216			212		
WMS39	6.4	X52	0.43	SS-FCAW	1.29	33.07	-3	209	206	212	208	213								212	218	206	214	204								218			211		
WMS40	8	X52	0.14	SS-FCAW	1.06	19.51	-12.5	220	223	229	224	226								192	186	177	185	182								192			184		
WMS41	8	X52	0.14	SS-FCAW	1.29	26.7	-6	228	221	227	222	224								178	190	180	188	185								190			184		
WMS44	11	X70	0.22	SS-FCAW	1.29	12.57	-22	195	199	203	198	199				205	205	206	204	244	234	225	237	234				221	221	218	223	244		223	235		221
WMS45	11	X70	0.22	SS-FCAW	1.99	29.54	-9	203	205	206	201	199				211	212	209	212	225	221	218	229	234				208	206	212	206	234		212	226		208
WMS46	16.1	X80	0.27	SS-FCAW	1.29	8.01	-20	183	185	186	184	183				194	196	197	197	277	271	268	274	277				246	241	239	239	277		246	273		241
WMS47	16.1	X80	0.27	SS-FCAW	1.99	15.59	-11.5	194	192	191	190	186				204	205	208	208	246	252	254	257	268				223	221	214	214	268		223	255		218
WMS48	19.1	X70	0.24	SS-FCAW	1.29	6.46	-36.5	196	190	202	194	192				195	197	190	192	241	257	227	246	252				244	239	257	252	257		257	245		248
WMS49	19.1	X70	0.24	SS-FCAW	1.99	11.68	-26.5	193	198	202	197	199				205	205	201	207	249	237	227	239	234				221	221	229	216	249		229	237		222

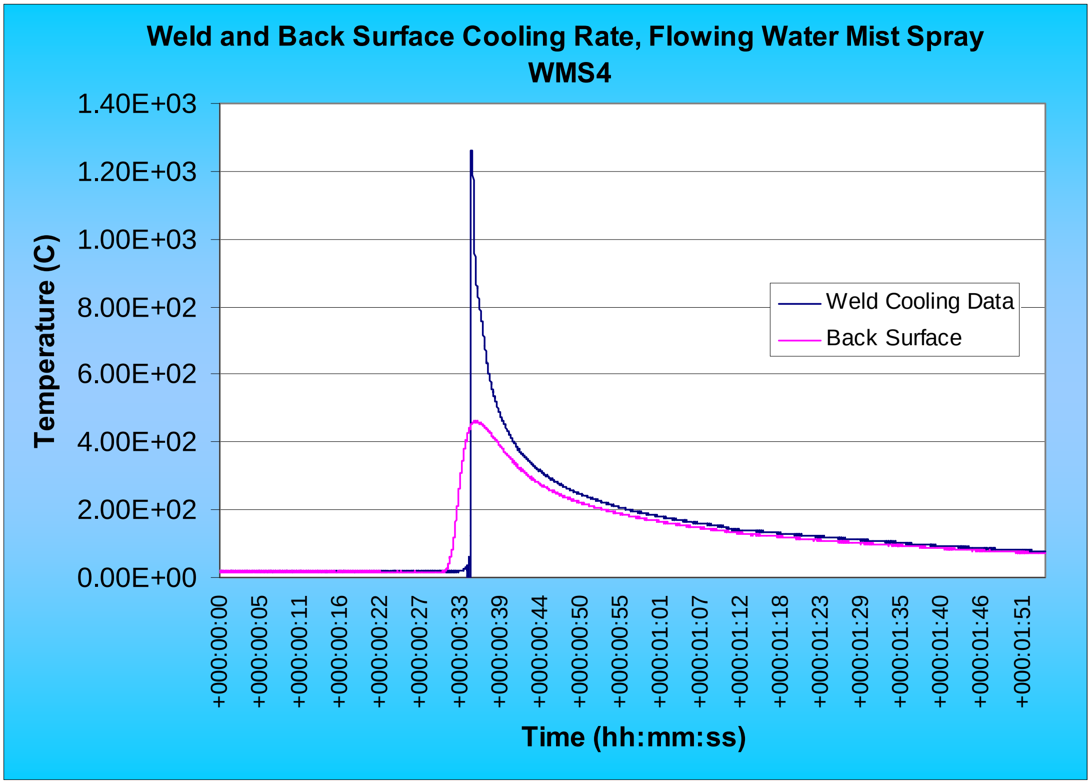

Figure 4.47: Weld and Back Surface Cooling Rate, Flowing Water Mist Spray

The sections that were removed from the mid-length of each bead on pipe weld (outside the contamination zone from the melted thermocouple) for HAZ hardness measurements for flowing air conditions are shown in **Appendix J**.

Trends were plotted between heat input and HAZ hardness for each weld / process over the range of materials evaluated. **Figure 4.48** is a plot for welds deposited on 0.43 CE X52 under flowing water mist spray conditions with each process. This plot shows that for a given heat input the differences in weld process arc efficiency has a direct influence on weld cooling rate and thus HAZ hardness. For example, the SS-FCAW process is a higher arc efficiency process compared to SMAW, and therefore transfers heat more efficiently at a given heat input in comparison. This higher arc efficiency at a given heat input results in slower weld cooling rates and a lower HAZ hardness.

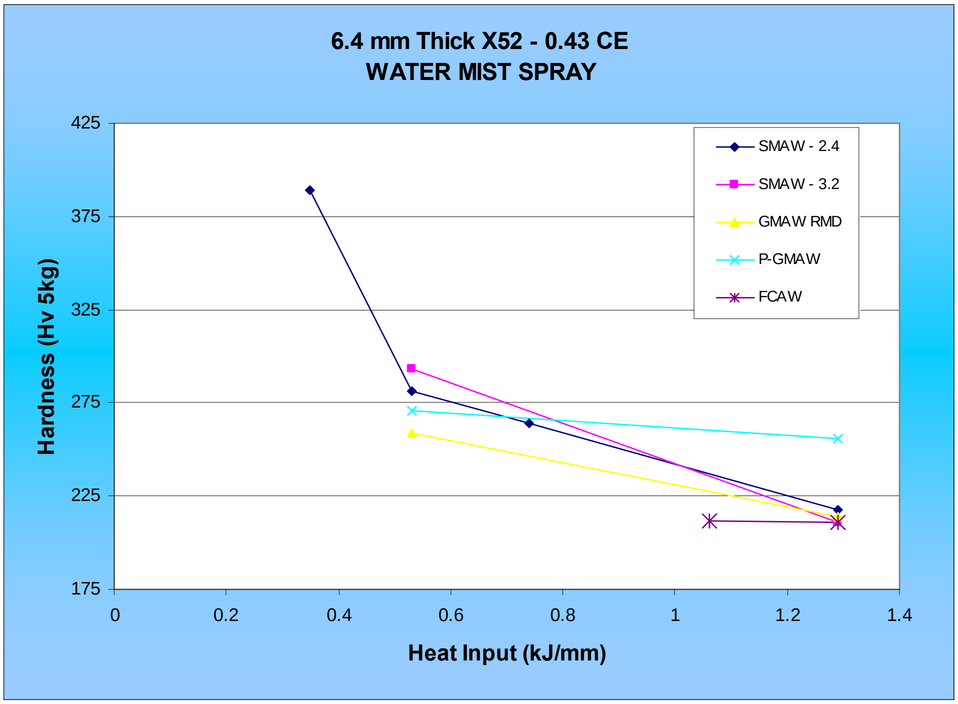

Figure 4.48: Heat Input vs. HAZ Hardness, Flowing Water Mist Spray

To examine the differences in arc efficiency between each of the welding processes and its influence on cooling rate, a trend is plotted for 0.53 kJ/mm and 1.29 kJ/mm heat inputs in **Figures 4.49** and **4.50**, respectively, for each process and conditions between static air, flowing air, and water mist spray. These plots demonstrate that cooing time from 1000°C to 100°C rate is less affected by the “external” cooling conditions or the process as thickness increases at the lower heat input setting, compared to at the higher heat input. As heat input increases the differences between arc efficiency of each process and cooling rate become more apparent. These plots also demonstrate that the heat sink has less of an influence on cooling rates as the pipe wall thickness approaches 20mm, in other words it is likely that the cooling rate of welds deposited on 20mm and higher thickness will not be influenced by the flowing fluid/gas. In addition, these plots demonstrate that for a given heat input, welding process, and heat sink condition, the SMAW process has the fastest cooling rate compared to the other welding processes. The SS-FCAW and P-GMAW processes provide the slowest cooling times and could be beneficial in terms of allowing more time for hydrogen to escape from the weld pool before returning to ambient or service temperature, and reduce the risk of hydrogen cracking. Furthermore, these plots demonstrate the effect of accelerated cooling as thickness decreases, as the flowing conditions draw more heat from the weld pool. For the low heat input welds, the effect of heat sink becomes most noticeable at a thickness of 6.4mm, as opposed to the higher heat input welds at 11mm, regardless of the welding process used.

In addition, each of the welds evaluated under static air, flowing air, and water mist spray were plotted for cooling rate (slope @ 540°C) vs. CGHAZ hardness, irrespective of the welding process or simulated in-service welding condition. The results are shown in **Figure 4.51**, and demonstrate how each material behaves with respect to cooling rate and hardness. As the pipeline materials carbon equivalent increases the slope of the hardening curves increases rapidly with increasing (higher) cooling rates. This type of plot could be useful for identifying lower heat input and cooling rate boundaries for specific material chemistries in order to produce a weld CGHAZ hardness below a desirable level to avoid cracking.

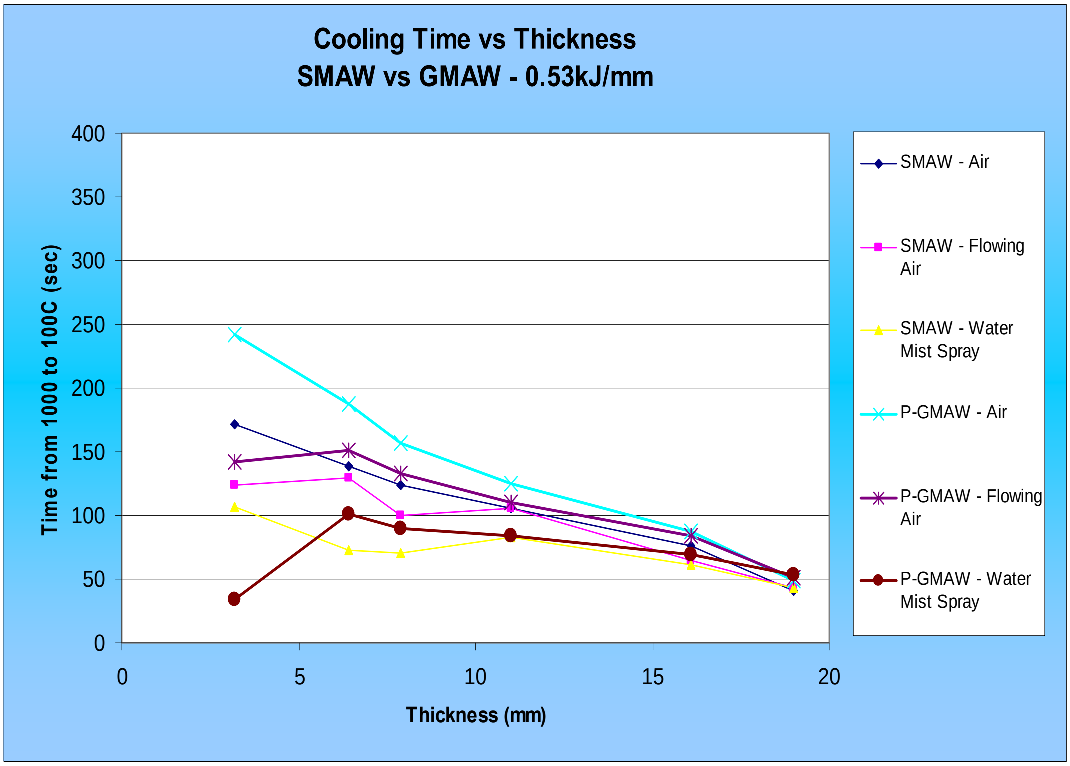

Figure 4.49: Cooling Time vs. Welding Process, 0.53kJ/mm Heat Input

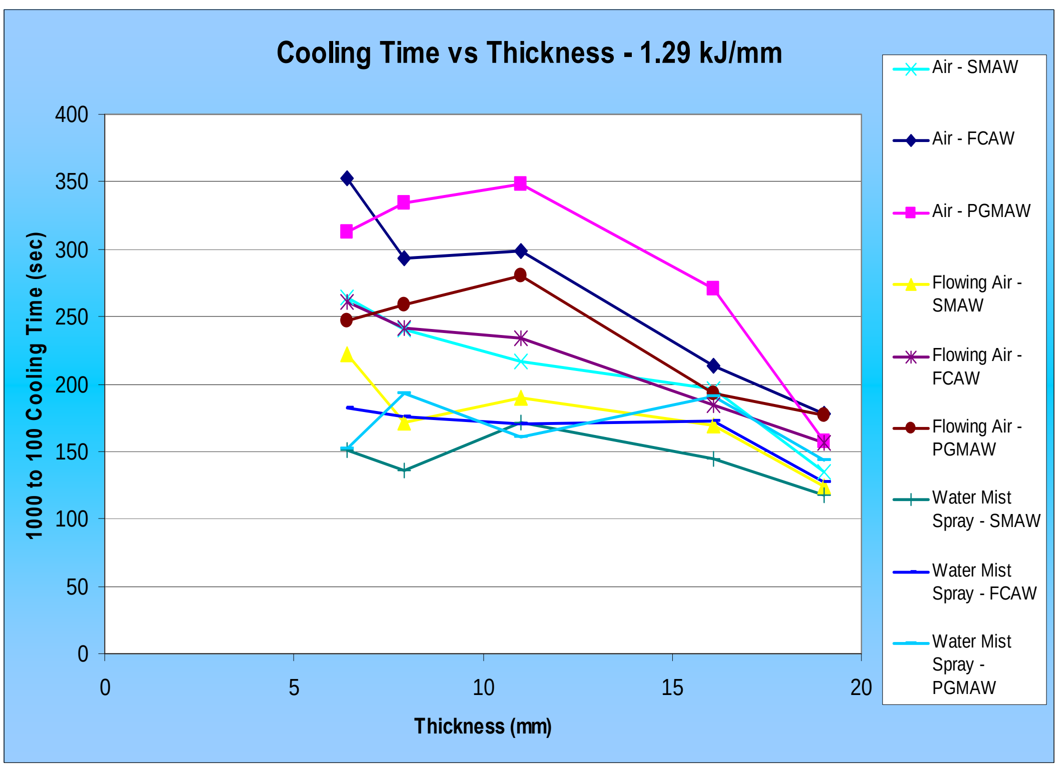

Figure 4.50: Cooling Time vs. Thickness, 1.29kJ/mm Heat Input

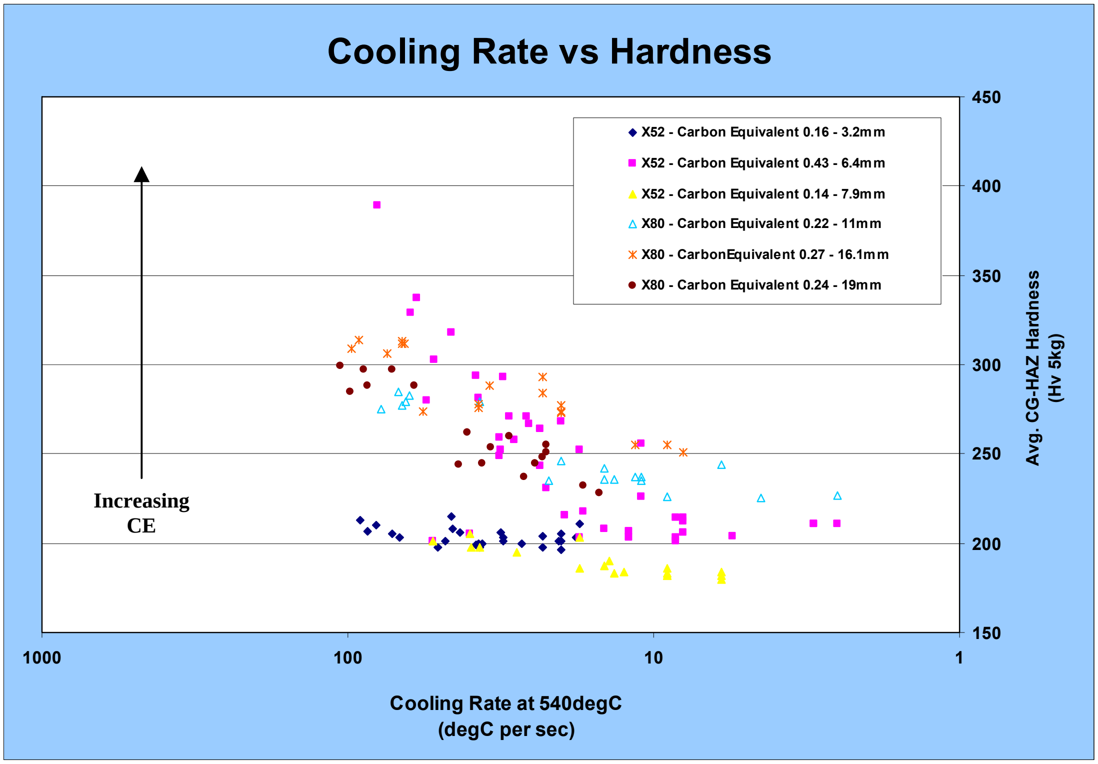

Figure 4.51: Coarse Grain Heat Affected Zone (CG-HAZ) Hardness (Hv) vs. Cooling Rate and Carbon Equivalent (CE), Regardless of Heat Sink Condition

4.9.3 Air and Water Backed Results for Bead on Pipe and Sleeve Fillet Welds

Sleeve fillet and bead on pipe welds were manufactured with both air and water backing to demonstrate how the cooling rates of the sleeve fillet welds compare back to the welds deposited on pipe with air backing. The plots of heat input vs. CGHAZ hardness for bead on pipe welds with air backing and each process in **Figures 4.28** to **4.32** can be referenced. To re-summarize, these plots shown a general trend of decreasing hardness with increasing heat input as expected, however there is an even more interesting trend that shows the SMAW process results in the highest hardness at a given heat input level, with a downward trend in hardness vs. process at a given heat input level from the PGMAW to FCAW to PMCAW processes. This indicates that the processes with the higher arc efficiencies (i.e., transfer more heat from the arc to the base material) result in lower CGHAZ hardnesses regardless of material type and thickness. Based on these results, the SMAW process has the lowest arc efficiency (as demonstrated by the highest hardness) and the PMCAW has the highest arc efficiency (as demonstrated by the lowest hardness).

The set-up for fillet welding the sleeves and bead on pipe welds with water backing was illustrated previously in **Figure 4.20**. In the case of the sleeves, thermocouples were positioned along the weld axis on the back surface, at the weld fusion line, and 10mm away from the edge of the sleeve, as shown in **Figure 4.52**.

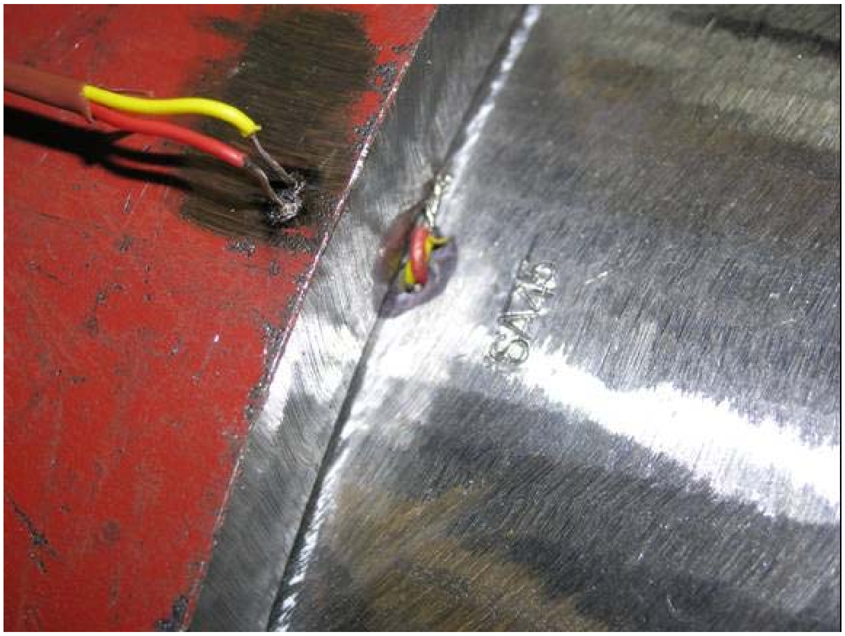

Figure 4.52: Thermocouple Locations

An example of a typical thermal history from each of the thermocouple positions is shown in **Figure 4.53**. For bead on plate welds, thermocouples were located as per previous tasks. Epoxy resin was used to seal the hole for the weld thermocouple to avoid water coming through and contaminating the weld. From each of the welds manufactured the cooling time (800 to 500°C), cooling rate (slope at 540°C), and peak back surface temperature were calculated. The cooling rate data and hardness results for the bead on pipe welds with water backing are shown in **Table 4.17** (note all welding data was provided as Appendix E), whereas the data for the sleeve fillet welds for air and water backing, are shown in **Tables 4.18** and **4.19**, respectively. All welding data for sleeve fillet welds with air and water backing are provide in **Appendix K** and **Appendix L**.

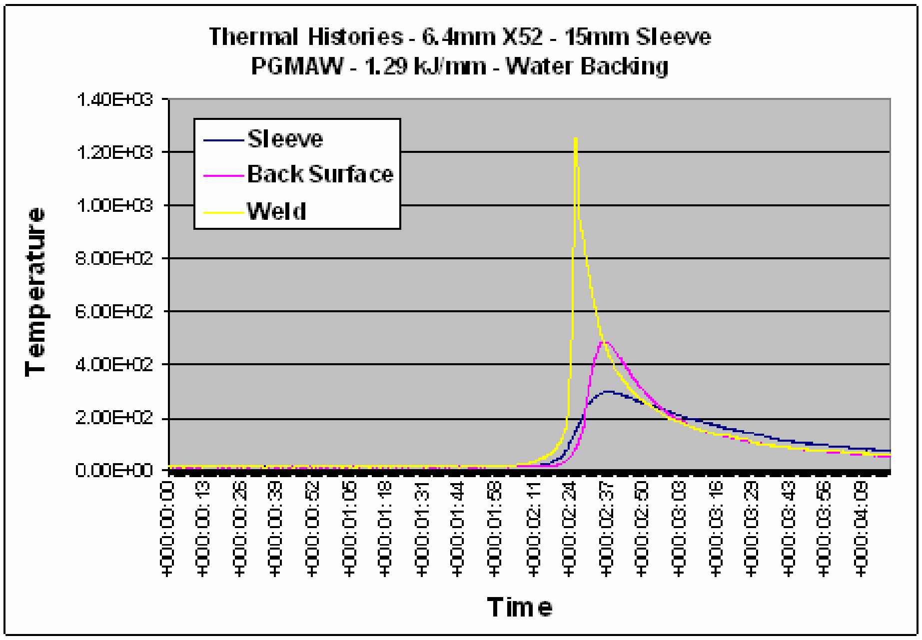

Figure 4.53: Typical Thermocouple Output

Table 4.17: Cooling Data and Hardness Results – Bead on Pipe – Water Backing

Weld ID	Pipe Thickness	Grade	C.E	Process	Heat Input	Cooling Rate		Location																								Peak Hardness (Hv5)			Average Hardness (Hv5)		
	(mm)				(kJ/mm)	ΔT 800-500C (s)	Slope at 540C (degC / sec)	Ocular Reading												Hardness (Hv5)												CGHAZ Pipe	CGHAZ Sleeve	Weld	CGHAZ Pipe	CGHAZ Sleeve	Weld
								CGHAZ - Pipe Side					CG-HAZ Sleeve			Weld				CGHAZ - Pipe Side					CG-HAZ Sleeve			Weld									
								1	2	3	4	5	1	2	3	1	2	3	4	1	2	3	4	5	1	2	3	1	2	3	4						
FW4	6.4	X52	0.43	SMAW	0.35	3.16	-63.25	162	165	175	183	161				198	196	195	196	353	341	303	277	358				237	241	244	241	358		244	326		241
FW5	6.4	X52	0.43	SMAW	0.53	4.12	-50.75	160	167	189	174	158				195	195	189	197	362	332	260	306	371				244	244	260	239	371		260	326		247
FW6	6.4	X52	0.43	SMAW	0.74	6.16	-33	182	183	195	168	179				204	205	205	206	280	277	244	329	289				223	221	221	218	329		223	284		221
FW7	6.4	X52	0.43	SMAW	1.29	10.92	-17.25	194	195	182	208	194				205	209	206	206	246	244	280	214	246				221	212	218	218	280		221	246		217
FW8	6.4	X52	0.43	SMAW	0.53	6.6	-27.25	196	195	196	165	173				202	203	202	203	241	244	241	341	310				227	225	227	225	341		227	275		226
FW9	6.4	X52	0.43	SMAW	1.29	16.04	-13.625	195	203	213	204	199				212	210	208	214	244	225	204	223	234				206	210	214	202	244		214	226		208
FW10	8	X52	0.14	SMAW	0.53	6.1	-44.4	213	216	224	218	217				199	200	199	199	204	199	185	195	197				234	232	234	234	204		234	196		234
FW11	8	X52	0.14	SMAW	1.29	5.75	-40.7	209	213	217	209	210				199	197	200	197	212	204	197	212	210				234	239	232	239	212		239	207		236
FW12	6.4	X52	0.43	P-GMAW	0.35	3.12	-64.75	155	155	180	150	150				190	189	189	189	386	386	286	412	412				257	260	260	260	412		260	376		259
FW14	11	X70	0.22	SMAW	0.53	3.55	-59.2	179	179	179	179	179				180	184	178	183	289	289	289	289	289				286	274	293	277	289		293	289		282
FW15	11	X70	0.22	SMAW	1.29	6.25	-57.4	190	189	189	190	190				191	193	192	191	257	260	260	257	257				254	249	252	254	260		254	258		252
FW23	6.4	X52	0.43	GMAW - RMD	0.53	6.8	-27.875	177	175	201	169	177				200	199	197	197	296	303	229	325	296				232	234	239	239	325		239	290		236
FW24	6.4	X52	0.43	GMAW - RMD	1.29	15.28	-13	197	195	210	189	200				211	205	206	204	239	244	210	260	232				208	221	218	223	260		223	237		218
FW28	6.4	X52	0.43	P-GMAW	0.53	5.56	-36.25	167	171	194	181	177				201	200	200	201	332	317	246	283	296				229	232	232	229	332		232	295		231
FW29	6.4	X52	0.43	P-GMAW	1.29	24.64	-9.25	204	194	214	183	207				213	213	216	214	223	246	202	277	216				204	204	199	202	277		204	233		202
FW30	8	X52	0.14	P-GMAW	0.53	3.9	-48.7	215	217	220	213	217				201	201	196	197	201	197	192	204	197				229	229	241	239	204		241	198		235
FW31	8	X52	0.14	P-GMAW	1.29	24.3	-7.9	220	226	223	226	225				218	214	214	214	192	182	186	182	183				195	202	202	202	192		202	185		201
FW32	11	X70	0.22	P-GMAW	0.53	3.05	-75.1	178	179	179	177	176				181	181	186	183	293	289	289	296	299				283	283	268	277	299		283	293		278
FW33	11	X70	0.22	P-GMAW	1.29	7.35	-33.2	178	177	177	178	178				185	189	187	192	293	296	296	293	293				271	260	265	252	296		271	294		262
FW50	6.4	X52	0.43	GS-FCAW	1.06	14.44	-19.875	198	210	212	186	205				204	202	199	207	237	210	206	268	221				223	227	234	216	268		234	228		225
FW51	6.4	X52	0.43	GS-FCAW	1.29	16.2	-11.5	205	202	192	179	202				211	203	209	214	221	227	252	289	227				208	225	212	202	289		225	243		212
FW52	8	X52	0.14	GS-FCAW	1.06	6.15	-22.2	209	209	216	212	208				194	200	196	199	212	212	199	206	214				246	232	241	234	214		246	209		238
FW53	8	X52	0.14	GS-FCAW	1.29	23.4	-10.3	224	224	222	222	222				216	216	216	217	185	185	188	188	188				199	199	199	197	188		199	187		198
FW54	11	X70	0.22	GS-FCAW	1.29	7.7	-28.57	190	191	191	190	189				194	193	198	193	257	254	254	257	260				246	249	237	249	260		249	256		245
FW55	11	X70	0.22	GS-FCAW	1.99	27.9	-6.3	200	194	196	196	200				200	202	203	205	232	246	241	241	232				232	227	225	221	246		232	239		226
FW60	6.4	X52	0.43	MCAW	0.53	7.48	-22.375	170	175	196	181	183				200	203	201	199	321	303	241	283	277				232	225	229	234	321		234	285		230
FW61	6.4	X52	0.43	MCAW	1.29	20.92	-11.375	200	194	219	196	205				211	214	215	214	232	246	193	241	221				208	202	201	202	246		208	227		203
FW62	8	X52	0.14	MCAW	0.53	3.55	-66.6	220	219	225	220	218				205	203	203	203	192	193	183	192	195				221	225	225	225	195		225	191		224
FW63	8	X52	0.14	MCAW	1.29	9.65	-25.8	213	212	211	213	213				192	195	192	193	204	206	208	204	204				252	244	252	249	208		252	206		249
FW64	11	X70	0.22	MCAW	0.53	2	-81.11	174	174	174	173	171				171	170	166	168	306	306	306	310	317				317	321	336	329	317		336	309		326
FW65	11	X70	0.22	MCAW	1.29	10.6	-18.18	192	193	193	190	195				186	189	188	193	252	249	249	257	244				268	260	262	249	257		268	250		260

Table 4.18: Cooling Data and Hardness Results – Sleeve Fillet Welds – Static Air (No Flow)

Weld ID	Pipe Thickness (mm)	Grade	C.E	Process	Welding Position	Heat Input (kJ/mm)	Cooling Rate ΔT 800-500C (s)	Cooling Rate Slope at 540C (degC / sec)	Location: Ocular Reading CGHAZ - Pipe Side 1	2	3	CG-HAZ Sleeve Side 1	2	3	Weld 1	2	Location: Hardness (Hv5) CGHAZ - Pipe Side 1	2	3	CG-HAZ Sleeve Side 1	2	3	Weld 1	2	Peak Hardness (Hv5) CGHAZ Pipe	CGHAZ Sleeve	Weld	Average Hardness (Hv5) CGHAZ Pipe	CGHAZ Sleeve	Weld
SA1	6.4	X52	0.43	SMAW	2F	0.53	5.55	-36.6	163	167	160	154	160	158	187	196	349	332	362	391	362	371	265	241	362	391	265	348	375	253
SA2	6.4	X52	0.43	SMAW	3F-UP	1.29	13.25	-17.3	198	185	186	185	170	169	196	196	237	271	268	271	321	325	241	241	271	325	241	258	305	241
SA3	6.4	X52	0.43	SMAW	2F	0.90	9.35	-19.5	177	180	180	173	174	173	196	195	296	286	286	310	306	310	241	244	296	310	244	289	309	243
SA4	6.4	X52	0.43	SMAW	3F-UP	1.29	13.85	-17.6	194	176	185	181	174	177	199	198	246	299	271	283	306	296	234	237	299	306	237	272	295	235
SA5	8	X52	0.14	SMAW	2F	0.90	5.05	-44.3	210	211	213	136	139	140	185	187	210	208	204	501	480	473	271	265	210	501	271	208	485	268
SA6	8	X52	0.14	SMAW	3F-UP	1.56	12.6	-15.7	220	213	214	164	161	160	192	195	192	204	202	345	358	362	252	244	204	362	252	199	355	248
SA7	11	X70	0.22	SMAW	3F-DWN	0.90	4	-88.3	179	179	180	148	150	156	160	165	289	289	286	423	412	381	362	341	289	423	362	288	405	351
SA8	11	X70	0.22	SMAW	2F	1.29	4.65	-45.2	184	183	183	160	157	153	165	169	274	277	277	362	376	396	341	325	277	396	341	276	378	333
SA9	16.1	X80	0.27	SMAW	3F-DWN	0.90	2	-71.42																						
SA10	16.1	X80	0.27	SMAW	2F	1.29	3.95	-67.1	170	168	167	140	144	142	159	163	321	329	332	473	447	460	367	349	332	473	367	327	460	358
SA11	19.1	X70	0.24	SMAW	3F-DWN	0.90	2.35	-99	174	173	175	137	137	139	147	147	306	310	303	494	494	480	429	429	310	494	429	306	489	429
SA12	19.1	X70	0.24	SMAW	2F	1.29	3.9	-60.8	177	178	179	139	141	140	160	160	296	293	289	480	466	473	362	362	296	480	362	293	473	362
SA13	6.4	X70	0.43	P-GMAW	3F-UP	0.53	8.2	-30.9	173	168	170	166	174	170	200	196	310	329	321	336	306	321	232	241	329	336	241	320	321	237
SA14	6.4	X70	0.43	P-GMAW	2F	1.29	10.65	-18.9	188	189	181	187	183	195	201	201	262	260	283	265	277	244	229	229	283	277	229	268	262	229
SA15	8	X80	0.14	P-GMAW	3F-UP	0.53	3.4	-65.2	217	216	216	148	150	149	192	191	197	199	199	423	412	418	252	254	199	423	254	198	418	253
SA16	8	X80	0.14	P-GMAW	2F	1.29	3.35	-60.8	218	218	218	159	150	155	192	193	195	195	195	367	412	386	252	249	195	412	252	195	388	250
SA17	11	X70	0.22	P-GMAW	3F-UP	0.53	2.9	-72.8	173	170	175	146	152	152	173	171	310	321	303	435	401	401	310	317	321	435	317	311	413	313
SA18	11	X70	0.22	P-GMAW	2F	1.29	5.25	-46.4	182	176	176	162	160	164	177	182	280	299	299	353	362	345	296	280	299	362	296	293	353	288
SA19	16.1	X80	0.27	P-GMAW	3F-UP	0.53	1.75	-80.64	166	167	167	140	142	140	166	160	336	332	332	473	460	473	336	362	336	473	362	334	469	349
SA20	16.1	X80	0.27	P-GMAW	2F	1.29	4.85	-47.5	173	174	173	141	147	147	182	182	310	306	310	466	429	429	280	280	310	466	280	309	442	280
SA21	19.1	X70	0.24	P-GMAW	3F-UP	0.53	2.05	-118.7	178	173	177	143	142	153	161	169	293	310	296	453	460	396	358	325	310	460	358	299	436	341
SA22	19.1	X70	0.24	P-GMAW	2F	1.29	3.8	-73.3	179	174	174	143	145	142	170	163	289	306	306	453	441	460	321	349	306	460	349	301	451	335
SA23	6.4	X52	0.43	SS-FCAW	3F-DWN	1.29	12.8	-18.4	203	186	202	185	182	193	204	209	225	268	227	271	280	249	223	212	268	280	223	240	267	218
SA24	6.4	X52	0.43	SS-FCAW	2F	1.99	21.8	-9.7	204	211	205	200	206	206	214	211	223	208	221	232	218	218	202	208	223	232	208	217	223	205
SA25	8	X52	0.14	SS-FCAW	3F-DWN	1.29	14.1	-17.7	214	213	211	152	150	150	204	202	202	204	208	401	412	412	223	227	208	412	227	205	408	225
SA26	8	X52	0.14	SS-FCAW	2F	1.99	30.4	-30.6	226	220	225	178	173	178	216	215	182	192	183	293	310	293	199	201	192	310	201	185	298	200
SA27	11	X70	0.22	SS-FCAW	3F-DWN	1.29	5	-38.8	185	185	184	160	160	171	182	188	271	271	274	362	362	317	280	262	274	362	280	272	347	271
SA28	11	X70	0.22	SS-FCAW	2F	1.99	11.7	-17.2	194	192	190	177	173	183	188	183	246	252	257	296	310	277	262	277	257	310	277	252	294	270
SA29	16.1	X80	0.27	SS-FCAW	3F-DWN	1.29	5	-47.6	170	172	168	148	146	150	180	180	321	313	329	423	435	412	286	286	329	435	286	321	423	286
SA30	16.1	X80	0.27	SS-FCAW	2F	1.99	5.45	-21.9	177	175	175	149	150	152	183	183	296	303	303	418	412	401	277	277	303	418	277	300	410	277
SA31	19.1	X70	0.24	SS-FCAW	3F-DWN	1.29	4.05	-56.7	182	180	184	148	145	155	181	179	280	286	274	423	441	386	283	289	286	441	289	280	417	286
SA32	19.1	X70	0.24	SS-FCAW	2F	1.99	6.35	-40.7	183	185	185	146	149	157	175	175	277	271	271	435	418	376	303	303	277	435	303	273	410	303
SA33	6.4	X80	0.43	GS-FCAW	3F-UP	1.99	21.4	-9.6	198	205	204	188	189	193	204	206	237	221	223	262	260	249	223	218	237	262	223	227	257	221
SA34	6.4	X80	0.43	GS-FCAW	2F	1.29	8.3	-22.3	183	178	182	172	161	168	192	192	277	293	280	313	358	329	252	252	293	358	252	283	333	252
SA35	8	X70	0.14	GS-FCAW	3F-UP	1.99	18.44	-18.54	211	217	216	184	182	174	204	208	208	197	199	274	280	306	223	214	208	306	223	201	287	219
SA36	8	X70	0.14	GS-FCAW	2F	1.29	8.16	-24	214	214	216	139	144	147	195	195	202	202	199	480	447	429	244	244	202	480	244	201	452	244
SA37	11	X70	0.22	GS-FCAW	3F-UP	1.99	2.05	-50	191	184	187	167	164	154	189	188	254	274	265	332	345	391	260	262	274	391	262	264	356	261
SA38	11	X70	0.22	GS-FCAW	2F	1.29	3.25	-63.7	187	187	186	160	163	171	182	186	265	265	268	362	349	317	280	268	268	362	280	266	343	274
SA39	16.1	X80	0.27	GS-FCAW	3F-UP	1.99	6.6	-24.4	176	174	175	151	146	149	178	179	299	306	303	407	435	418	293	289	306	435	293	303	420	291
SA40	16.1	X80	0.27	GS-FCAW	2F	1.29	5.1	-50	171	170	171	137	145	145	175	180	317	321	317	494	441	441	303	286	321	494	303	318	459	294
SA41	19.1	X70	0.24	GS-FCAW	3F-UP	1.99	5.05	-52.85	180	179	178	148	145	149	172	168	286	289	293	423	441	418	313	329	293	441	329	289	427	321
SA42	19.1	X70	0.24	GS-FCAW	2F	1.29	3.25	-68.7	175	175	180	147	143	143	184	180	303	303	286	429	453	453	274	286	303	453	286	297	445	280
SA43	6.4	X80	0.43	MCAW	3F-UP	0.53	6.6	-33.7	175	172	172	165	167	180	194	194	303	313	313	341	332	286	246	246	313	341	246	310	320	246
SA44	6.4	X80	0.43	MCAW	2F	1.29	7	-31.2	167	164	183	164	170	182	199	198	332	345	277	345	321	280	234	237	345	345	237	318	315	235
SA45	8	X70	0.14	MCAW	3F-UP	0.53	5.48	-39.375	213	212	214	144	141	143	193	193	204	206	202	447	466	453	249	249	206	466	249	204	456	249
SA46	8	X70	0.14	MCAW	2F	1.29	4.52	-35.97	210	215	215	140	139	139	191	191	210	201	201	473	480	480	254	254	210	480	254	204	478	254
SA47	11	X70	0.22	MCAW	3F-UP	0.53	3.7	-59.7	177	175	176	148	154	153	153	151	296	303	299	423	391	396	396	407	303	423	407	299	403	401
SA48	11	X70	0.22	MCAW	2F	1.29	3.5	-57.33	185	182	182	152	161	158	174	173	271	280	280	401	358	371	306	310	280	401	310	277	377	308
SA49	16.1	X80	0.27	MCAW	3F-UP	0.53	3.4	-80.8	168	167	168	138	143	145	158	156	329	332	329	487	453	441	371	381	332	487	381	330	460	376
SA50	16.1	X80	0.27	MCAW	2F	1.29	3.45	-68.2	168	169	168	137	141	148	160	159	329	325	329	494	466	423	362	367	329	494	367	327	461	364
SA51	19.1	X70	0.24	MCAW	3F-UP	0.53	2.7	-95.3	173	173	174	140	143	141	154	159	310	310	306	473	453	466	391	367	310	473	391	309	464	379
SA52	19.1	X70	0.24	MCAW	2F	1.29	4.85	-52.7	176	179	180	142	145	154	156	160	299	289	286	460	441	391	381	362	299	460	381	292	431	372

Table 4.19: Cooling Data and Hardness Results – Sleeve Fillet Welds – Water Backing

Weld ID	Pipe Thickness (mm)	Grade	C.E	Process	Welding Position	Heat Input (kJ/mm)	Cooling Rate		Location																Peak Hardness (Hv5)			Average Hardness (Hv5)		
									Ocular Reading								Hardness (Hv5)													
									CGHAZ - Pipe Side			CG-HAZ Sleeve Side			Weld		CGHAZ - Pipe Side			CG-HAZ Sleeve Side			Weld							
							ΔT 800-500C (s)	Slope at 540C (degC / sec)	1	2	3	1	2	3	1	2	1	2	3	1	2	3	1	2	CGHAZ Pipe	CGHAZ Sleeve	Weld	CGHAZ Pipe	CGHAZ Sleeve	Weld
SW1	6.4	X52	0.43	SMAW	2F	0.53	3.56	-63.25	143	153	145	146	149	147	177	177	453	396	441	435	418	429	296	296	453	435	296	430	427	296
SW2	6.4	X52	0.43	SMAW	3F-UP	1.29	6.28	-37.25	180	151	158	164	162	160	186	193	286	407	371	345	353	362	268	249	407	362	268	355	353	258
SW3	6.4	X52	0.43	SMAW	2F	0.90	3.48	-92.5	149	144	142	150	151	150	167	171	418	447	460	412	407	412	332	317	460	412	332	442	410	325
SW4	6.4	X52	0.43	SMAW	3F-UP	1.29	4	-64.5	147	145	152	153	152	153	184	189	429	441	401	396	401	396	274	260	441	401	274	424	398	267
SW5	8	X52	0.14	SMAW	2F	0.90	4.25	-42.6	210	209	216	139	139	140	174	185	210	212	199	480	480	473	306	271	212	480	306	207	478	289
SW6	8	X52	0.14	SMAW	3F-UP	1.56	7	-32.8	211	211	217	137	142	139	191	189	208	208	197	494	460	480	254	260	208	494	260	204	478	257
SW7	11	X70	0.22	SMAW	3F-DWN	0.90	4.25	-53.3																						
SW8	11	X70	0.22	SMAW	2F	1.29	7	-30.2																						
SW13	6.4	X70	0.43	P-GMAW	3F-UP	0.53	6.24	-43.47	139	143	143	146	154	148	182	180	480	453	453	435	391	423	280	286	480	435	286	462	416	283
SW14	6.4	X70	0.43	P-GMAW	2F	1.29	5.8	-40.25	151	141	152	159	159	158	190	187	407	466	401	367	367	371	257	265	466	371	265	425	368	261
SW15	8	X80	0.14	P-GMAW	3F-UP	0.53	3.35	-68.9	208	210	215	144	138	138	182	181	214	210	201	447	487	487	280	283	214	487	283	208	474	281
SW16	8	X80	0.14	P-GMAW	2F	1.29	4.15	-50.8	216	218	217	139	140	140	190	193	199	195	197	480	473	473	257	249	199	480	257	197	475	253
SW17	11	X70	0.22	P-GMAW	3F-UP	0.53	2	-115.1	174	172	173	148	149	148	162	169	306	313	310	423	418	423	353	325	313	423	353	310	421	339
SW18	11	X70	0.22	P-GMAW	2F	1.29	3.85	-68.3	182	176	179	165	162	154	179	178	280	299	289	341	353	391	289	293	299	391	293	290	362	291
SW33	6.4	X80	0.43	GS-FCAW	3F-UP	1.99	10.08	-23.125	163	167	151	167	164	173	191	193	349	332	407	332	345	310	254	249	407	345	254	363	329	252
SW34	6.4	X80	0.43	GS-FCAW	2F	1.29	3.84	-50	153	148	157	164	156	165	194	182	396	423	376	345	381	341	246	280	423	381	280	399	355	263
SW35	8	X70	0.14	GS-FCAW	3F-UP	1.99	10.6	-25.7	210	210	210	138	140	141	191	191	210	210	210	487	473	466	254	254	210	487	254	210	475	254
SW36	8	X70	0.14	GS-FCAW	2F	1.29	5.85	-32.6	216	214	215	141	146	151	198	190	199	202	201	466	435	407	237	257	202	466	257	201	436	247
SW37	11	X70	0.22	GS-FCAW	3F-UP	1.99	4.35	-22.7	178	179	178	166	162	161	178	177	293	289	293	336	353	358	293	296	293	358	296	292	349	294
SW38	11	X70	0.22	GS-FCAW	2F	1.29	7.8	-33.34	184	184	182	158	157	159	170	173	274	274	280	371	376	367	321	310	280	376	321	276	371	315
SW43	6.4	X80	0.43	MCAW	3F-UP	0.53	3.04	-90.9	140	144	143	150	149	150	186	187	473	447	453	412	418	412	268	265	473	418	268	458	414	267
SW44	6.4	X80	0.43	MCAW	2F	1.29	5.8	-28.57	143	156	146	163	152	157	187	184	453	381	435	349	401	376	265	274	453	401	274	423	375	270
SW45	8	X70	0.14	MCAW	3F-UP	0.53	3.2	-76.3	206	211	210	136	139	139	184	184	218	208	210	501	480	480	274	274	218	501	274	212	487	274
SW46	8	X70	0.14	MCAW	2F	1.29	5.7	-40	215	212	216	140	149	157	195	192	201	206	199	473	418	376	244	252	206	473	252	202	422	248
SW47	11	X70	0.22	MCAW	3F-UP	0.53	4	-62.5	179	178	177	158	157	160	169	169	289	293	296	371	376	362	325	325	296	376	325	293	370	325
SW48	11	X70	0.22	MCAW	2F	1.29	4.5	-50.4	184	184	183	163	162	166	170	169	274	274	277	349	353	336	321	325	277	353	325	275	346	323

Cooling rate comparisons between bead on pipe and fillet welds for 0.53 and 1.29kJ/mm heat inputs and each process are shown in **Figures 4.54** and **4.55**. These comparisons show that the weld cooling rate for the fillet welded sleeves increase considerably over the bead on pipe welds for the same heat inputs. This is due to the additional mass and heat sink capacity when the sleeve is attached.

Cross-sections were extracted from each weld and hardness measurements were made to develop a relationship between heat input, cooling rate, and CGHAZ hardness in the base metal (i.e., carrier pipe). Cross-sections for air and water backed sleeve fillet welds are provided as **Appendix M and Appendix N** (note that air and water backed bead on pipe cross-sections are included as Appendix D and Appendix F, as previously discussed in Task 3). **Figures 4.56** to **4.60** show the general trend of increasing hardness with increasing heat sink capacity going from bead on pipe with air backing, to sleeve fillet welds with air backing, to sleeve fillet welds with water backing. These examples are shown for the 6.4mm thick X52 pipe with the highest carbon equivalent (C.E.) of all materials evaluated.

Figures 4.61 to **4.63** shows the result of the CGHAZ hardness of the carrier pipe for each repair scenario (i.e., direct bead on pipe with air backing, sleeve fillet welding with air backing, and sleeve fillet welding with water backing) as a comparison with each welding process. To the right of each plot are the cooling times (800 to 500°C in seconds) vs. heat input to show the relationship between the resulting hardnesses and “actual” cooling times for each weld deposited. The trend of increasing hardness with shorter cooling times (i.e., faster cooling rates) is apparent, however there does not appear to be a trend of any process resulting in softer CGHAZ’s at a given cooling rate compared to the others. The water backed sleeve fillet welds demonstrate overall higher hardnesses and the air backed bead on pipe welds have the lowest hardnesses over the same heat input range.

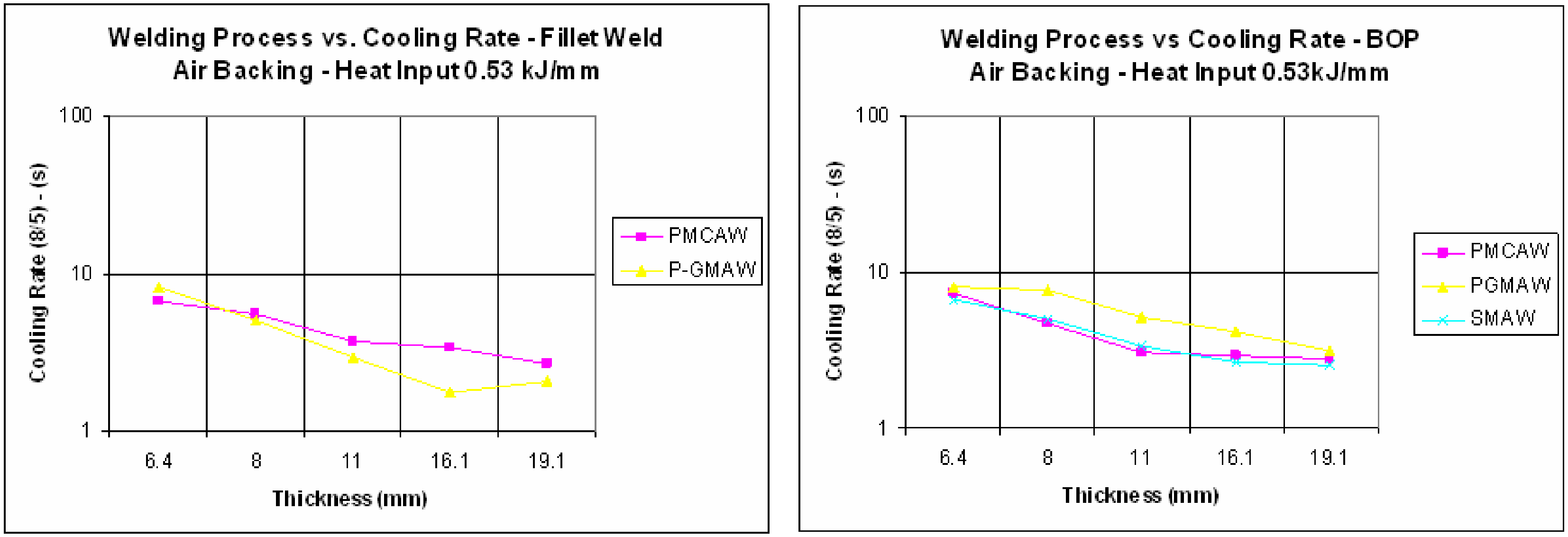

Figure 4.54: Welding Process vs. Cooling Rate, Fillet Weld vs. Bead on Pipe, 0.53 kJ/mm

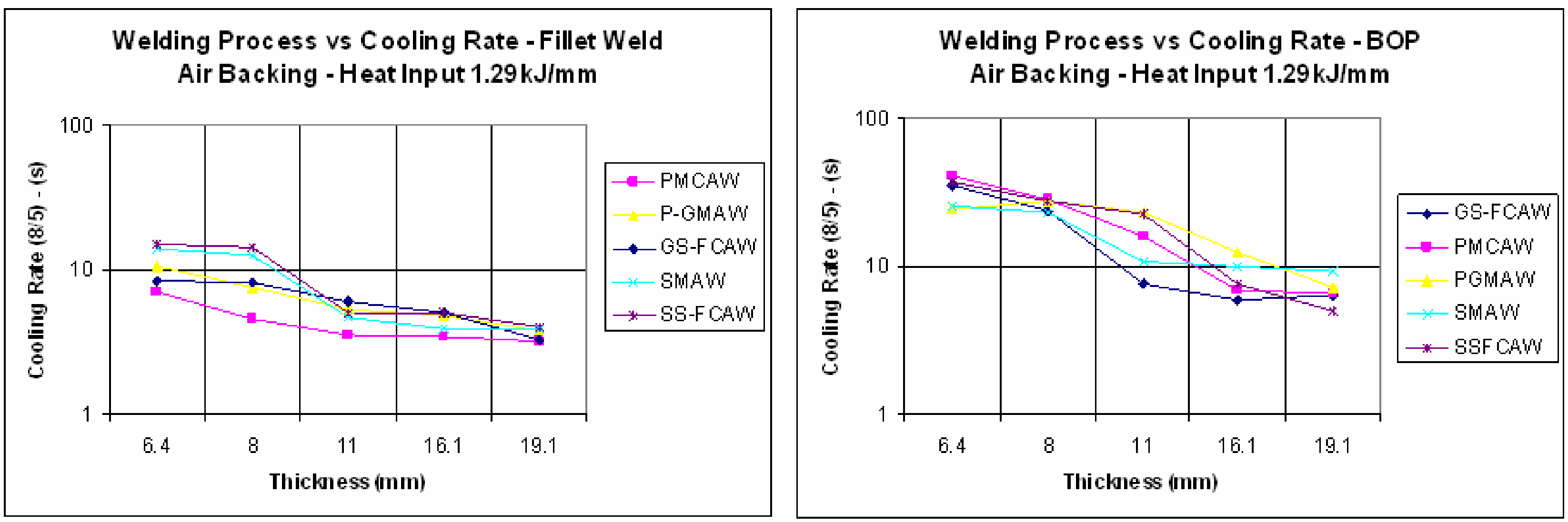

Figure 4.55: Welding Process vs. Cooling Rate, Fillet Weld vs. Bead on Pipe, 1.29 kJ/mm

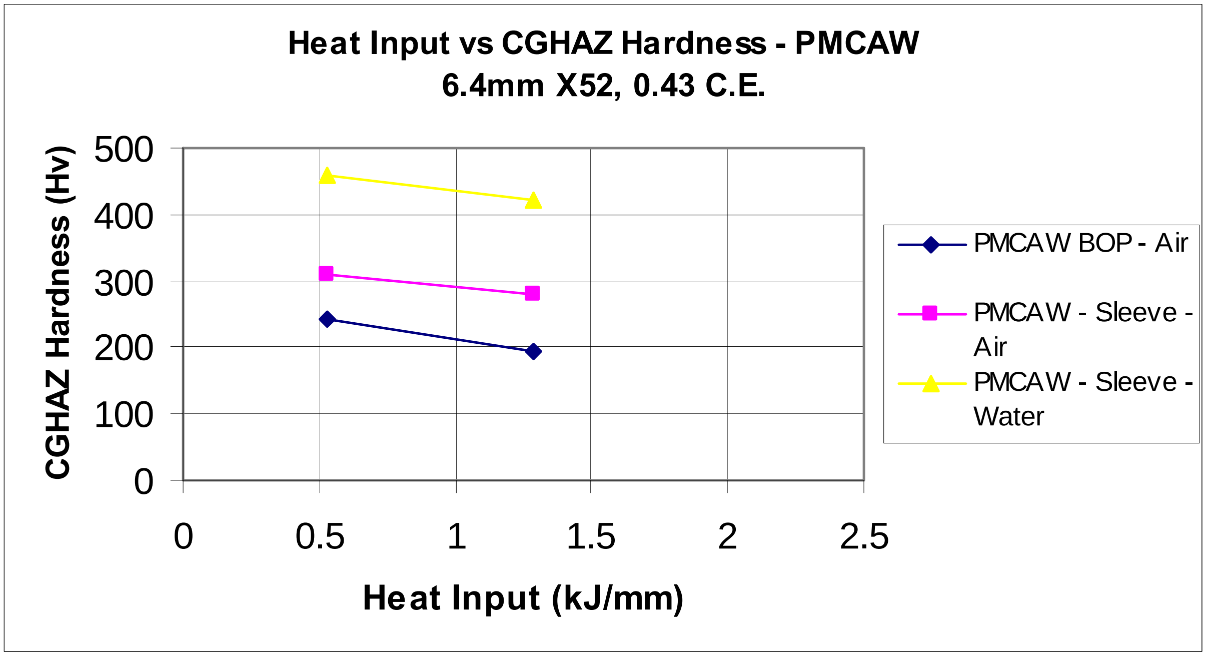

Figure 4.56: Heat Input vs. Hardness, PMCAW

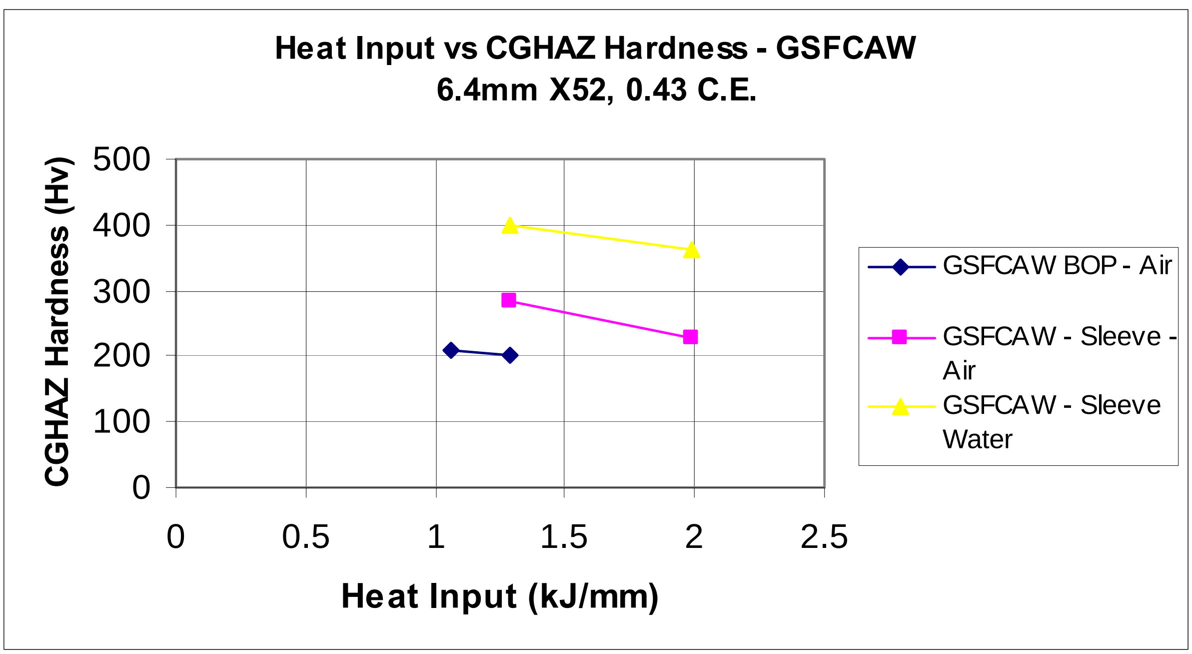

Figure 4.57: Heat Input vs. Hardness, GSFCAW

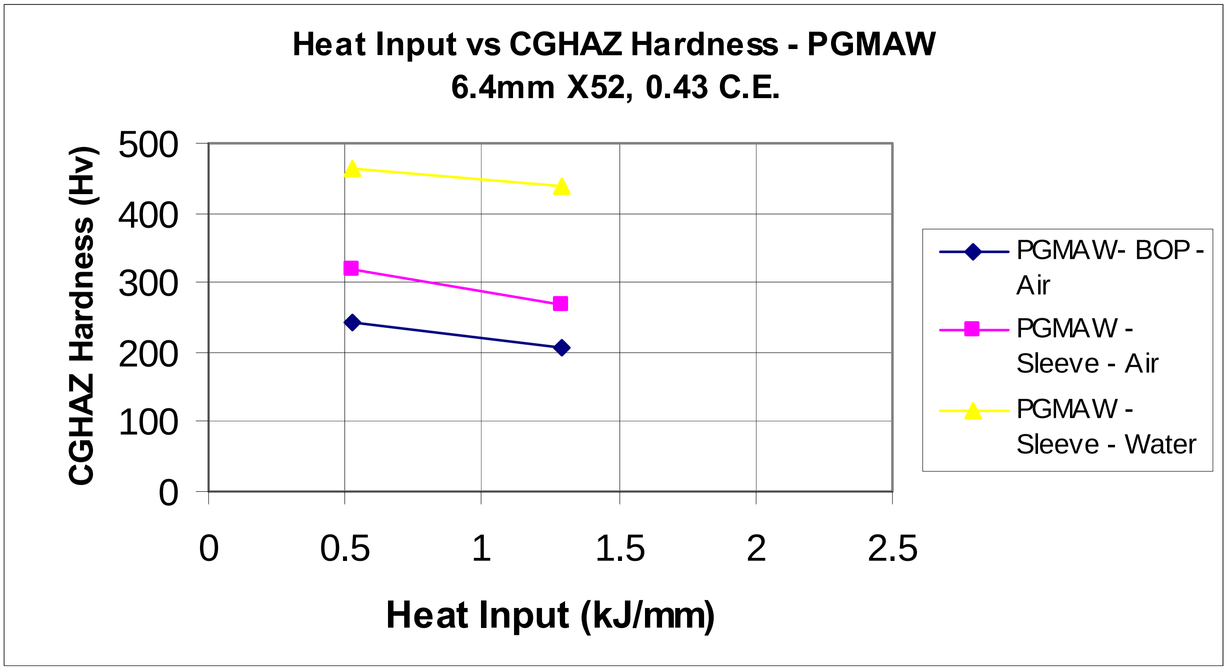

Figure 4.58: Heat Input vs. Hardness, PGCAW

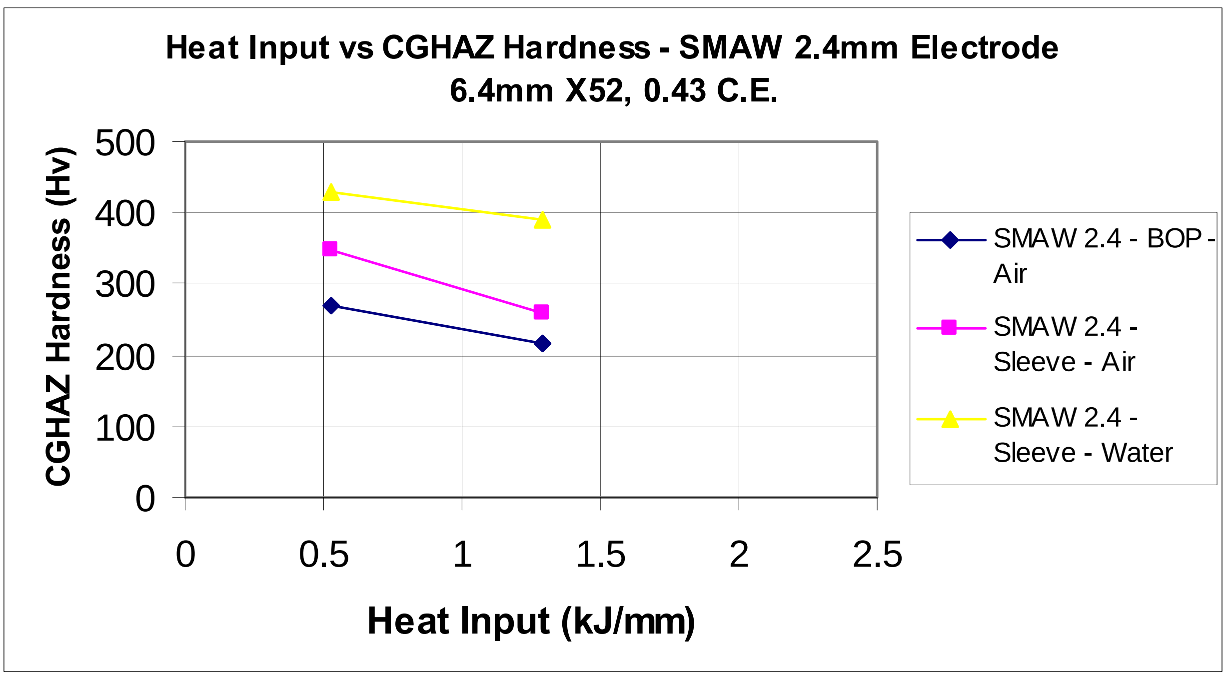

Figure 4.59: Heat Input vs. Hardness, SMAW, 2.4mm Diameter Electrode

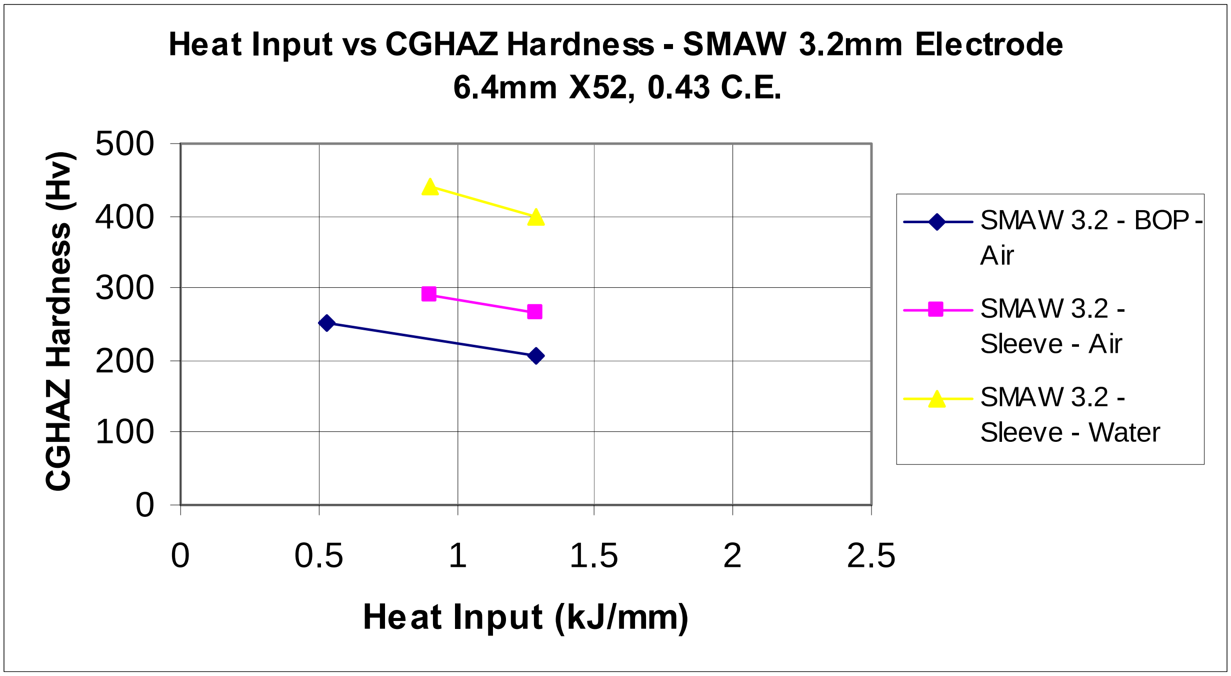

Figure 4.60: Heat Input vs. Hardness, SMAW, 3.2mm Diameter Electrode

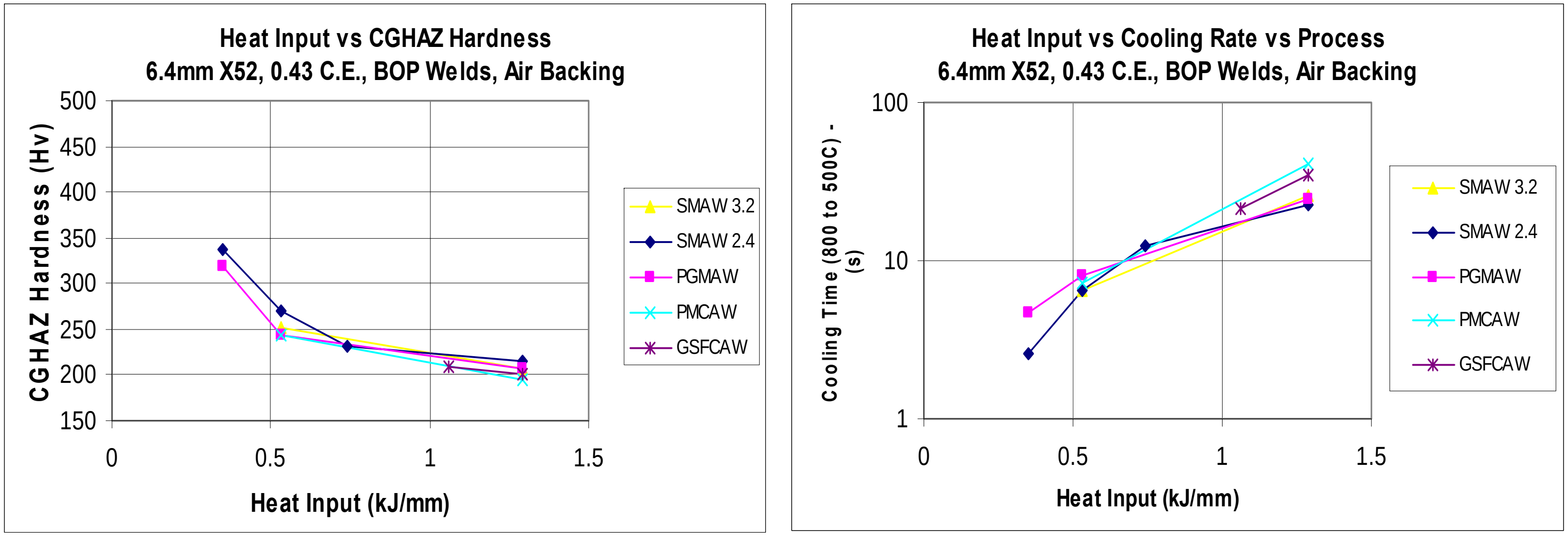

Figure 4.61: Heat Input vs. Hardness vs. Cooling Rate, Bead on Pipe, Air Backing

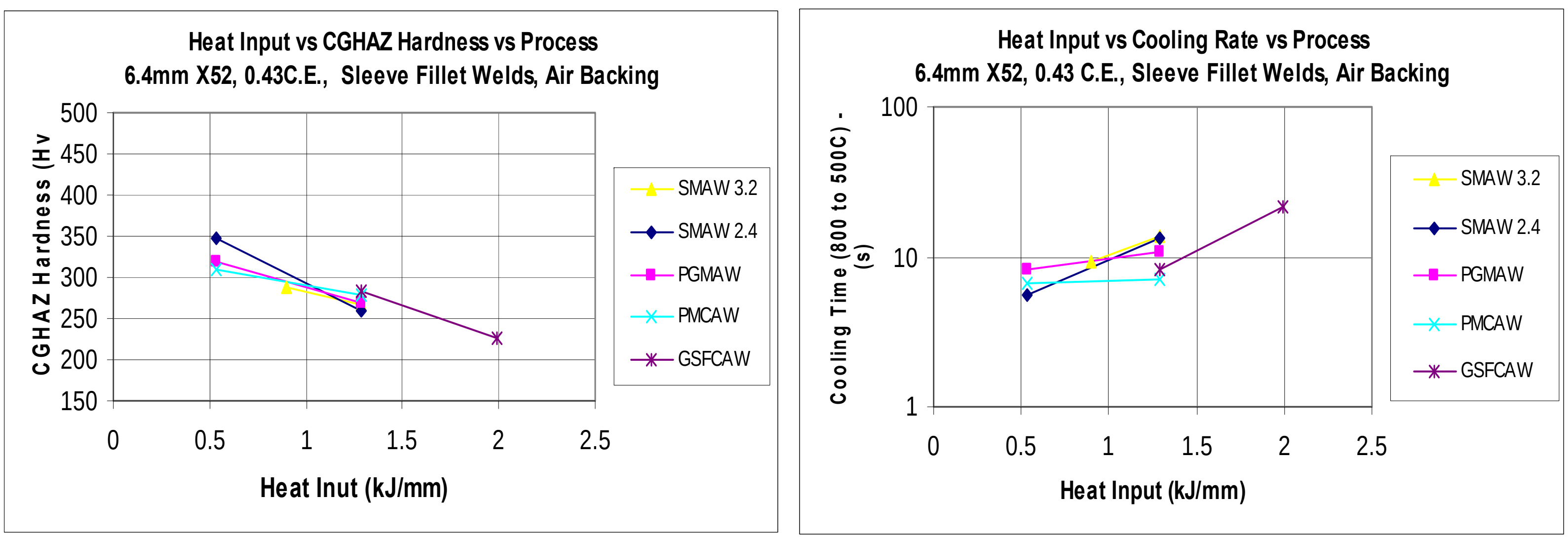

Figure 4.62: Heat Input vs. Hardness vs. Cooling Rate, Sleeve Fillet Welding, Air Backing

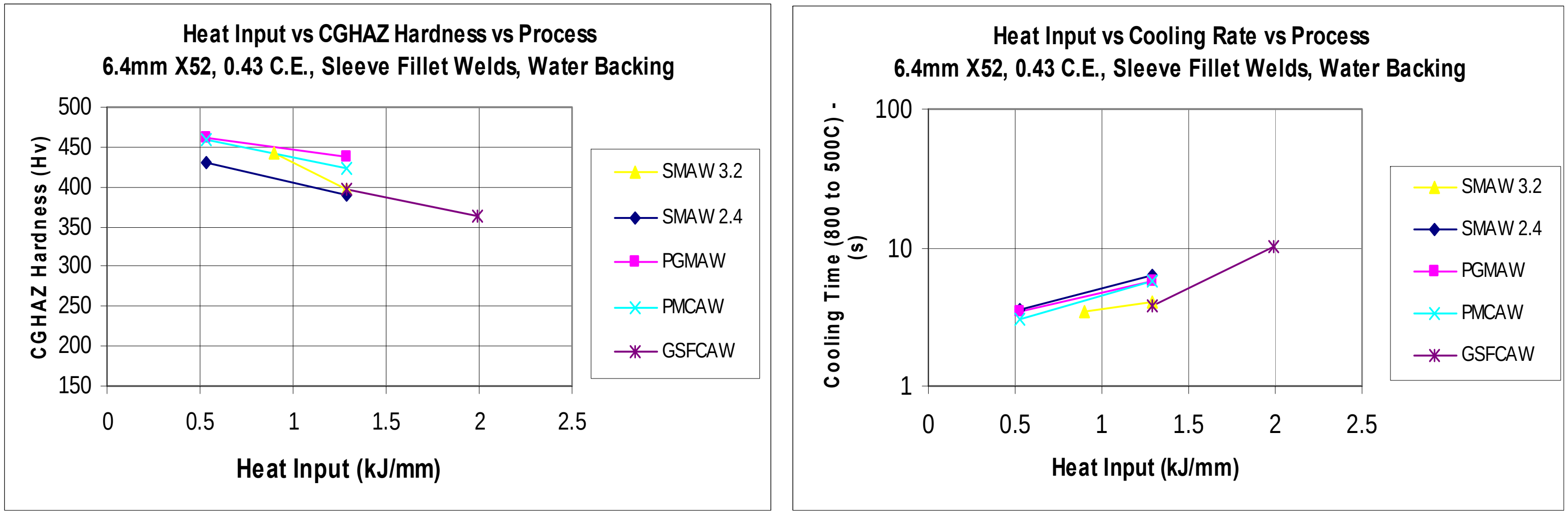

Figure 4.63: Heat Input vs. Hardness vs. Cooling Rate, Sleeve Fillet Welding, Water Backing

4.10 Task 8: Hot-tap Joint Simulation

An NPS36 X70 pipe (19mm thickness) and a 25mm thick sleeve (ASTM A516 Gr70, C.E .46) was used for the test assembly as supplied by Williamson Industries. The long seams of the sleeves were positioned at the 12 o'clock and 6 o'clock positions (see **Figure 4.64**) to allow a continuous non-interrupted fillet weld to be deposited with vertical up progression from the bottom of the pipe to the top. This method allowed for procedures to be developed for all positions of welding with each process for a three pass fillet weld. The target final fillet weld size had a leg length of 13mm. The good fit-up between the Williamson Industries provided sleeve and the NPS36 pipe is shown in **Figure 4.65**.

The processes that were successfully evaluated included pulsed gas metal arc welding (PGMAW), pulsed metal cored arc welding (PMCAW) and gas shielded flux cored arc welding (FCAW). An attempt was made to implement self shielded FCAW however the welding control system and power source could not accurately control the parameters required to deposit a sound weld with a 2mm diameter electrode. However, a fillet weld will be made semi-automatically at a later date to compare the results of the weld zone hardnesses between all of the processes investigated.

The welding equipment used included Miller's Pipe Pro Axcess 450 power source (serial number LF310619) and Pipe Pro feeder. The welding head used for this evaluation was from RMS Welding Systems, which is a modified "bug and band" circumferential welding system with torch fixturing that was designed specifically to perform fillet welding. The welding head is shown in **Figure 4.66**.

The welding procedures that were developed for each of the welding processes are shown in **Table 4.20**. It should be noted that the welding parameters for each individual weld pass for each process application did not change as the weld head progressed around the sleeve. This is an obvious advantage in that complex welding procedures do not have to be implemented for this application.

The first, second, and third pass of the FCAW process are shown in **Figure 4.67**, **4.68**, and **4.69**, respectively. The first, second, and third pass of the PMCAW process are shown in **Figures 4.70**, **4.71**, and **4.72**, respectively. The first, second, and third pass of the PGMAW process are shown in **Figures 4.73**, **4.74**, and **4.75**, respectively. An example of the mechanized welding system in operation is shown in **Figure 4.76**.

Figure 4.64: Sleeve Assembly

Figure 4.65: Sleeve Fit-up

Figure 4.66: Mechanized Welding Head and Travel Band Set-up

Table 4.20: Mechanized Fillet Welding Procedures

Weld Process	Weld Pass	Wire Feed Speed	VTAT Amperage Setting	Arc Control	Trim	Voltage	Travel Speed	Heat Input		Oscillation Rate	Oscillation Dwell	Oscillation Width Setting
	(#)	(ipm)	(A)			(V)	(IPM)	(kJ/in)	(kJ/mm)	(BPM)	(ms)	
FCAW	1	285	200	NA	NA	24	8	36.0	1.42	100	250	275
FCAW	2	250	200	NA	NA	24	10	28.8	1.13	250	50	130
FCAW	3	265	200	NA	NA	24	8	36.0	1.42	100	250	185
MCAW-P	1	170	135	41	37	19	6	25.7	1.01	100	300	275
MCAW-P	2	140	120	41	37	16.5	9	13.2	0.52	250	50	200
MCAW-P	3	155	130	41	37	19	7	21.2	0.83	100	250	185
GMAW-P	1	170	130	45	27	17.5	6	22.8	0.90	100	300	275
GMAW-P	2	130	115	30	27	18	9	13.8	0.54	250	50	200
GMAW-P	3	150	130	30	23.5	18	7	20.1	0.79	100	250	185

FCAW Electrode 1.2mm ESAB Dual Shield 70T12MJ, C25 Gas, Constant Voltage
MCAW Electrode 1.2mm Hobart / Trimark Metalloy 71, C10 Gas, AccuPulse Mode
GMAW Electrode 1.2mm Thyssen K-Nova, C10 Gas, Synergic Pulse Mode

Figure 4.67: FCAW First Pass

Figure 4.68: FCAW Second Pass

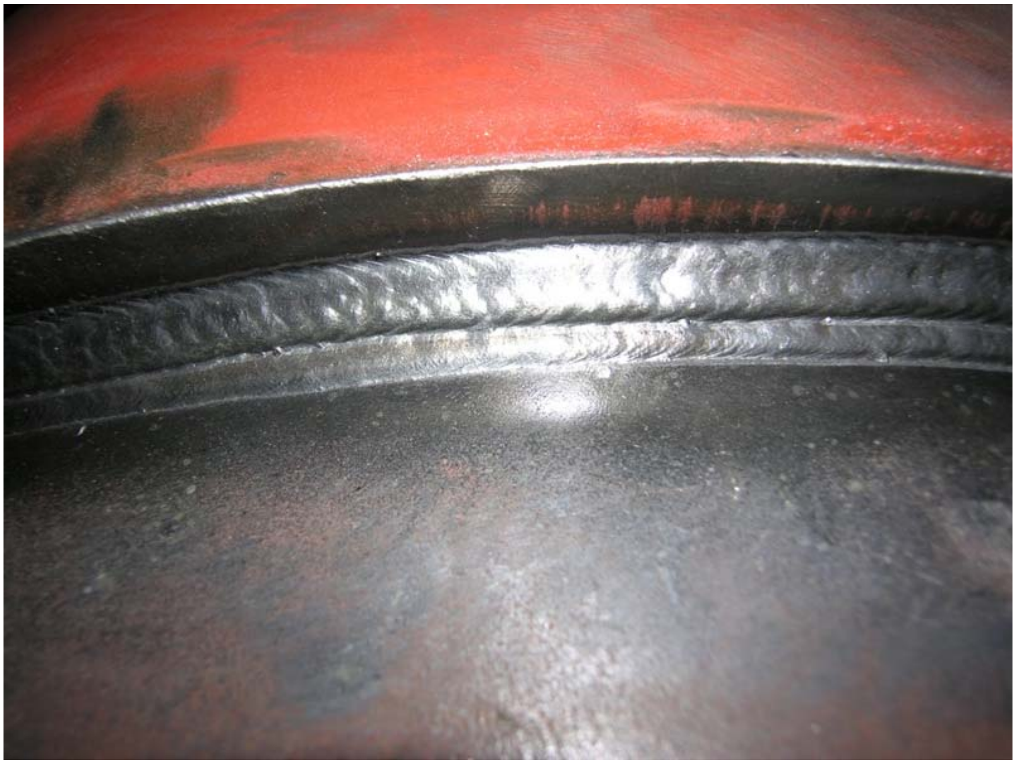

Figure 4.69: FCAW Third Pass

Figure 4.70: PMCAW First Pass

Figure 4.71: PMCAW Second Pass

Figure 4.72: PMCAW Third Pass

Figure 4.73: PGMAW First Pass

Figure 4.74: PGMAW Second Pass

Figure 4.75: PGMAW Third Pass

Figure 4.76: Mechanized Fillet Welding

The ends of the welds for each pass for each process were staggered by approximately four (4) inches (see **Figure 4.77**), to demonstrate the effectiveness of weld and HAZ tempering from subsequent passes by each process evaluated.

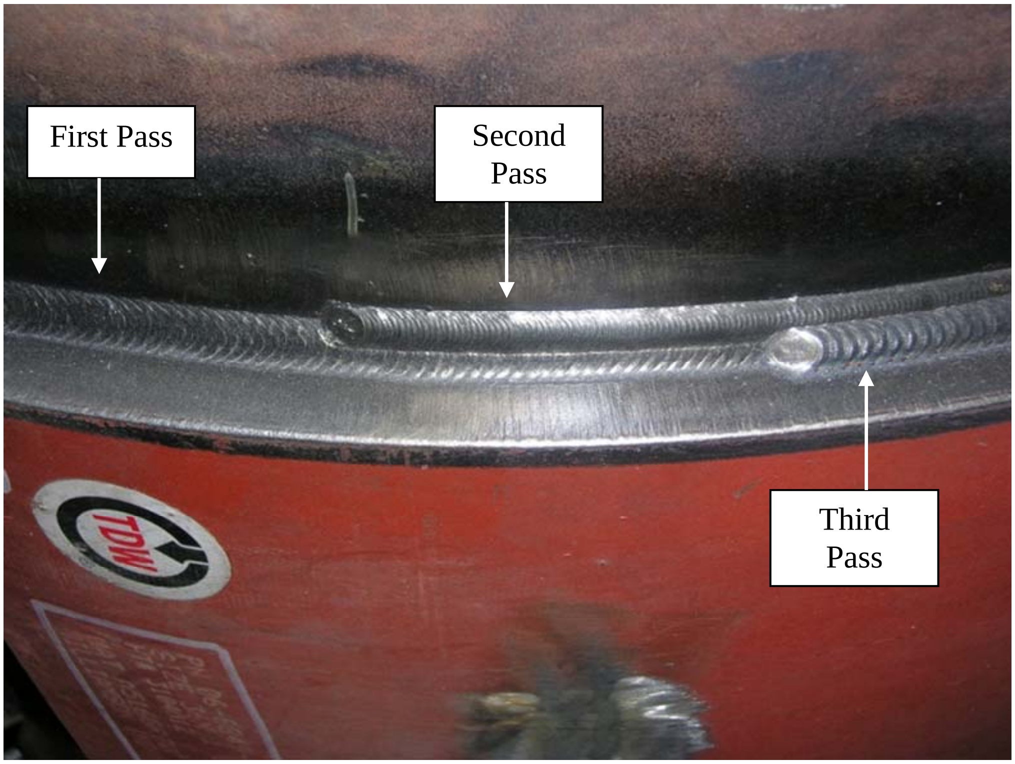

Figure 4.77: Weld Pass Staggering

Macro and micro sections were extracted from each of the mechanized welds and then prepared for weld bead penetration profile examination and hardness evaluations, as well as nick break and face bend tests. The macro cross-section of each completed fillet weld and each weld pass for each process are shown in **Figures 4.78** to **4.80**. Shown on each of the cross-sections are the heat inputs and average HAZ hardness measurements for each weld pass that demonstrate the degree of tempering of the previous weld deposits by the subsequent weld passes. It is interesting to note that each weld with each process demonstrated similar hardness results and degree of hardness reductions (i.e., tempering), however the PGMAW and PMCAW processes achieved the same degree of tempering at heat inputs 50% less than those of the FCAW process. This infers that the FCAW process is not as effective at tempering compared to the other two processes. The PMCAW and PGMAW processes therefore have the potential to provide weld zones that are less susceptible to hydrogen induced cracking compared to the FCAW process, since increasing hardness and susceptibility to cracking are directly related.

Face bend specimens were extracted from each completed mechanized fillet weld and tested in accordance with API 1104. The results are shown in **Figures 4.81** to **4.83**. Each weld was acceptable in that they demonstrated no signs of discontinuity exceeding 1/8" in size.

Nick break specimens were also extracted from each weld and tested in accordance with API 1104. The results are shown in **Figures 4.84** to **4.86**. Each weld was acceptable in that they demonstrated good fusion with no signs of cracks, lack of fusion, slag inclusions, or porosity exceeding the acceptance criteria.

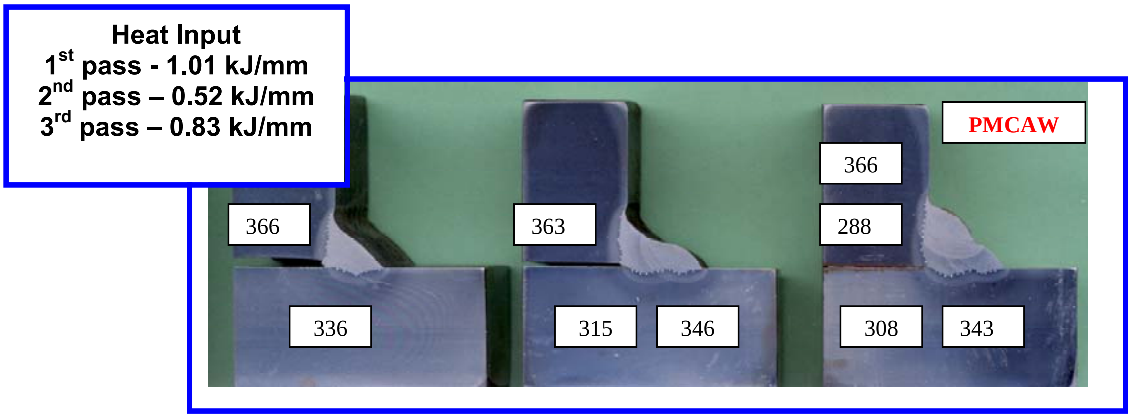

Figure 4.78: PMCAW Weld Passes and Average CGHAZ Hardness per Pass

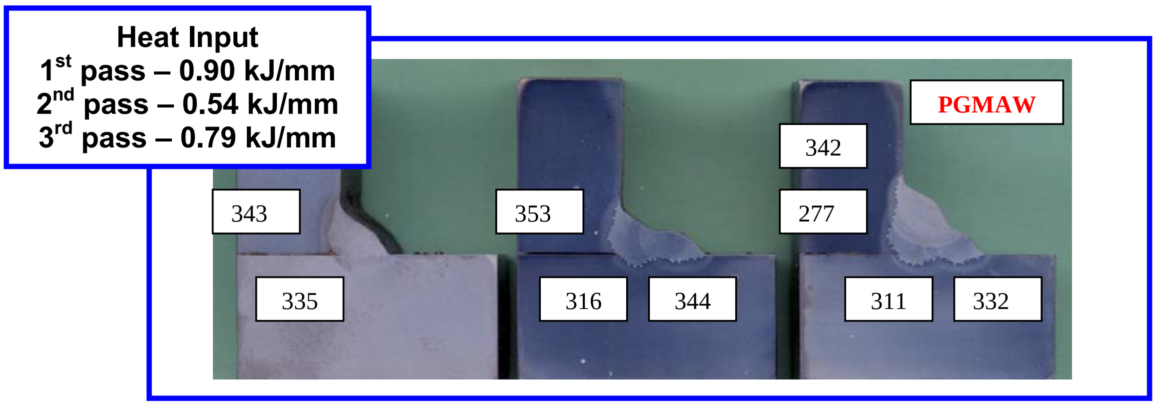

Figure 4.79: PGMAW Weld Passes and Average CGHAZ Hardness per Pass

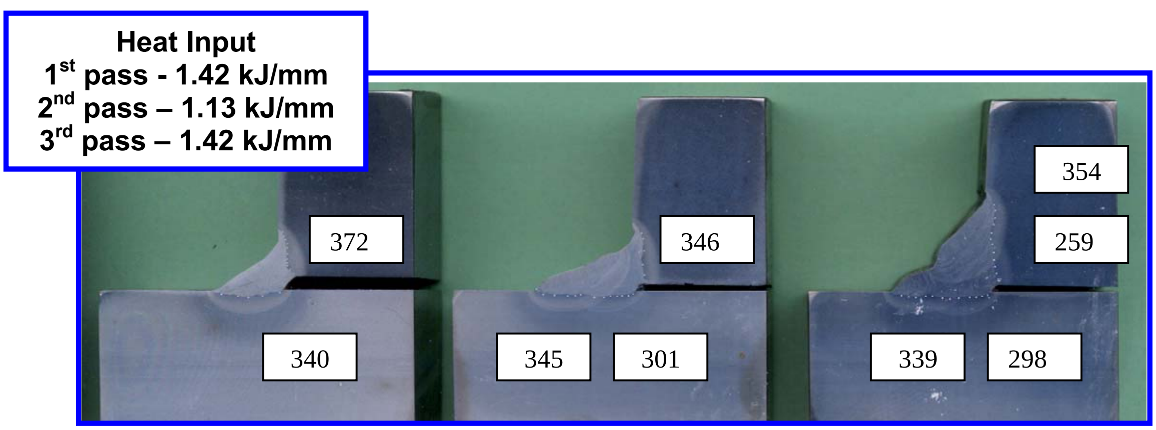

Figure 4.80: FCAW Weld Passes and Average CGHAZ Hardness per Pass

Figure 4.81: FCAW Face Bend Test Results

Figure 4.82: PGMAW Face Bend Results

Figure 4.83: PMCAW Face Bend Results

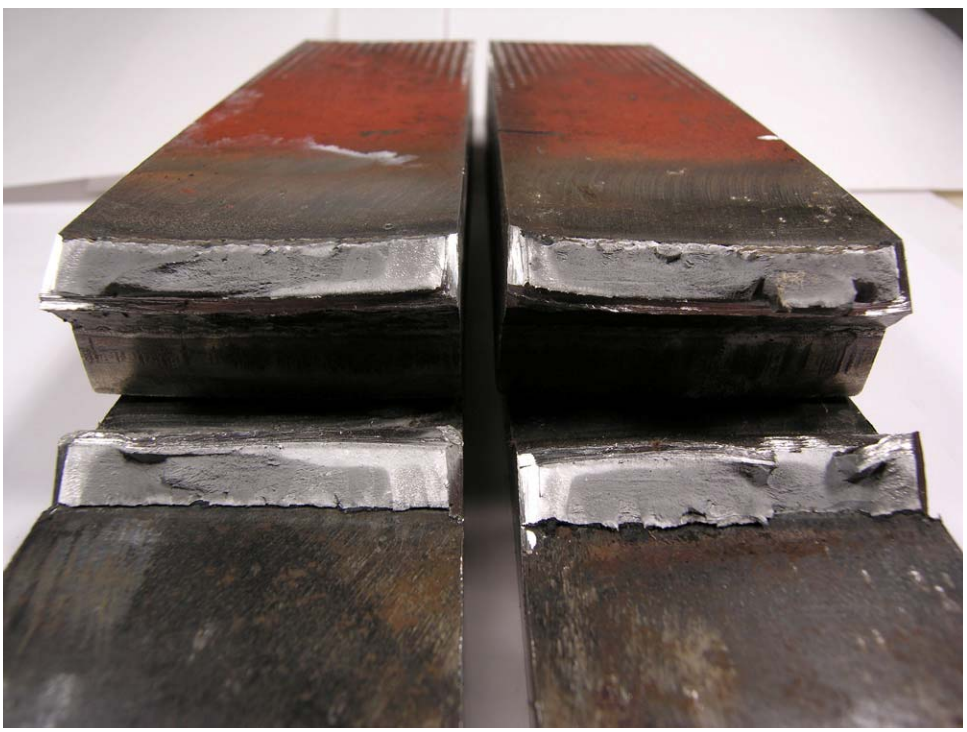

Figure 4.84: FCAW Nick Break Results

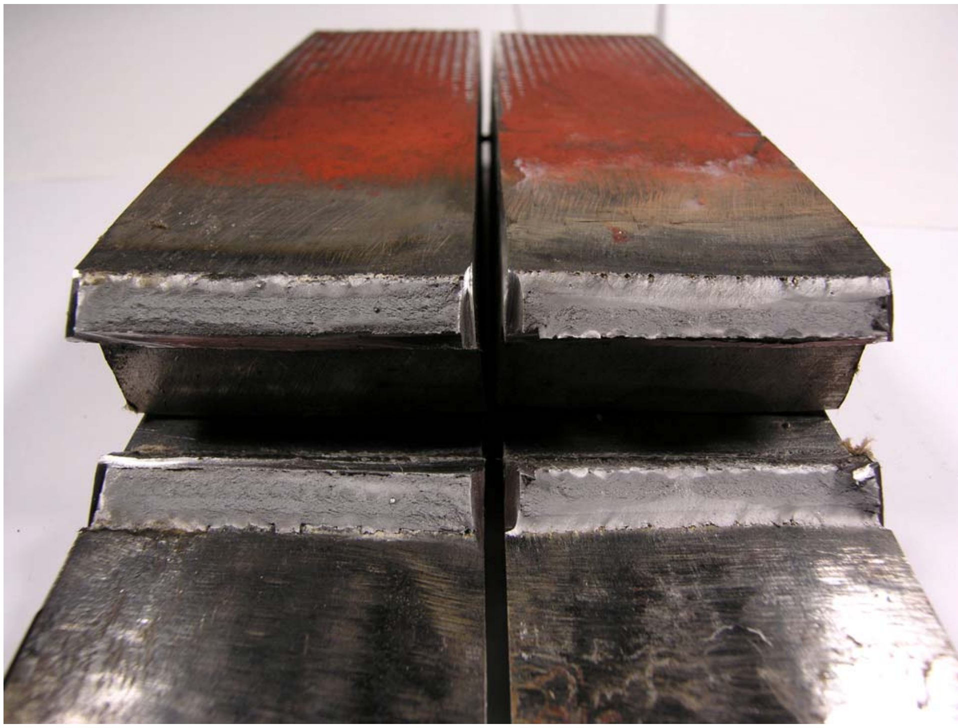

Figure 4.85: PGMAW Nick Break Results

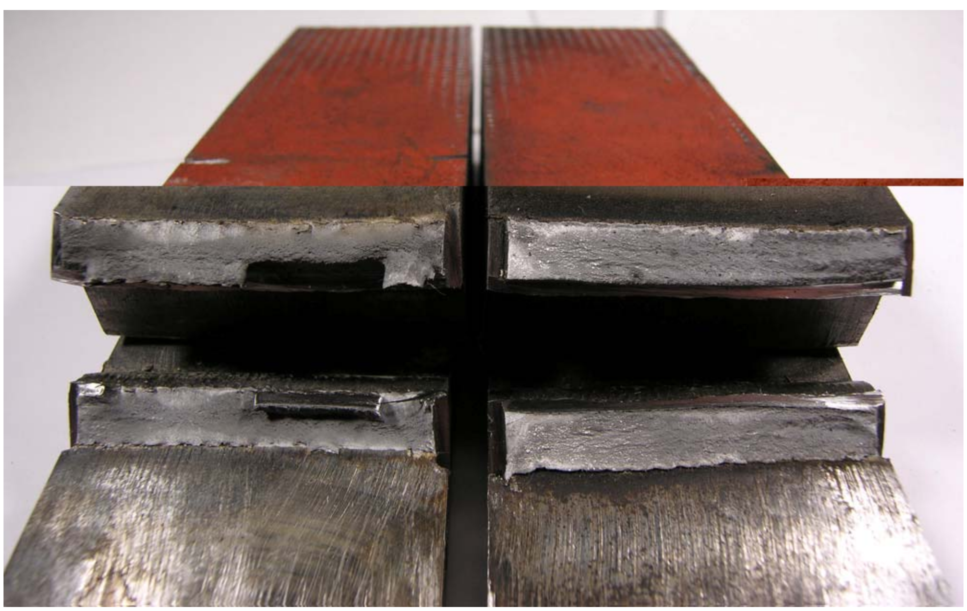

Figure 4.86: PMCAW Nick Break Results

5 CONCLUSIONS

Based on the results of the alternative welding processes evaluated

(a) Each have the potential to provide slower cooling rates over a range of heat inputs, compared to the SMAW process.
- Slower cooling resulted in lower CGHAZ hardness and thus lower susceptibility to hydrogen cracking
- PMCAW and PGMAW demonstrated lower CGHAZ hardness compared to SMAW at the same calculated heat input level.

(b) Each alternative process exhibited a higher susceptibility to burn-though compared to SMAW, likely due to their higher process arc efficiencies and resulting higher peak inside surface temperature for a given calculated heat input level. The SSFCAW process had demonstrated the highest susceptibility to burn-through, however SMAW with 2.4mm electrodes had demonstrated the lowest.

(c) Possible that adjusting pulse waveform parameters could reduce their susceptibility

(d) Alternative processes offer the advantage of mechanization to enhance consistency of the welding procedure in all positions of welding as well as enhanced productivity with continuous wire feed and less interruptions.

(e) PMCAW and PMCAW processes demonstrated enhanced tempering of HAZ's in previously weld deposits at heat inputs 50% lower than the FCAW process, as demonstrated in Task 8.

(f) Alternate welding processes passed the requirements for bend and nick break testing as per API 1104 specifications.

(g) Each process demonstrated longer hydrogen delay times in the simulated hydrogen model when welding on water filled pipe compared to the static air conditions.